MAPPING, ANALYSIS, AND INTERPRETATION OF THE GLACIER INVENTORY DATA FROM JOTUNHEIMEN, SOUTH NORWAY, SINCE THE MAXIMUM OF THE 'LITTLE ICE AGE'

Inaugural-Dissertation
zur Erlangung der Doktorwürde der
Philosophischen Fakultät III
der
Julius-Maximilians-Universität Würzburg

Vorgelegt von
Sabine Christine Baumann
aus Gröbenzell

Würzburg
2009

Erstgutachter: Professor Dr. Heiko Paeth

Zweitgutachter: Professor Dr. Atle Nesje

Tag des Kolloquiums: 10.02.2010

Photographs on previous page:

Upper image: Glacier foreland of Tverråbreen, 01.08.2008, S. Baumann

Central image: Moraines and glacier foreland of a nameless glacier and S. Illåbreen, 27.07.2008, S. Baumann

Lower image: Moraines and glacier foreland of Styggebreen, 31.07.2008, S. Baumann

Summary

Glaciers are good indicators of climate changes on various time-scales, especially maritime glaciers, which react very sensitively. Despite this, a respective part of the research is still focusing and is based on the European Alps and does not clearly differentiate between glaciers in varying climate regimes. This has a special impact on forecasts of glacier behaviour by models and simulations. This study contributes to a more detailed differentiation between maritime and continental glaciers from the 'Little Ice Age' maximum until 2003. The study area is Jotunheimen in central South Norway, situated in a transitional zone between maritime and continental climate.

Glacier outlines during the 'Little Ice Age' maximum in Jotunheimen were mapped by using remote sensing techniques (vertical aerial photos and satellite imagery), glacier outlines from the 1980s and 2003, a digital terrain model (DTM), geomorphological maps of individual glaciers, and field-GPS measurements. The related inventory data (surface area, minimum and maximum altitude) and several other variables (e.g. slope, range) were calculated automatically by using a geographical information system. The length of the glacier flowline was mapped manually based on the glacier outlines at the maximum of the 'Little Ice Age' and the DTM.

During the maximum of the 'Little Ice Age', there were 233 glaciers in Jotunheimen with a total area of 290 km². Only three glaciers were larger than 10 km². More than 50% were smaller than 0.5 km² (representing 9% of the total area). The mean glacier size was 1.24 km². Maximum altitude ranged between 1500 and 2500 m a.s.l. (mean 2010 m a.s.l.), while the minimum altitude ranged between 1000 and 2400 m a.s.l. (mean 1590 m a.s.l.). Central flowline length of the glaciers varied between 134 and 6818 m (mean 1554 m). Two thirds of the flowlines were shorter than the mean. Only eight flow lines were longer than 5.0 km.

The glacier data during the maximum of the 'Little Ice Age' were compared with the Norwegian glacier inventory of 2003. The glacier area decreased from 290 km² to 190 km² (35%), and the mean flow-length from about 1.55 km to 1.03 km (34%).

Based on the glacier inventories during the maximum of the 'Little Ice Age', the 1980s and 2003, a simple parameterization after HAEBERLI & HOELZLE (1995) was performed to estimate unmeasured glacier variables, as e.g. surface velocity or mean net mass balance. Input data were composed of surface glacier area, minimum and maximum elevation, and glacier length. Some additional variables

and parameters (e.g. value of mass balance gradient, glacier bed geometry) had to be estimated in advance. Selection of glaciers was done according to minimum glacier size of 0.2 km² related to the area of the 1980s and comparability of the glacier length. Thus, 125 glaciers (57%) of the 1980s inventory with a total area of 182.5 km² (88%) remained. For adjusting the parameterisation, available mass balance data from Jotunheimen (Stor-, Hellstugu-, and Gråsubreen) were used. The outcome was a separation of the area into a more maritime western and a more continental eastern part.

The results of the parameterization were compared with the results of previous parameterizations in the European Alps and the Southern Alps of New Zealand (HAEBERLI & HOELZLE 1995; HOELZLE et al. 2007). In Jotunheimen, a mean value of -0.05 m w.e./a of the specific net mass balance for the more maritime part was calculated, and -0.03 m w.e./a for the eastern part. These values are much higher than in the two abovementioned regions (European Alps: -0.33 m w.e./a; New Zealand: -0.67 to -0.57 m w.e./a). The calculated values fit very well to the measured data for Stor- and Hellstugubreen.

A relationship between these results of the inventories and of the parameterization and climate and climate changes was made. For glacier behaviour the influence of temperature and precipitation is important. Maritime glaciers are more influenced by winter precipitation and continental glaciers by summer temperature. Therefore, it is fundamental not to use mean annual values, but to make a seasonal differentiation. A strong impact on glacier behaviour is seen by the influence of atmospheric circulation patterns. The main factor is the North Atlantic Oscillation in Norway and the European Alps as well as the Southern Oscillation in New Zealand. Strong influences of these circulation patterns were visible in the glacier changes, especially concerning the long period since the maximum of the ‘Little Ice Age’.

Zusammenfassung

Gletscher sind gute Indikatoren des Klimawandels auf verschiedenen Zeitskalen, besonders maritim geprägte Gletscher, die sehr sensibel reagieren. Trotzdem konzentriert sich und basiert ein ansehnlicher Teil der Forschung auf den Europäischen Alpen und differenziert nur gering zwischen Gletschern unterschiedlicher klimatischer Regime. Dies hat besonders Auswirkungen auf Vorhersagen des Gletscherverhaltens in Modellen und Simulationen. Diese Untersuchung trägt zu einer detaillierteren Unterscheidung zwischen maritim und kontinental geprägten Gletschern vom Maximum der „Kleinen Eiszeit“ bis 2003 bei. Das Untersuchungsgebiet ist Jotunheimen im zentralen Südnorwegen, das in einem Übergangsbereich von maritimem zu kontinentalen Klima liegt.

Die Gletscherumrisse während des Maximalstandes der „Kleinen Eiszeit“ in Jotunheimen wurden unter der Verwendung von Fernerkundungstechniken (vertikale Luftbilder und Satellitenbilder), von Gletscherumrissen aus den 1980er Jahren und von 2003, von einem digitalen Geländemodel (DTM), von geomorphologischen Karten einzelner Gletscher und von GPS-Messungen im Gelände kartiert. Die daraus erzielten Inventardaten (Gletscherfläche, minimale und maximale Höhe) und einige andere Variablen (z.B. Hangneigung, Höhendifferenz) wurden automatisch mit einem geographischen Informationssystem berechnet. Die Länge der Gletscherfließlinie wurde basierend auf den Gletscherumrissen zum Maximum der „Kleinen Eiszeit“ und dem DTM manuell kartiert.

Zum Maximalstand der „Kleinen Eiszeit“ gab es 233 Gletscher in Jotunheimen mit einer Gesamtfläche von 290 km². Nur drei Gletscher waren größer als 10 km². Mehr als 50% waren kleiner als 0,5 km² (9% der Gesamtfläche). Die mittlere Gletschergröße war 1,24 km². Die maximale Höhe lag zwischen 1500 und 2500 m ü.M. (Mittelwert 2010 m ü.M.), während sich die minimale Höhe zwischen 1000 und 2400 m ü.M. (Mittelwert 1590 m ü.M.) bewegte. Die Länge der zentralen Fließlinie der Gletscher variierte zwischen 134 und 6818 m (Mittelwert 1554 m). Zwei Drittel der Fließlinien waren kürzer als der Mittelwert. Nur acht Fließlinien waren länger als 5,0 km.

Die Gletscherdaten zum Maximalstand der „Kleinen Eiszeit“ wurden mit dem Gletscherinventar von 2003 verglichen. Die Gletscherfläche verringerte sich von 290 km² auf 190 km² (35%) und die mittlere Fließlänge von 1,55 km auf 1,03 km (34%).

Basierend auf den Gletscherinventaren zum Maximum der „Kleinen Eiszeit“, von den 1980er Jahren und von 2003 wurde eine einfache Parametrisierung nach HAEBERLI & HOELZLE (1995) durchgeführt, um ungemessene Gletschervariablen, wie z.B. Oberflächengeschwindigkeit oder mittlere Netto-Massenbilanz, abzuschätzen. Eingabedaten bestanden aus Gletscherfläche, minimaler und ma-

ximale Höhe und der Gletscherlänge. Einige weitere Variablen und Parameter (z.B. Wert des Massenbilanzgradienten, Gletscherbettgeometrie) mussten im Voraus abgeschätzt werden. Eine Auswahl der Gletscher wurde aufgrund der Mindestgröße von 0,2 km² bezogen auf die Fläche aus den 1980er Jahren und aufgrund der Vergleichbarkeit der Gletscherlänge vollzogen. Somit verblieben 125 Gletscher (57%) des 1980er Inventars mit einer Gesamtfläche von 182,5 km² (88%). Zur Anpassung der Parametrisierung wurden vorhandene Massenbilanzdaten aus Jotunheimen (Stor-, Hellstugu- und Gråsubreen) verwendet. Das Ergebnis war eine Trennung des Gebiets in einen eher maritimen westlichen und einen eher kontinentalen östlichen Teil.

Die Resultate der Parametrisierung wurden mit den Ergebnissen früherer Parametrisierungen aus den Europäischen Alpen und den Southern Alps auf Neuseeland verglichen (HAEBERLI & HOELZLE 1995; HOELZLE et al. 2007). In Jotunheimen wurde der Mittelwert der spezifischen Netto-Massenbilanz mit -0,05 m w.e./a im maritimen Teil und mit -0,03 m w.e./a im östlichen Teil berechnet. Diese Werte sind viel höher als in den zwei vorhergenannten Regionen (Europäische Alpen: -0,33 m w.e./a; Neuseeland: -0,67 und -0,57 m w.e./a). Die berechneten Werte passten sehr gut zu den gemessenen Daten des Stor- und Hellstugubreen.

Eine Verbindung zwischen diesen Ergebnissen aus den Inventaren und der Parametrisierung und dem Klima und der Klimaänderung wurde hergestellt. Für das Gletscherverhalten ist der Einfluss der Temperatur und des Niederschlags wichtig. Maritime Gletscher sind stärker durch Winterniederschlag und kontinentale stärker durch Sommertemperaturen beeinflusst. Deswegen ist es elementar, nicht die Mittelwerte zu verwenden, sondern eine saisonale Differenzierung durchzuführen. Einen großen Einfluss auf das Gletscherverhalten haben atmosphärische Zirkulationsmuster. Der Hauptfaktor in Norwegen und den Europäischen Alpen ist die nordatlantische Oszillation und in Neuseeland die „Southern Oscillation“. Ein starker Einfluss dieser Zirkulationsmuster ist in den Gletscherveränderungen sichtbar, besonders bezogen auf die lange Dauer seit dem Maximum der „Kleinen Eiszeit“.

Outline

List of tables

List of figures

List of abbreviations

AAR	Accumulation area ratio
AAR_0	Mean accumulation area ratio
AD	Anno domini (after Christ)
AO	Arctic Oscillation
a.s.l.	Above sea level
ASTER	Advanced Spaceborne Thermal Emission and Reflection Radiometer
AWS	Automatic weather station
bn	Specific glacier net mass balance
$\bar{b}n$	Mean specific glacier net mass balance
BP	Before present
bs	Specific glacier summer mass balance
b_t	Ablation at the glacier tongue
BUK	Bukkeholsbreen
bw	Specific glacier winter mass balance
cal.	Calibrated (by radiocarbon calibration)
db/dH	Mass balance gradient
DEM	Digital elevation model
DFG	Deutsche Forschungsgemeinschaft (German research community)
DTM	Digital terrain model
DTM 25	Digital terrain model with 25m resolution derived from N50 by Statens Kartverk
E	East
e.g.	Exempli gratia (for example)
ELA	Equilibrium line altitude
ELA_0	Mean equilibrium line atlitude
ENSO	El Niño/Southern Oscillation
Equ.	Equation
ETM+	Enhanced Thematic Mapper Plus
f	Geometry shape factor
GCOS	Global climate-related observing system
GCP	Ground control point
GHOST	Global hierarchical observing strategy
GIS	Geographical information system
GLIMS	Global land ice measurements from space
GPS	Global positioning system

GRA	Gråsubreen
GRJ	Grjotbreen
GTN-G	Global terrestrial network for glaciers
GTOS	Global terrestrial observing system
h_{max}	maximum ice thickness
H_{max}	Maximum glacier altitude
H_{mean}	Mean glacier altitude
H_{min}	Minimum glacier altitude
HEL	Hellstugubreen
ID	Identification number
i.e.	Id est (that means)
L_0	Original glacier length
LIA	'Little Ice Age'
MaMoGla	Recent and Holocene Glacier Dynamics of Maritime Mountain Glaciers
MEM	Memurubreen
N	North
N50	Digital topographic map in 1:50000 of Norway at AD 1980s by Statens Kartverk
NAO	North Atlantic Oscillation
NAM	Northern Annular Mode
NIG	Nigardsbreen
NVE	Norges vassdrags- og energi directorat (Norwegian Water Resources and Energy Directorate)
RMSE	Root mean square error
SLP	Sea level pressure
SOI	Southern Oscillation index
SOL	Soleibotnbreen
STD	Styggedalsbreen
STO	Storbreen
TM	Thematic Mapper
t_{relax}	Relaxation time
t_{resp}	Response time
t-test	Student's t-test
$u_{b,a}$	Mean sliding velocity
$u_{d,a}$	Velocity of ice deformation
ü.M.	Über Meer
$u_{s,a}$	Mean surface flow velocity
V	Glacier volume
VIS	Visbreen

VR	Velocity ratio
vs.	Versus (against)
w	Half width
W	West
w.e.	Water equivalent
WGMS	World glacier monitoring service
z.B.	Zum Beispiel
α	Surface slope
δb	Mass balance disturbance
δELA	Change in equilibrium line altitude
δL	Change in glacier length
ΔS	Difference of glacier surface area between two points of time
ΔV	Difference of glacier volume between two points of time
σ	Standard deviation
τ	Mean basal shear stress

1 Foreword

The present thesis was connected to the project 'MaMoGla', supported from the *Deutsche Forschungsgemeinschaft* (DFG) and lead by PD Dr. Stefan Winkler. This project was focused on the comparison between glaciers from Norway and New Zealand concerning a more detailed regional differentiation in using glaciers as climate indicators. The Norwegian part dealt with the monitoring of seasonal and annual changes of glacier snout positions and of glacier outlines at the snout at several glaciers in South Norway. This thesis was also connected to the Norwegian Directorate of Water Resources and Energy (Norges vassdrags- og energi directorat; NVE). A contract was concluded for exchanging data and submitting of thereof derived data. Hence, parts of this thesis will be included in the planned New Norwegian glacier inventory and stored in NVE's online database.

1.1 Motivation

Changes during recent decades of mountain landscapes and glaciers have been in the focus of public interest since 2003. The remarkably warm summer of that year was accompanied by a large reduction of snow and ice, rock fall, and rock- and landslides in the mountain regions. Many tourists and hikers were affected by severe dangers, e.g. caused by newly exposed rock areas at the glaciers or dangerously changed accesses onto the glaciers. This development of changing glaciers, and especially the glacier reduction since the beginning of the present millennium was not new for science, but the public started only now to become aware of what was going on in the mountains. In the media, discussions about climate change and climate warming became a popular topic.

But these discussions often presented a very simplified picture of the relationship between glacier behaviour and climate and were strongly focussed on the European Alps (WINKLER et al. submitted). Global glacier behaviour was postulated based on the strong increase of temperature. This explanation was correct for the European Alps, but did not represent the glacier behaviour world-wide. In science, a stronger differentiation of the glacier responses to climate changes of the individual mountain regions was initiated. Still, many open questions concerning the complete understanding of the complex system of mountain glaciers are still unanswered. Influences of climatic and non-climatic

factors aggravate this understanding. Despite the more intensive research on this topic during the last decade, a deficit concerning the regional differentiation of high-mountain glaciers still exists, even if only concentrating on the glaciers of the mid-latitudes.

This missing knowledge and the simplified image of a global behaviour raised my interest in explaining at least a small piece of this complex relationship. Because of several private trips to Scandinavia, I am familiar with the landscape of Norway. Due to private and professional mountaineering experience in the European Alps, I have already been aware of the ongoing changing processes myself. During an internship at the World glacier monitoring service (WGMS) I had the chance to broaden my knowledge about glaciers world-wide and to experience the great variety and differences of glaciers. Therefore, the research topic of my thesis is based on my gained knowledge on glaciers and mountains, their impressive variety, and my great interest in former development and future of the glaciers.

1.2 Acknowledgements

Working on this study for the last three years was only possible because of being supported by the Chair of the Physical Geography at the University of Würzburg, Prof. Dr. Roland Baumhauer, and the provision of the entire needed infrastructure. My special thanks go to my reviewers and supervisors Prof. Dr. Heiko Paeth (University of Würzburg) and Prof. Dr. Atle Nesje (Bjerknes Centre of Climate Research; University of Bergen). I also thank my mentor PD Dr. Stefan Winkler for his helpful, fruitful, and intense discussions, hints, and support during the last years not only in working on the thesis and all related projects, but also in supporting me mentally and psychologically.

I would like to thank Liss M. Andreassen (NVE), Martin Hoelzle (University of Fribourg), and L.A. Rasmussen (University of Washington) for their fruitful comments and discussions during my research.

I thank the NVE and especially Liss M. Andreassen in providing the following material: satellite image, digital terrain model, topographical map, digital glacier shapes of the 1980s, and unpublished glacier shapes and glacier inventory data of 2003 from Jotunheimen, as well as digital glacier shapes of the 1980s from Jostedalsbreen. Martin Hoelzle supported my study in providing detailed data bases of parameterization data of the European Alps and the Southern Alps of New Zealand.

A non scientific but also very important role played my family and friends in giving me power, energy and support during the three years. I especially want to thank my mother, Stephan, Sandra, Stephanie, Daniel, and Wesley.

This study is supported by a personal grant from the *Bayerische Graduierten-förderung nach dem Bayerischen Eliteförderungsgesetz*, a personal grant from the *Qualifikationsprogramm für Wissenschaftlerinnen an der Universität Würzburg*, a grant for fieldwork in 2008 in Norway from the *Universitätsbund der Universität Würzburg,* and a travelling grant to Norway in 2009 from the *Jubiläums-Stiftung zum 400-jährigen Bestehen der Universität* (University of Würzburg). The study is connected to the DFG-funded project 'MaMoGla' and NVE.

2 Introduction

Glaciers offer a high potential to serve as key indicators for climate change (IPCC 2007). They are showing indications of short-, middle-, and long-scale changes of climate. In this context, a detailed knowledge of glacial chronology during the later Holocene is important. It serves as an opportunity to verify forecasts and simulations of future glacier behaviour.

Additional to their function as indicators, glaciers and their behaviour exhibit a specific importance for practical meaning. For example, they serve as providers of drinking water in the subtropics or are used for production of hydropower in the mid-latitudes. Furthermore, they are important elements in the geo-ecosystem of high mountains (WINKLER et al. submitted). Especially in Norway, knowledge of the behaviour of glaciers and their response to changes of climatic factors is important for power production. 98% of the domestic electricity is produced using hydropower and 15% of the exploited runoff is derived from glacierized river basins (ANDREASSEN et al. 2008a; NESJE et al. 2008a). Up to 80% of the discharge occurs due to summer melting (NESJE et al. 2008a). For example, in the extraordinary warm summer of 2002 in Norway, the glaciers in Jotunheimen showed larger than normal melting and an altered drainage regime (NESJE et al. 2008a). Rapid melting of glaciers can cause outburst floods or jökulhaups (NESJE et al. 2008a). This and other natural hazards caused directly or indirectly by glaciers can be a threat for population and infrastructure.

However, for any successful application of this information provided by the variations of glaciers, it is necessary to gain a representative regional climate signal from the glacier cover rather than signals from few selected individual glaciers. One individual glacier in most cases hardly represents a whole mountain system (HOELZLE et al. 2007; UNEP & WGMS 2008). Therefore, it would give an unreliable and subjective basis for further investigations and related conclusions. In addition, global effects of climate change can be achieved only by comparing long-term behaviour of glaciers within different mountain systems (HOELZLE et al. 2007).

Mapping the ‘Little Ice Age’ (LIA) maximum glacier extent (that was between about 1600 and 1900 depending on regional differences) by conventional field work is time consuming and is seldom applied to investigate more than a few selected glaciers. To study a whole region with a large number of individual glaciers, many difficult to visit on foot, remote sensing provides an alternative. By using a huge data base, regional averages can be detected to minimize the dangers of misinterpreting specific local behaviour of selected individual ‘key-

glaciers' as common trend. Those regionally based results are more reliable. It is particularly important to understand the actual behaviour of mountain glaciers and their changes during the geologically recent past, not only concerning the assessment of future glacier reactions on assumed climate changes.

2.1 Scientific background

A lot of work has been done on glaciers in the European Alps, Scandinavia, and North America, as well as to a lesser amount in New Zealand, South America, Greenland, and Antarctica. Out of a large variety of studies, some examples are CHINN (1996), DYURGEROV & MEIER (1997), ARENDT et al. (2002), DYURGEROV (2002), RASMUSSEN & CONWAY (2004), ANDREASSEN et al. (2005), VUILLE et al. (2008), ZEMP et al. (2008). Research on the recent dynamics of mountain glaciers is mainly motivated by questions of reasons and meanings of the actual climate change. An evaluation of the actual glacier reduction in many mountain regions and an assessment of the glacier development during the next decades are in scientific focus (e.g. HAEBERLI & BENISTON (1998); HAEBERLI et al. (1999); HOELZLE et al. (2000); OERLEMANS (2001); HOELZLE et al. (2007); IPCC (2007); NESJE et al. (2008a)).

Many results from research on continental or continentally influenced mountain regions cannot be adopted to the maritime glaciers of Norway (WINKLER et al. 1997, submitted; WINKLER & HAAKENSEN 1999; WINKLER 2002; CHINN et al. 2005). That means that due to different glaciological regimes, glaciers in maritime regions are influenced more strongly by precipitation during winter than continental glaciers (cf. NESJE & DAHL (2003)). For this reason, models based on the European Alps (GREUELL & BÖHM 1998; OERLEMANS 2005; SCHAEFER et al. 2009) do not work in the maritime regions, e.g. maritime Norway and New Zealand, even if modifications have been applied, or show contrary results to the observations (WINKLER et al. 1997; NESJE et al. 2001; CHINN et al. 2005). Only models especially constructed for maritime glaciers are consistent with observations (e.g. JÒHANNESSON et al. (1989a); LAUMANN & REEH (1993); HOCK (2003); RASMUSSEN & CONWAY (2005); BRAITHWAITE (2008); LAUMANN & NESJE (2009)).

Large regional differences during the LIA regarding dimension, number, and timing of the individual glacier advances became evident during the recent years (WINKLER 2002). Evidence from dating of LIA maximum extents, from detailed chronologies, and from their patterns were related to the recent glaciological

development and conditions. Hence, a similar global pattern of holocene glacier chronology (RÖTHLISBERGER 1986) was not determined according to these findings (e.g. HORMES et al. (2001); NESJE et al. (2001); WINKLER (2002); MATTHEWS & BRIFFA (2005); NESJE (2009)).

Studies on recent maritime glaciers show the similarity and parallelism between the reaction of the glacier tongues and climatic forcing factors driving mass balance of southern Norway and New Zealand (WINKLER 2001, 2003; CHINN et al. 2005). This similarity was also found for the maximum advance during LIA (BOGEN et al. 1989; BICKERTON & MATTHEWS 1993; WINKLER 2004b). These are good reasons for a trans-regional comparison in contrast to the continentally influenced mountain regions, as e.g. the European Alps.

Previous studies in other regions have shown the potential of using satellite imagery as an efficient tool for mapping the maximum LIA extent of glaciers on the regional scale (SOLOMINA et al. 2004; CSATHO et al. 2005; PAUL & KÄÄB 2005; WOLKEN 2006; PAUL & SVOBODA 2009). Therefore, glaciological data not only on selected individual glaciers, but on whole glacier regions are needed for a profound analysis (KARGEL et al. 2005; HOELZLE et al. 2007; UNEP & WGMS 2008; ZEMP et al. 2008) in order to reconstruct climate change and create future scenarios.

Investigations of the glacier maximum extent during the LIA in South Norway have, until recently, mainly been carried out as locally focused studies on selected glaciers (e.g. FÆGRI (1948); HOEL & WERENSKIOLD (1962); MATTHEWS (1977), (2005); ERIKSTAD & SOLLID (1986); BOGEN et al. (1989); WINKLER (2002)). These investigations included dating of moraines, e.g. by application of lichenometry, and mapping of selected glaciers. Previous studies have focused on the region of Jostedalbreen and a few individual glaciers in Jotunheimen, e.g. Storbreen (STO) in Visdalen.

The parameterization, developed by HAEBERLI & HOELZLE (1995), has already successfully been applied to the European Alps (HAEBERLI & HOELZLE 1995) and the Southern Alps of New Zealand (HOELZLE et al. 2007).

2.2 Objectives of this study

This study will provide deeper knowledge about the regional differentiation between maritime and continental glaciers for a better understanding of the glaciological regimes and the glacier characteristics. The work is concentrated on Jotunheimen in southern Norway. This area has been chosen because of the

very well established glacier data since decades of glacier measurements and the setting of the glacier area in a transitional zone between maritime and continental climate.

The aim of this study is to reconstruct the glacier area during LIA maximum on a regional scale. Out of these results and a digital terrain model, the LIA maximum inventory data (e.g. minimum and maximum altitude) will be determined using a geographical information system (GIS). The data will be used to analyze the area change since LIA maximum until 2003, and to detect spatial differences in glacier behaviour.

One method of analyzing is the parameterization developed by HAEBERLI & HOELZLE (1995). This study presents the application of this parameterization scheme on the available inventory data from Jotunheimen. The results will be compared with previous studies using the same method.

The derived data will be connected to climate and climate changes to detect the sensitivity of these glaciers concerning climatic forces. By establishing this connection not only the mechanisms of global climate features, but also the impact of local differences resulting in individual glacier regimes will be analyzed.

2.3 Structure of this study

This thesis is divided into nine parts. Section 1 is the foreword including motivation and acknowledgements. The introduction in section 2 gives the scientific background and aims of this study. Section 3 is an overview of the study area and the other glacier areas used for comparison. Section 4 summarizes the scientific and thematic background on which this thesis is based. It briefly describes the theory of glaciers and relevant climatic factors as well as glacier history during the Holocene and the ‘Little Ice Age’ especially in Jotunheimen. All methods used in this thesis are described in section 5 with a focus on remote sensing, the data sources, the mapping process, and the scheme and input data of the parameterization. Results of the sensitivity analysis, of mapping the glacier inventory at ‘Little Ice Age’ maximum in Jotunheimen, and of the parameterization of Jotunheimen are shown in section 6. In section 7, the comparison with other inventories of Norway, the comparison with other glacier regions of the inventory and the parameterization data, as well as a relationship to climate are made. The discussion is described in section 8. It contains questions and uncertainties about

mapping and remote sensing, comparison of sources, usability of and selection of variables for the parameterization, analysis of mapping results, comparison between glacier areas, and the relationship between glaciers and climate. Section 9 closes the thesis with the conclusions and the outlook.

3 Study area

The study area is Jotunheimen. All investigations as compilation of the inventory and inventory data of LIA maximum and the application of the parameterization were done with data from this area. These results were compared with other regions which are also briefly described in the following.

3.1 Geography

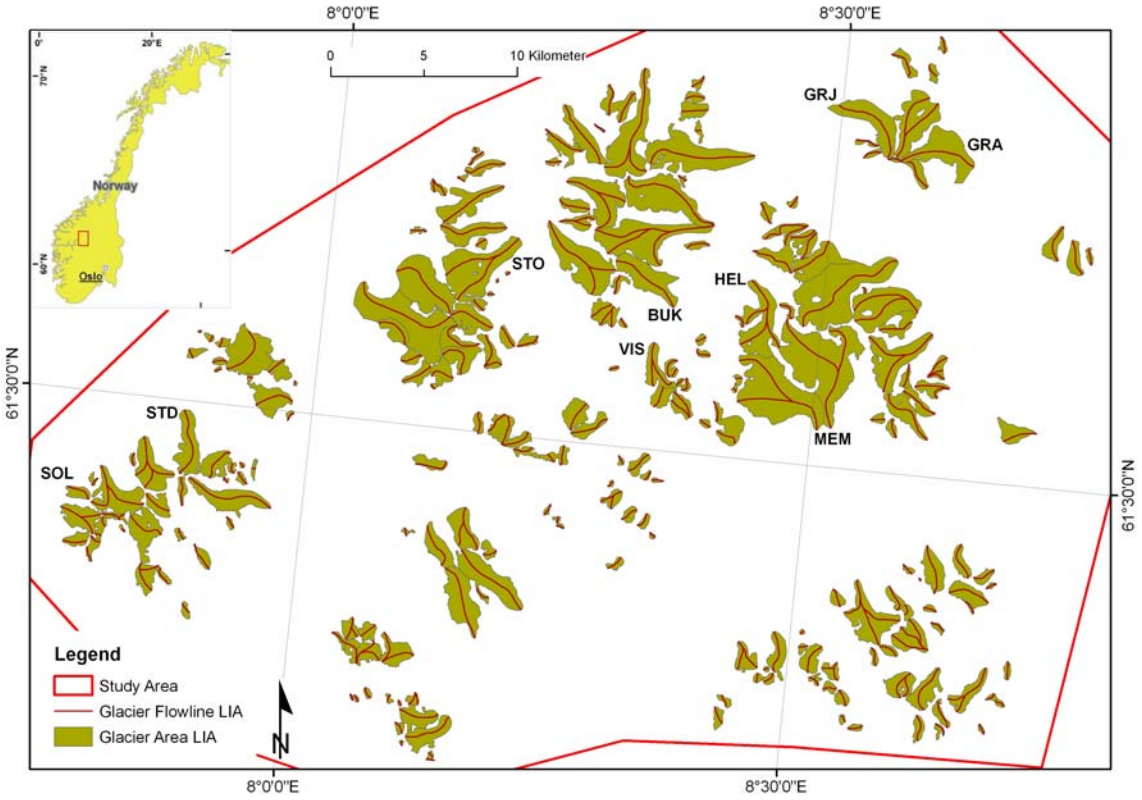

Figure 1: Location of the study area Jotunheimen (inset) and glaciers (> 0.01 km²) with flowlines during LIA maximum. Letter codes denote: SOL = Soleibotnbreen, STD = Styggedalsbreen, STO = Storbreen, VIS = Visbreen, BUK = Bukkeholsbreen, HEL = Hellstugubreen, MEM = Memurubreen, GRJ = Grjotbreen, GRA = Gråsubreen (Inset map: ESRI Templates).

The study area of Jotunheimen is located in central South Norway (61.5° N; 8.3° E) (Figure 1) covering about 3500 km² and belongs to the fylkene (Norwegian administrative unit) Sogn og Fjordane and Oppland. It has a high-alpine character and the highest points of Norway are located here (Galdhøpiggen 2469 m a.s.l.; Glittertind 2464 m a.s.l.). 101 of all 137 peaks higher than 2000 m a.s.l. in Scandinavia are in Jotunheimen (BAXTER 2009). The area can be divided into 14 separate mountain massifs, as e.g. Hurrungane in the very West of Jotunheimen (BAXTER 2009).

West of Jotunheimen, there are the glacier areas Breheimen and Jostedalsbreen (Figure 2) and to the East, the region Rondane. Some small towns around the area are Lom, Vågå, and Øvre Årdal. 1145 km² of Jotunheimen were designated as national park in 1980 (JOTUNHEIMEN REISELIV 2007). Mountain huts and hiking routes are well established, attracting a lot of tourists and hikers.

MOEN (1999) described the vegetation cover of Jotunheimen. The area lies in the boreal zone. This zone is dominated by cold winters, long-lasting snow-cover and a short growing season. Jotunheimen is composed of a high, middle, and low alpine as well as a northern boreal zone, accompanied by the typical vegetation. The alpine zone is above the timberline, which is at about 1250 m a.s.l in Jotunheimen. The high alpine zone is sporadically covered with bryophytes and lichens. The middle alpine zone is dominated by grass heaths, the low alpine zone by bilberry heather and dwarf scrubs of juniper and birch. The typical vegetation of the northern boreal zone consists of birch woodland and some coniferous trees.

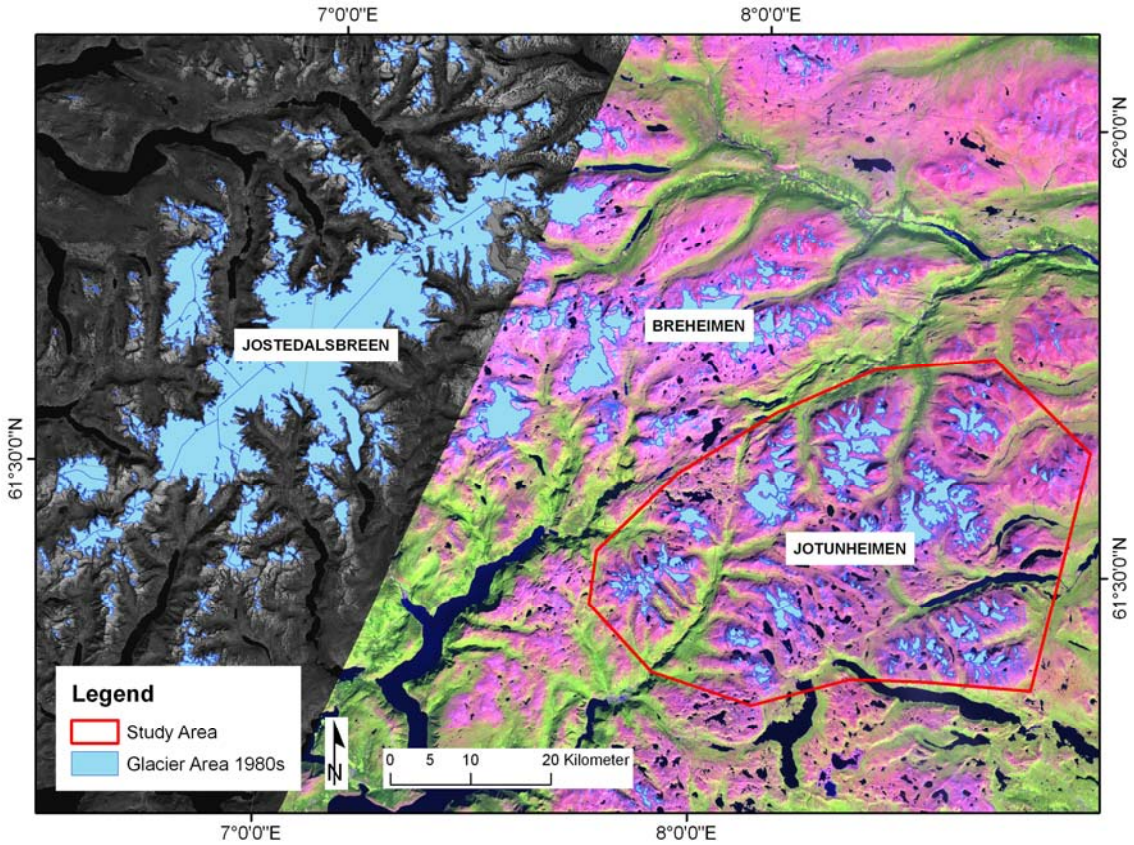

Figure 2: Location of Jotunheimen, Breheimen, and Jostedalsbreen on the satellite images used in this study (Glacier outline 1980s: Statens Kartverk N50, satellite image Jotunheimen/Breheimen: Norsk Satellittdataarkivet, satellite image Jostedalsbreen: GLCF 2008).

3.2 Geology

The origin of the mountain area of Jotunheimen is described by FOSSEN et al. (2008). The area of Jotunheimen is part of the Caledonian orogenic belt, formed between 500 and 400 million years BP with its main phase of orogeny during the Silurian Period. Reasons of the Caledonian orogeny were the collision between Laurentia (North American continent including Greenland) and Baltica (northern and eastern Europe) following the closure of the Iapetus Ocean. The whole Caledonian mountain chain stretches from western Europe via Ireland, Scotland, and Scandinavia to Svalbard, but is best developed and preserved in Norway. The rocks in the Jotun Nappe complex have been pushed over younger Late Precambrian-Ordovician sandstones and shales which overlie an autochthonous basement (NORDGULEN & ANDRESEN 2008).

The denudation and erosion of the Caledonian mountains took place until early Paleogene (KLEMSDAL 2000). The climate of these times is described as tropical and subtropical with chemical weathering and mass movement by sheet flows and erosion by running water (KLEMSDAL 2000). This led to an undulating topography in the peripheral parts and rounded mountain landforms in the more central parts, called paleic surfaces and paleic mountains (KLEMSDAL 2000). This surface is a composite landscape of Palaeozoic, Mesozoic, and Palaeogene landforms and surfaces (MARTINSEN & NØTTVEDT 2008).

The uplifted surface of today is a result of irregular uplift processes that occurred during the spreading of the North American and European continental mass, following the North Atlantic rift in the Tertiary (KLEMSDAL 2000; LIDMAR-BERGSTRÖM et al. 2000; MARTINSEN & NØTTVEDT 2008). This uplift was not evenly distributed over Scandinavia, but rather had a stronger impact in the western part, i.e. in Norway (KLEMSDAL 2000; LIDMAR-BERGSTRÖM et al. 2000). The climate cooled down during Neogene, followed by mechanical weathering, mostly frost weathering, and transformation of the paleic valleys into V-shaped valleys by strong fluvial activity (KLEMSDAL 2000; LIDMAR-BERGSTRÖM et al. 2000). During Pliocene and Pleistocene, several periods of glaciation occurred and the landscape of today is dominated by traces of the past glaciations (KLEMSDAL 2000; LIDMAR-BERGSTRÖM et al. 2000). The cirque- and valley-glaciers at the beginning of the glaciation eroded the paleic landscape and developed U-shaped valleys and steep rock walls, leading to the glacial mountain landform (KLEMSDAL 2000). Further erosion by glaciers led to steep, sharp peaks with no traces of the paleic surface, i.e. the alpine mountain landform (KLEMSDAL 2000).

During the Holocene, mainland Norway has risen very rapidly in response to isostatic rebound following the last glacial period in Quaternary in order to reach equilibrium (MARTINSEN & NØTTVEDT 2008). Other causes may be masked due to the great velocity of the uplift (MARTINSEN & NØTTVEDT 2008). The uplift was greatest where the ice sheet had once been thickest (where the Gulf of Bothnia is today), with an ice sheet thickness of 3000 m, producing an isostatic depression of 1000 m (VORREN et al. 2008). The rate of uplift there was about 9 mm/a (VORREN et al. 2008). During the last glacial maximum, global sea level lowered by about 120 m (VORREN et al. 2008). As melting occurred, global sea level began to rise, but the uplift in Norway, for most of the land and most of the time, rose faster than the sea level (VORREN et al. 2008). The rebound of Scandinavia still continues today, but the uplift has nearly ceased in the northern and western coastal areas of Norway (VORREN et al. 2008).

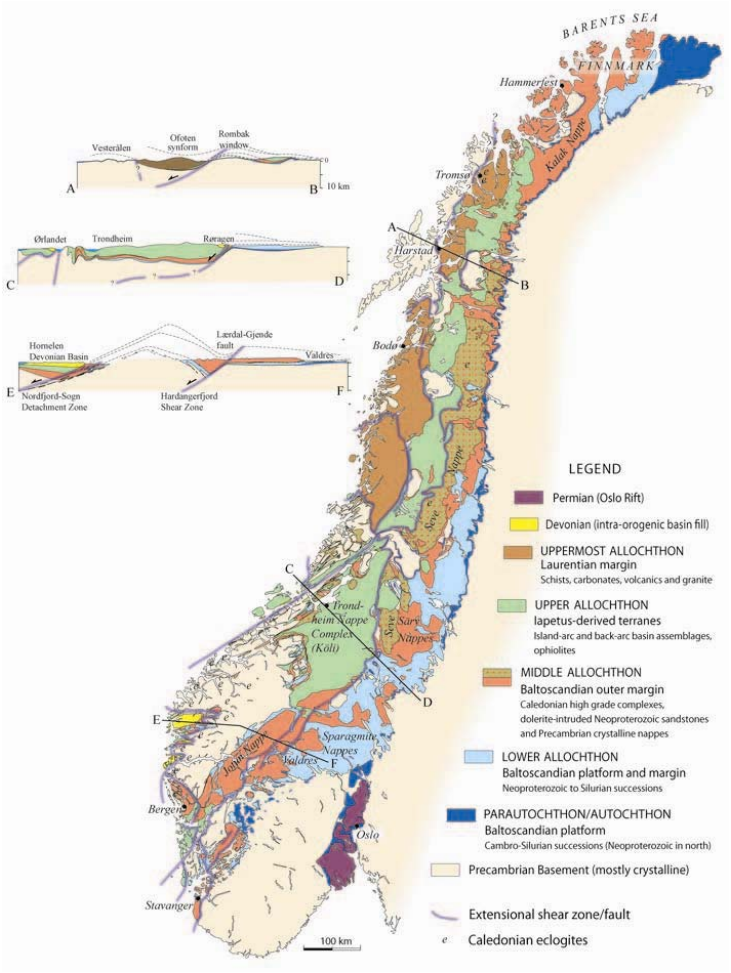

Figure 3: Geological map of the Caledonides in Norway (Figure after GEE et al. (2008)).

The bedrock in Jotunheimen is divided in a triplex structure (SCHOLZ & JONASSON 2004). Lowermost is the basement with the sub-Cambrian peneplain,

in the middle a layer of phyllite, and uppermost the remains of basement rocks in the Jotun Nappe (KOESTLER 1983) (Figure 3). The latter ones are of the Middle Allochton (FOSSEN et al. 2008), corresponding to gabbro, diorite, anorthosite, and to a lower part augen gneiss, sandstone, schist, quartzite, and amphibolite (SOLLI & NORDGULEN 2008). Overall, Jotunheimen consists of gabbro and gabbrogneiss variations (BAXTER 2009).

Jotunheimen is the highest and most alpine mountain region in northern Europe because of the quality of gabbro showing a high erosion resistance (REUBER & REUBER 1999). The rock formation of Jotunheimen contrasts to the neighbouring areas: Breheimen is largely composed of gneiss and Rondane of sparagmite, a sedimentary sandstone with lower resistance (BAXTER 2009).

3.3 Climatology

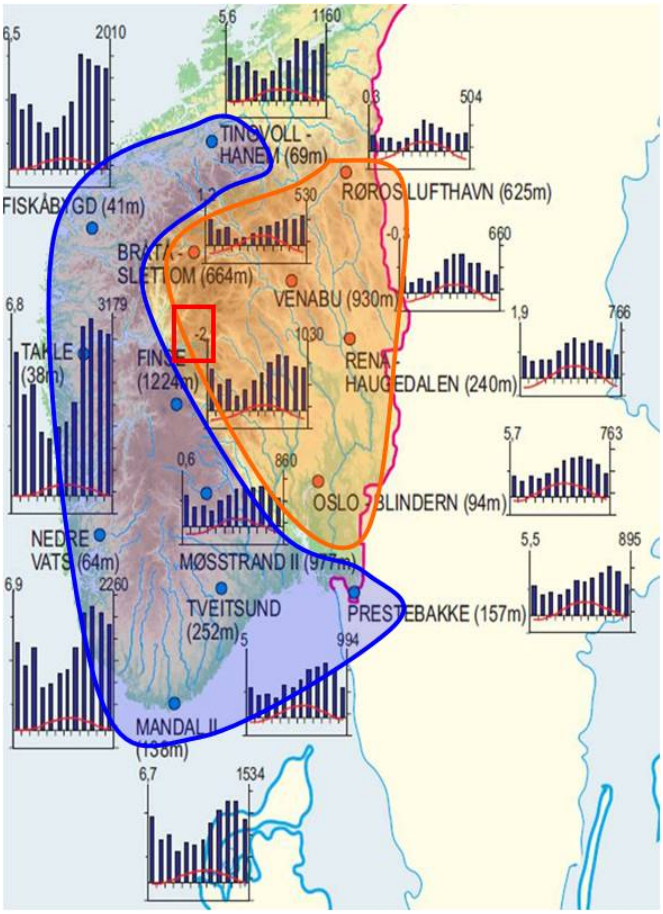

Figure 4: Selection of meteorological data from several stations in South Norway. Blue points, line, and area are maritime sites, red points, line, and area continental sites (temperature range > 20°C). Climate diagram: temperature in [°C] shown as red line, precipitation in [mm] as blue bars in monthly means over the year for the period 1961 – 1990. Location of Jotunheimen indicated by red rectangle (Data source: http://eklima.met.no) (Figure modified after MANNIG (2007)).

According to the climate system of Köppen, Jotunheimen is categorized as an ET-climate (KLEMSDAL 2000). It has therefore a cold tundra climate with the mean temperature of the warmest month between 0° and 10°C (KLEMSDAL 2000).

Meteorological data from various stations in South Norway show a remarkable difference between western and central Norway on a horizontal distance of about 150 km (Figure 4) (WINKLER & HAAKENSEN 1999; NESJE et al. 2000). Annual precipitation (up to > 3000 mm/a) and the amount each month are much higher at the weather stations westwards and in the maritime mountains, and the temperature amplitude of seasonal variation is smoother. The stations in the inland and eastwards measure less annual precipitation (around 700 mm/a) and a higher temperature difference between winter and summer. This pattern is typical for a huge climate gradient in continentality from the coast eastwards to the interior (HOEL & WERENSKIOLD 1962; ØSTREM et al. 1988; MOEN 1999; ANDREASSEN et al. 2008a; WINKLER 2009). The area more westwards has a maritime climate, whereas the area more eastwards has a continental one. This is also recorded by long-term mass balance measurements along a West-East profile on five glaciers (Figure 5) (e.g. ØSTREM et al. (1988); RASMUSSEN et al. (2007); KJØLLMOEN (2009)). Changes of other climatic factors along this gradient are e.g. a decrease of the mean annual air temperature and an increase in frequency of summer snowfall events (WINKLER & HAAKENSEN 1999). Glacier altitudes also increase eastwards (WINKLER & HAAKENSEN 1999). Jotunheimen lies in a transitional zone between maritime and continental climate (ØSTREM et al. 1988).

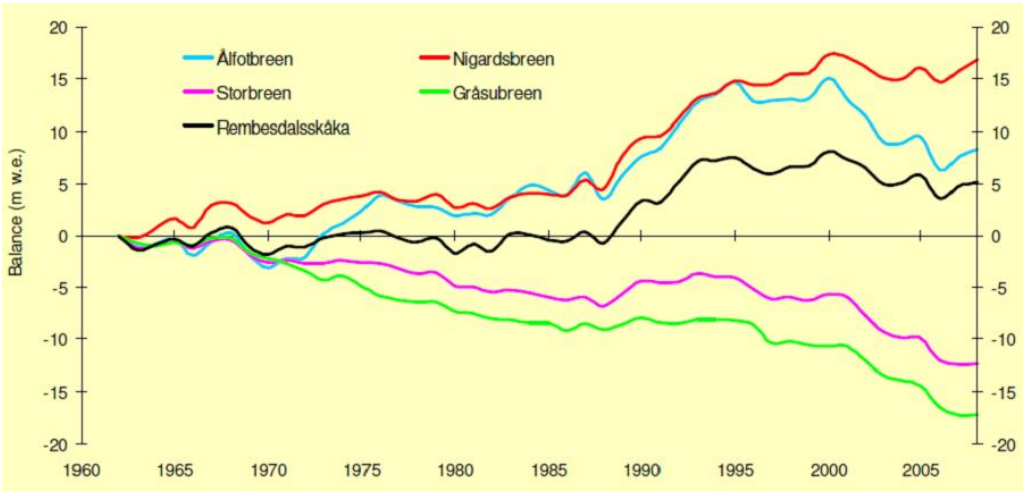

Figure 5: Cumulative net balance of five glaciers in southern Norway during the period 1963 – 2008 (Figure after KJØLLMOEN (2009)).

The North Atlantic Oscillation (NAO) index (winter period; Figure 6) is especially connected to the annual winter balance and therefore to maritime glaciers in western Norway due to their strong correlation of winter and net

balance (LAUMANN & REEH 1993; POHJOLA & ROGERS 1997; NESJE et al. 2000, 2008a, b; REICHERT et al. 2001; SIX et al. 2001; NESJE 2009). But this pressure system also has an impact on continental glaciers (NESJE et al. 2008a), even if there is a gradual decrease of the effect with increasing continentality (NESJE et al. 2000). The regression correlation between accumulation and NAO index still explains more than 50% of the accumulation on Stor-, Hellstugu-, and Gråsubreen (STO, HEL, GRA, respectively; see Figure 1 for location) if the NAO is taken as the only circulation index (NORDLI et al. 2005). The glacier advance at LIA maximum in western Norway was related to a strengthened positive mode of the NAO index with increasing winter precipitation (MANN 2000; JANSEN et al. 2005; NESJE et al. 2008b). Since the 1940s, a negative NAO index was recorded, coinciding with an enhanced retreat.

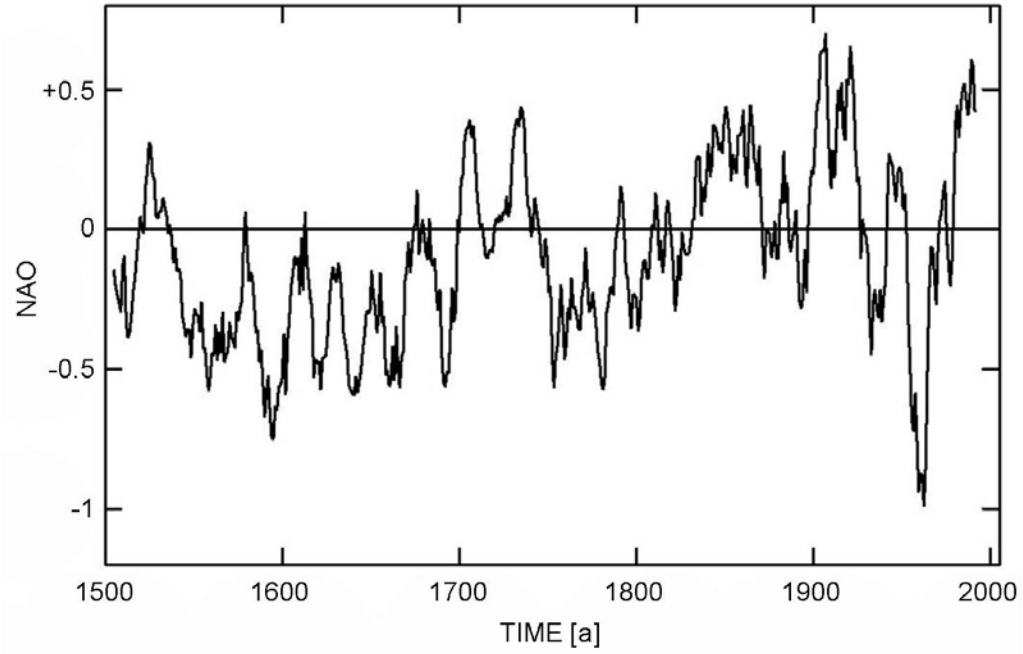

Figure 6: 11-year unweighted average of December – February NAO index. (Figure modified after RASMUSSEN et al. (submitted)).

A positive NAO index over 1989 – 1995 was related to positive net balances in the 1990s at the continental glaciers in Jotunheimen by deeper penetration of moist air masses onto the land (FEALY & SWEENEY 2007). A change in atmospheric circulation over the North Atlantic, i.e. a strongly positive NAO index (HURRELL 1995), brought warmer air to Scandinavia. This resulted in increased winter precipitation, but not in a shift from snow to rain (RASMUSSEN & CONWAY 2005) and, therefore, in a slightly positive net balance. Since the mid-1990s, the intensity of the NAO has decreased, followed by a decline of glacier mass balance on the continental glaciers in Norway since 2000 (FEALY & SWEENEY 2007).

3.4 Glaciology

The present glaciers [2003] in Jotunheimen are mostly small individual valley-type and cirque-type glaciers, separated by steep rock-walls, ranging from 1300 to 2300 m a.s.l. (ANDREASSEN et al. 2008a). Smørstabbreen is the only ice cap in the area. The glacier area of Jotunheimen shows the most continental glaciological regime in Norway (ØSTREM et al. 1988) including a gradient with a relatively maritime regime in the West and a relatively continental East (MATTHEWS 2005). Since LIA maximum, the glaciers retreated more or less continuously until the 1980s. Cumulative glacier length variations of four regions in Norway, including Jotunheimen, have shown a rather slight but overall retreat from LIA maximum until the 1930s/40s (NESJE et al. 2008a; NESJE 2009). This retreat was shortly interrupted by a readvance around 1920, followed by a more rapid retreat (HOEL & WERENSKIOLD 1962; NESJE et al. 2008a; NESJE 2009). This retreat and also the retreat after 2000 were mainly caused by increased summer and annual temperature (NESJE 2009). Since then, the increase in volume of the maritime glaciers in Norway especially in the 1990s (MATTHEWS & BRIFFA 2005) until the end of the 20th century was also visible at the glaciers of Jotunheimen by a slightly positive net balance in the early 1990s (RASMUSSEN & CONWAY 2005; KJØLLMOEN 2009; NESJE 2009). Between 1981 and 2003, many of the larger glaciers in Jotunheimen experienced only small reductions in area. This advance was a response to higher winter precipitation in the first part of the 1990s (NESJE et al. 2008a). However, glaciers in eastern and southeastern Jotunheimen had a notable reduction (ANDREASSEN et al. 2008a). The total area reduction of this period was ~8% (RASMUSSEN et al. submitted). Since 2000, length and volume retreat continued again with a slight slow-down in 2008 (last year of observations) (KJØLLMOEN 2009).

Jostedalsbreen to the West of Jotunheimen (see Figure 2) is the largest ice mass on mainland Europe. This ice cap with several outlet glaciers consists in general of larger glaciers than Jotunheimen. Breheimen, between Jotunheimen and Jostedalsbreen, has, as Jotunheimen, mostly individual glaciers, but a smoother topography (ANDREASSEN et al. 2008a). Two ice caps and one glacier complex exist in this area, slightly smaller in size than the ice cap of Jotunheimen (ANDREASSEN et al. 2008a).

There are some high-altitude, often cirque-type, probably non-temperate glaciers in Jotunheimen with a glacier foreland surrounded by an ice-cored moraine, e.g. Gråsubreen (GRA) and Nautgardsbreane (ØSTREM 1964; WINKLER

2001). Glaciers with ice-cored moraines indicate a glacier type where the snout remains nearly in the same position for long times or where the variability of the front is restricted to a certain extent (ØSTREM 1964). Gråsubreen has a huge ice-cored moraine (see Figure 33) and might be polythermal (LIE et al. 2004) or possibly cold-based (personal comment N. Haakensen, 01/2007).

3.5 Other glacier regions used for comparison

Other glacier regions used for comparison with Jotunheimen are the European Alps, the Southern Alps of New Zealand (hereinafter referred to as 'New Zealand Alps'), and Baffin Island in the Canadian Arctic.

The European Alps are one of the most comprehensively analyzed mountain areas of the world (RÖTHLISBERGER 1986; ZEMP et al. 2008). They range according to CIPRA (2007) roughly between Grenoble (France) in the West, Vienna (Austria) in the East, Kempten (Germany) in the North and Lake Garda (Italy) in the South and have a curved shape. This huge area consists of several different climatic zones and lies in the Westerlies. Precipitation is higher in the external than in the internal areas because of orographic effects (ROTT et al. 1993). This results in a more humid area in the external northern Alps, dry inner-alpine regions, a maritime western and a continental eastern part, and a Mediterranean influenced region in the South (BÄTZING 2005).

In the European Alps, glacier advances during the 'Little Ice Age' occurred in the decades around 1320, 1600, 1700 and 1810 (GROVE 2001; GROVE 2004). Three maxima within the LIA, remarkably similar in extent, were identified around 1350, 1650 and 1850 in the Swiss Alps (MATTHEWS & BRIFFA 2005). Although a certain degree of spatial differentiation of the timing of the LIA maxima has to be mentioned for the European Alps, the general pattern of three roughly similar maxima is a good approximation. Reasons for these advances are lower temperatures, especially during winter and spring and for the last maximum also during summer, and higher precipitation, mainly during summer (RÖTHLISBERGER 1986; HOLZHAUSER et al. 2005). Retreat of the glaciers was initiated by lower precipitation (i.e. snowing) during summer and winter (RÖTHLISBERGER 1986; VINCENT et al. 2005; ZEMP et al. 2008). Since LIA maximum, the glaciers in the European Alps showed three phases of intermittent advance: in the 1890s, 1920s, and 1970 – 1980s (ZEMP et al. 2008). The area declined mainly after 1985, and the acceleration of the retreat was more pronounced in 1985 – 1999 compared to 1850 – 1973 (PAUL et al. 2004b, 2007).

The New Zealand Alps are situated along the West coast of the Southern Island of New Zealand (42.0° – 45.9° S, 167.3° – 173.8° E). The glaciers are located in three main areas: Rakaia and Rangitata region, Mt Cook and Mt Tasman region, and Mt Aspiring region (RÖTHLISBERGER 1986). New Zealand has a humid maritime climate with a strong gradient in precipitation (CHINN et al. 2005). The mean annual precipitation, evenly distributed over the whole year, is 3000 mm along the Western coastal plains, and rises to 15000 mm in the western part of the Southern Alps west of the Main divide (CHINN 2000). In the eastern ranges, precipitation is about 1000 mm/a. Many of the largest valley glaciers in New Zealand are debris-covered (RÖTHLISBERGER 1986) and exhibit proglacial lakes (CHINN et al. 2005). Probably, the debris-cover existed already during the last millennia because of the huge moraine walls still visible today (RÖTHLISBERGER 1986). The small seasonal amplitude of temperature and the heavy rainfall are favourable for the low minimum altitude of the snow line (RÖTHLISBERGER 1986). It is about 250 m lower on the western compared with the eastern side of the Main divide (RÖTHLISBERGER 1986).

In New Zealand, the range of dates of the dated LIA moraines reveals no clear regional pattern. The tentative conclusion relating this different timing to response times of the glaciers needed to be taken with certain care as methodological problems with the applied dating techniques might highly influence any interpretation (cf. RÖTHLISBERGER (1986); WINKLER (2004b); BURROWS (2005); SCHAEFER et al. (2009)). The earliest maximum related to the LIA was assumed to be about 1600 or even earlier. Later maxima or re-advances occurred between mid- to late 1700s, early to mid-1800s, and around 1900. A maximum advance at several glaciers in Mt Cook National park was dated ~1750 (WINKLER 2004b), comparable to Jotunheimen. It was followed by several re-advances, closely reaching the maximum or even overriding it (Tasman glacier) (WINKLER 2004b). However, during the decades from 1750 until 1900 and partly until 1930, most glaciers seem to have not varied much and kept quite close to their maximum positions (CHINN et al. 2005). After termination of the LIA, glaciers shrank in area and volume until the mid-1970s (CHINN et al. 2008). Comparable with South Norway, an advance started in the early 1980s until about 2000 (CHINN et al. 2005). This advance was recorded at the majority of the index glaciers throughout the New Zealand Alps (CHINN et al. 2005), but not at those large debris-covered valley glaciers with proglacial lakes (DYKES et al. submitted; WINKLER et al. submitted). The debris-covered glaciers with proglacial lakes have generally experienced massive mass loss during recent years (CHINN et al. 2008). Since mid-2005, the glacier tongues of Franz Josef and Fox glacier started again to advance (WINKLER 2009).

Jotunheimen, as well as the European and New Zealand Alps, have a high-alpine character with mostly individual glaciers of alpine morphology (HOEL & WERENSKIOLD 1962; ØSTREM et al. 1988; CHINN 2001; FITZSIMONS & VEIT 2001; LAWSON & FITZSIMONS 2001; ANDREASSEN et al. 2008a; ZEMP et al. 2008) and a climate gradient in continentality (AUNE 1993; FØRLAND 1993; MOEN 1999; SALINGER 2001; STURMAN 2001a, b; STURMAN & WANNER 2001; BÄTZING 2005). The European Alps and the New Zealand Alps represent whole mountain systems. Jotunheimen, however, represents one single mountain region within Norway. Therefore, the areal extent of the study areas and the number of glaciers differ remarkably. The European and the New Zealand Alps are at about the same latitude, only in opposite hemispheres. The area covered by both regions is roughly the same.

In Jotunheimen (~1750) and the European Alps (~1850), the term ‘maximum’ seems to describe more or less correctly the former circumstances, because no other glacier extent during LIA was larger than this one (ERIKSTAD & SOLLID 1986; MATTHEWS 2005; GROVE 2008; MATTHEWS & DRESSER 2008; NESJE et al. 2008a; NESJE 2009). In New Zealand, the LIA maximum showed a different pattern as indicated by the available dating: no clear regional maximum is identifiable yet, just a rather broad time span between 1600 (or earlier) and around 1900 (BURROWS 2005).

Baffin Island is the largest of the Arctic islands in north-eastern Canada in the Canadian Arctic (63° - 83° N, 62° - 90° W) with a rugged mountain region (TRENHAILE 2004). It has an area of about 500000 km² (DISCOVERY COMMUNICATIONS 2008), 37000 km² covered by ice (TRENHAILE 2004). Cumberland Peninsula is in the south-eastern part of Baffin Island, located on the Arctic Circle. There are many ice fields and alpine cirque and valley glaciers because of higher snowfall compared to the central and western parts (TRENHAILE 2004). Due to its topography and geographical position, it is peculiarly sensitive to climate changes (GROVE 1988). LIA maximum glacier extent at Baffin Island (about the 1920s (PAUL & KÄÄB 2005)) was detected by a trimline and moraine survey via remote sensing (PAUL & KÄÄB 2005; PAUL & SVOBODA 2009). Dating was done by lichenometry dependent on radiocarbon dating (GROVE 1988). The glaciers of Baffin Island in the Canadian Arctic are larger compared with the other regions mentioned above.

4 Glaciers and climate

The cryosphere consists of snow, river and lake ice, sea ice, glaciers, ice caps, ice shelves, ice sheets, and frozen ground (GROVE 1988; IPCC 2007). 10% of the land surface of the earth is covered permanently by ice, but mountain glaciers only contribute to a small amount (IPCC 2007). 1% of mainland Norway is covered by glaciers (ANDREASSEN et al. 2005). The existence of glaciers depends on climate, and their behaviour is in permanent interaction to changes in the climatic system.

4.1 Glaciers

Background on glacier formation, zones and types of glaciers, and reactions and responses to climate and climate changes are described in the following.

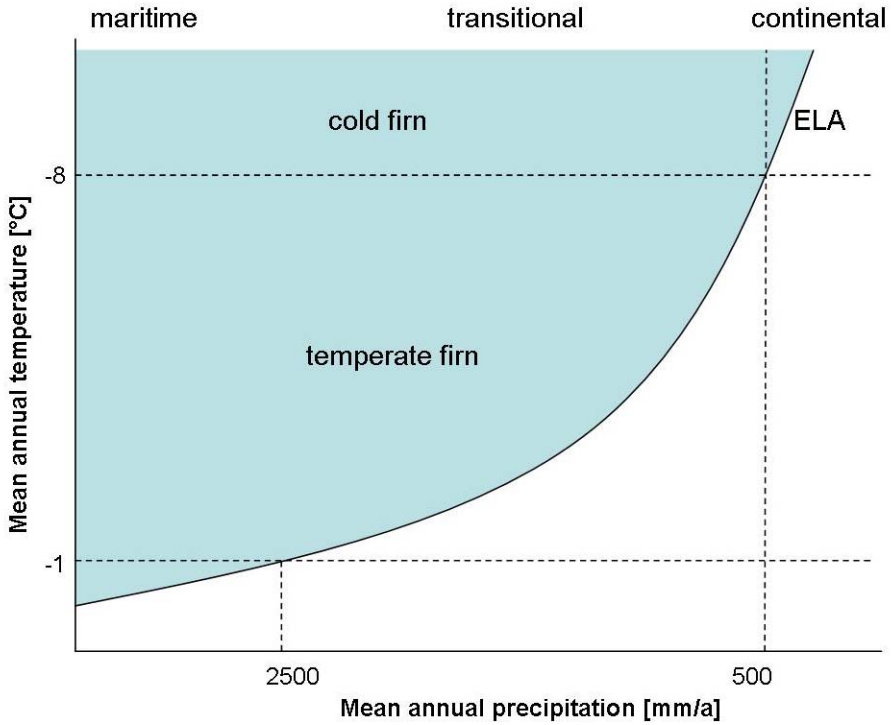

Figure 7: Schematic diagram of glacier limits as a function of mean annual temperature and mean annual precipitation. ELA = equilibrium line altitude (Figure modified after HAEBERLI et al. (1989)).

4.1.1 Formation of glaciers

In former glacier theory and as a simplified picture, the occurrence of glaciers is depending on mean annual temperature and mean annual precipitation (SHUMSKII 1964) (Figure 7). Glaciers can be formed where the (winter) accumula-

tion (i.e. snow) does not melt away totally during the warm (summer) period, for at least in most years. Topography of the mountains must be higher than the altitude of the equilibrium line, so that snow accumulation can occur. The climatic regime depends on the mean annual precipitation. High precipitation is related to a maritime climate regime, while low precipitation to a continental one.

Snow is needed for the formation of glacier ice and transformed by metamorphosis. The method and time of this transformation depend on the climatic regime and, therefore, temperature (PATERSON 1994). The density of snow can vary between 0.050 and 0.400 g/cm³.

Transformation of snow is caused by mechanical processes as wind erosion, pressure, compaction, condensation, and melting and refreezing (WINKLER 2009). Processes concerning melting enhance the transformation and appear only in temperate regions (PATERSON 1994). Old snow that survived one summer is called firn (WINKLER 2009). The transformation of firn to ice is much slower than the transformation from snow to firn and is mainly caused by further compression (PAUL 2007). Firn becomes glacier ice when the connection between the air bubbles is cut off. That occurs at a density of 0.830 g/cm³ (PATERSON 1994). Glacier ice has usually a density of 0.917 g/cm³, resulting from a further compression of the air bubbles (PATERSON 1994).

4.1.2 Zones and types of glaciers

Different zones on a glacier can be discerned. They depend on the occurrence of melting, percolation of water, temperature of ice, and ablation (PATERSON 1994). These zones are the dry-snow zone, the percolation zone, the wet-snow zone, and the superimposed ice zone in the accumulation area, followed by the ablation area. Their distribution on a glacier is shown in Figure 8. The dry snow zone occurs only where there is no melting (PATERSON 1994). The only dry-snow zones found are in the interiors of Greenland and Antarctica and near the summits of the highest mountains in Alaska, the Yukon, and possibly central Asia (PATERSON 1994; TRENHAILE 2004). Water of surface melting seeps down in the percolation zone and latent heat released on refreezing raises the temperature of the snow to the pressure melting point (TRENHAILE 2004). The wet-snow zone is entirely penetrated by melting to the base of the annual snow layer and is therefore at the pressure melting point (TRENHAILE 2004). The ice merges into a continuous mass in the superimposed-ice zone due to the large amount of refreezing meltwater (TRENHAILE 2004).

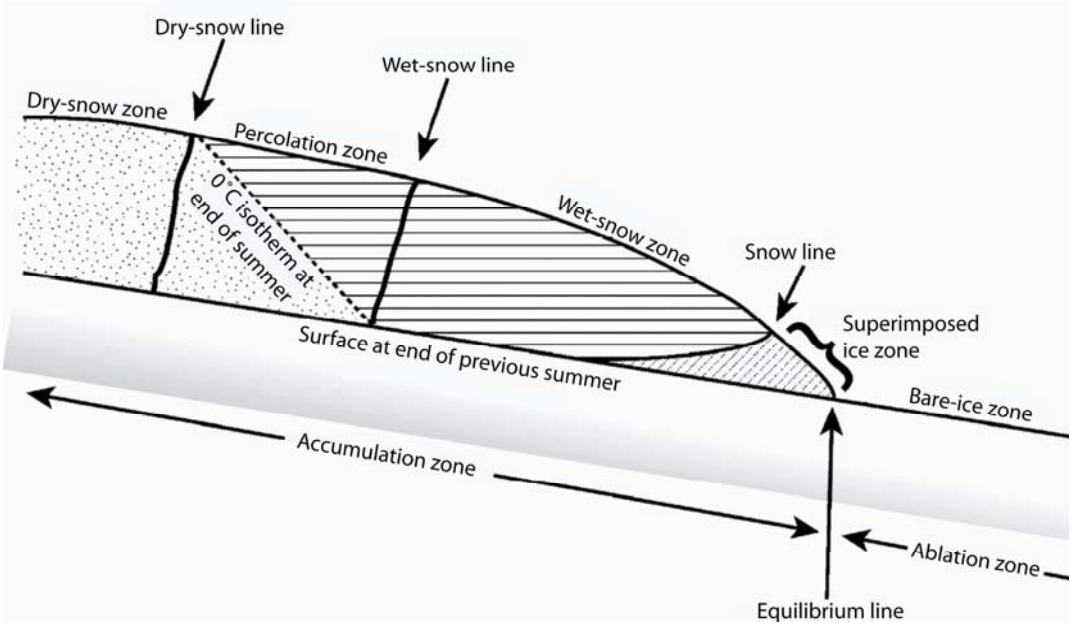

Figure 8: Glacier zones (Figure modified after PATERSON (1994)).

There exist three types of glaciers based on the temperature of the ice and therefore connected to altitude and climate. These types are temperate, cold-based, and polythermal glaciers. The temperature of temperate glaciers' ice is close to the local melting point throughout the whole glacier, except for the surface layer, which is colder for parts of the year (PATERSON 1994). No dry-snow and percolation zones exist on temperate glaciers because those zones are by definition colder than 0°C, at least partly (PATERSON 1994). The equilibrium and snow line coincide and, therefore, no superimposed ice zone exists. Thus, on a temperate glacier, there are only wet-snow and ablation zones (PATERSON 1994). A cold-based glaciers' ice is below the local melting point (BLATTER & HUTTER 1991). The dry-snow zone occurs there, because it only exists in glacier ice colder than the local melting point. Polythermal glaciers have both, a temperate and a cold ice zone. The distribution of these zones can differ widely and depends on heating by surface melt, by strain and/or geothermal heat, and advection and conduction (D. Benn, personal communication, 03/2009).

4.1.3 Glacier fluctuations and climate

Glaciers react in a complex way to changes of climate factors. Temperature and precipitation are the leading climate forces influencing glacier behaviour (see Figure 7). Topography dominates the local climate and, therefore, distribution and pattern of temperature and precipitation. Temperature and precipitation control mass balance to a high degree and, therefore, also advance or retreat of the glacier tongue (Figure 9).

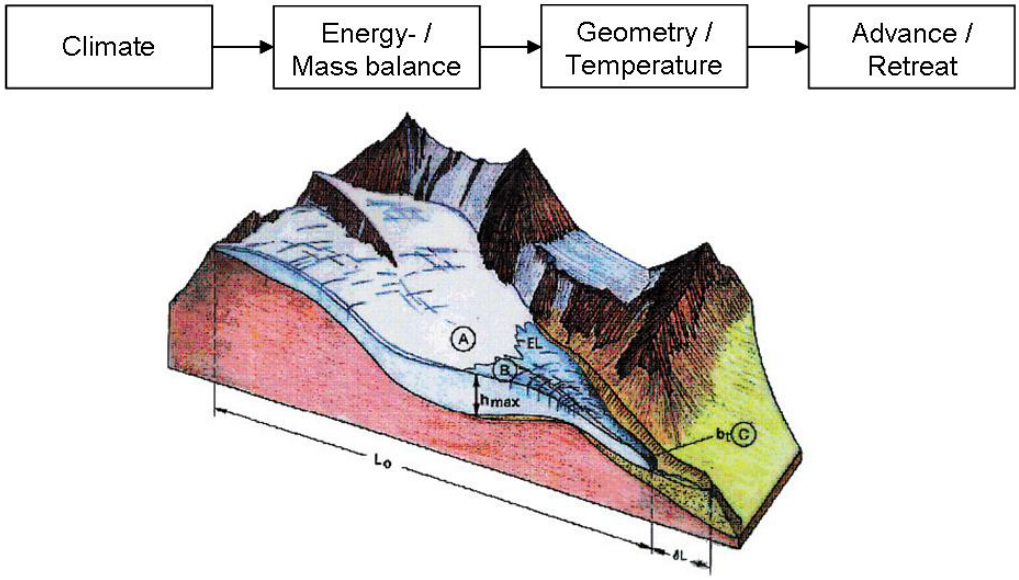

Figure 9: Simple scheme of a mountain glacier and reaction to climate. (A) = accumulation area, (B) = ablation area, (C) = glacier terminus, EL = equilibrium line, h_{max} = maximum glacier thickness, b_t = ablation at the glacier tongue, L_0 = glacier length, δL = length change (Figure after HAEBERLI et al. (1989)).

Mass balance is the direct and underlying signal to climate forcing (NESJE 2009), change in glacier length the result of the mass balance (WINKLER et al. submitted). It is, therefore, delayed and smoothed, but can also function as an enhanced signal (HAEBERLI 1995). In the glacier areas outside of the Tropics, the monsoonal areas, and polar regions (WINKLER et al. submitted), accumulation mostly takes place during winter by snowing and to a lower amount by avalanches, wind drift (PATERSON 1994), resublimation, and condensation (KASER et al. 2003). Melting followed by run-off is the dominant factor during the summer season for ablation (PATERSON 1994). On high altitudes and low latitudes, sublimation also plays an important role (FRANCOU et al. 2003; KASER et al. 2003). Other factors of ablation are wind deflation, avalanching from the front, calving, and evaporation (NESJE et al. 2000). Therefore, winter precipitation and summer temperature are the driving climate factors. Summer melting takes place mostly at the lower parts of the glacier and results in a mass surplus of the higher area. The glacier ice is moving down the glacier due to gravity by plastic deformation, basal sliding, and deformation of the glacier bed (PATERSON 1994). This process goes on until the glacier reaches a steady-state position, i.e. that the net mass balance over the entire glacier equals zero. If a glacier is not in steady-state the glacier tongue must advance (e.g. after several years of positive mass balance) or retreat (e.g. after several years of negative mass balance) during a certain time, called response time (t_{resp}) to reach a new steady-state (HOELZLE 1994). The response time depends mainly on the climatic regime, i.e. climate sensitivity as e.g. seen in the mass balance gradient, and glacier geometry, e.g. mean slope

and glacier length (JÒHANNESSON et al. 1989a). The concept of glaciers in steady-state is a more theoretical one for explaining glacier mechanisms and behaviour and for calculations but not for observations in the field (JÒHANNESSON et al. 1989a).

At the end of the ablation period, the snow covered area in the higher parts is called accumulation area, the snow-free area in the lower part ablation area. The line of equal annual accumulation and ablation between these two areas is called equilibrium line altitude (ELA) (see Figure 9).

4.1.4 Differentiation of glacier response to climate

The influence of temperature and precipitation is different in the individual climatic regimes and during the seasons of the year. Principal climatic variables controlling mass balance processes are winter precipitation as well as winter temperature mainly for accumulation and summer temperature mainly for ablation (RASMUSSEN & CONWAY 2005). In maritime climates, winter precipitation has more influence on the net mass balance than summer temperatures (NESJE et al. 2000; RASMUSSEN & ANDREASSEN 2005; RASMUSSEN et al. 2007; WINKLER 2009; WINKLER et al. 2009). Winter precipitation and temperature are positively correlated in South Norway, so greater precipitation occurs with increasing temperature, but only on average over a large number of glaciers, not in every individual case (L.A. Rasmussen, personal communication, 12/2009). An increase in winter temperature causes mild winters with a high amount of precipitation (RASMUSSEN & CONWAY 2005; WINKLER in print). Until today, this results in a positive net mass balance by enhanced snowing (RASMUSSEN & CONWAY 2005; WINKLER in print), but winter warming can also cause more of the precipitation to fall as rain instead of snow (L.A. Rasmussen, personal communication, 12/2009). However, an increase in summer temperature enhances ablation, but does not compensate accumulation due to high winter precipitation at maritime glaciers in South Norway (WINKLER & HAAKENSEN 1999). Net mass balance in continental climates is rather dominated by summer temperature than by winter precipitation, seen by a higher correlation of summer balance with net balance than of winter balance with net balance (NESJE et al. 2000; RASMUSSEN & ANDREASSEN 2005; RASMUSSEN et al. 2007; NESJE et al. 2008a; WINKLER 2009). The negative effect on mass balance caused by lower winter precipitation is exceeded by the effect of higher spring and summer temperatures (NESJE & DAHL 2003; STEINER et al. 2008). Storbreen shows a remarkably higher correlation coefficient between net and winter balance compared to a lower value for Hellstugu- and Gråsubreen (Figure 10) (NESJE et al. 2000; MATTHEWS & BRIFFA 2005; RASMUSSEN & ANDREASSEN 2005; WINKLER in print). The two last mentioned

glaciers exhibit a very high correlation coefficient between net and summer balance.

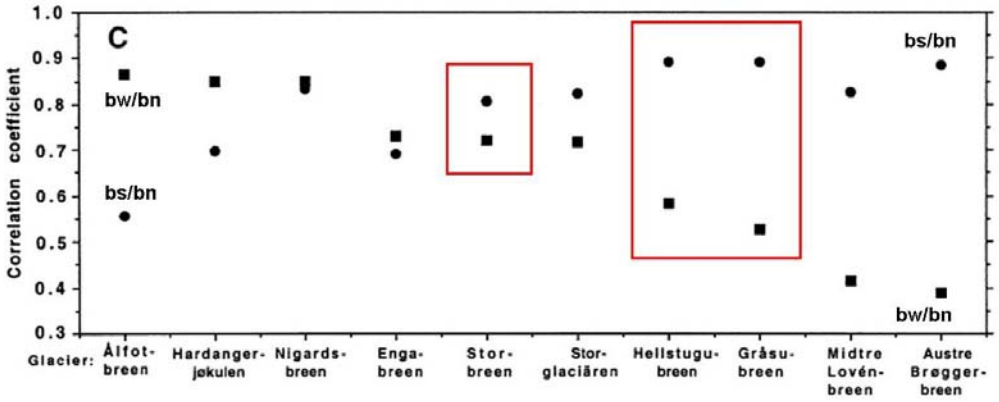

Figure 10: Correlation of winter and summer balance (bw and bs, respectively) with net balance (bn) at Scandinavian (including Svalbard) glaciers (raw data: Kjøllmoen, 2005) (Figure modified after NESJE et al. (2008a)).

In recent times, not only glacier retreat caused by negative mass balances was recognised, but also a down-wasting process at the glacier tongue (e.g. HAEBERLI (2004); PAUL et al. (2004b); ZEMP et al. (2008); WINKLER & NESJE (2009); WINKLER in print). Down-wasting occurs due to high summer temperatures. Especially at maritime glaciers, glacier tongues react without any response time, and glacier length changes are decoupled from mass balance (WINKLER & NESJE 2009).

4.2 Circulation indices

The climate of Jotunheimen and of all of Norway is characterized by predominating westerly airflow and zonal circulation patterns. The circulation index of the NAO as well as of the Northern Annular Mode (NAM; previously called Arctic Oscillation, AO (IPCC 2007)) are good measures of the strength of zonal air flow in Northwest Europe (HURRELL 1995; NESJE et al. 2000; BENISTON 2005; LINDERHOLM et al. 2007; WANNER et al. 2008; WINKLER & NESJE 2009).

The NAO index is the difference in sea level pressure (SLP) between Iceland and the Azores (IPCC 2001). When the index is high, i.e. SLP increases from north to south, the air flow is strongly westerly (IPCC 2001). The time scale of the pressure difference fluctuates between days and decades (IPCC 2001). The NAO has the strongest signature in the winter months – December to March – and is the dominant mode of winter climate variability in the North Atlantic region, e.g. in Europe (IPCC 2001; NESJE 2009).

The NAM is a winter fluctuation characterized by low surface pressure in the Arctic and strong mid-latitude westerlies (IPCC 2007). It is the leading annular mode of climate variability in the Northern Hemisphere and its pattern has a large correlation with the NAO (RASMUSSEN & CONWAY 2005; FEALY & SWEENEY 2007). Therefore, NAM and NAO are often taken together into one index (IPCC 2007). Both, the NAO and the NAM modulate the transport and convergence of atmospheric moisture and the distribution of evaporation and precipitation (IPCC 2007). RASMUSSEN & CONWAY (2005) made a correlation between the October until May NAM and NAO results with modelled winter and net balances (bw and bn, respectively). These correlations were over 1949 – 1999 for STO and over 1962 – 1999 for HEL and GRA. The correlation between the balance values and NAM was better for STO and HEL than between the balance values and NAO. For GRA, it was the other way round. Correlation with the summer balance (bs) is negligible. Generally, the correlation is stronger for western than for eastern glaciers in Norway (RASMUSSEN et al. 2007).

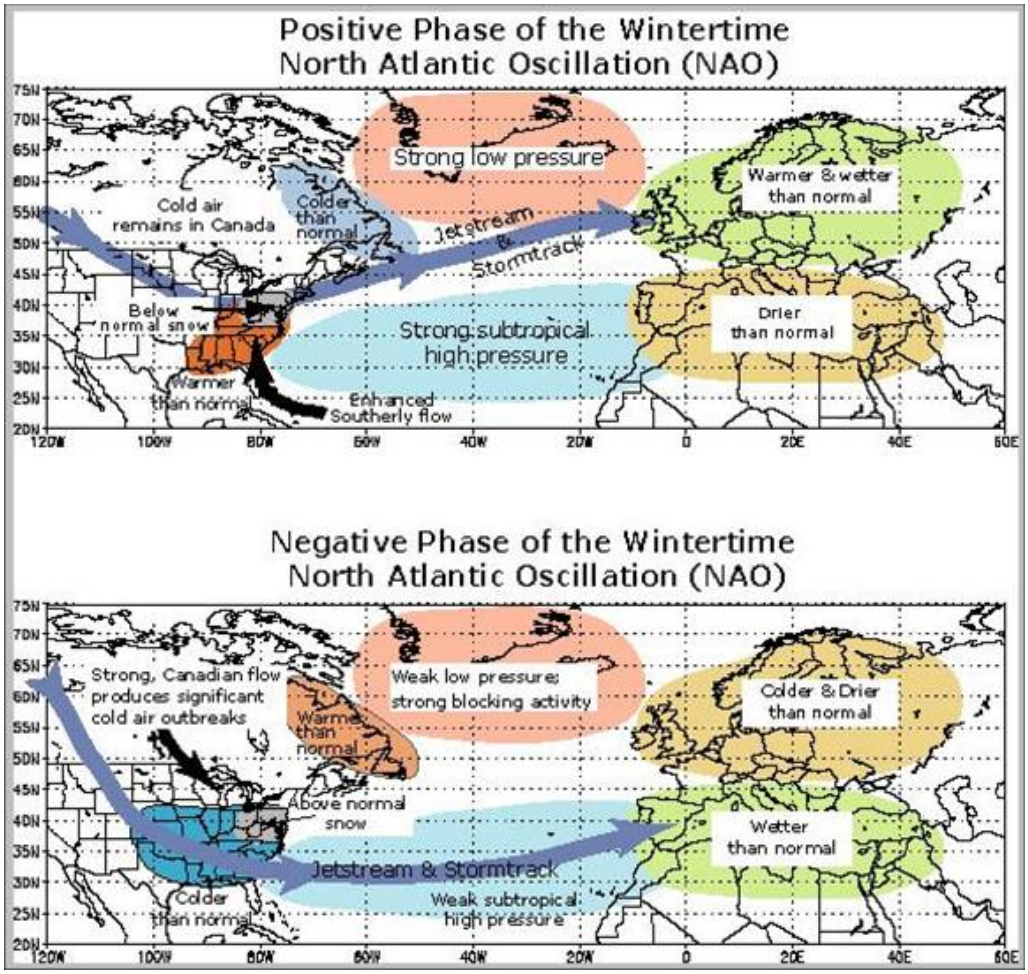

Figure 11: Variations of the North Atlantic Oscillation (NAO) during winter (Figure after NCDC (2008)).

The variability of the NAO is expressed by the NAO index (see Figure 6). A positive index is associated with a north-eastward shift in the Atlantic storm activity (Figure 11) (IPCC 2007). It means enhanced westerly flow across the North Atlantic in the winter months with warm and moist maritime air over much of Europe, bringing wet conditions to northern Europe and dry conditions to southern Europe, i.e. more precipitation than normal falls over Scandinavia and less over central and southern Europe (HURRELL 1995; NESJE & DAHL 2003; FEALY & SWEENEY 2007; IPCC 2007).

In New Zealand, the Southern Oscillation Index (SOI) and Pacific Decadal Oscillation can be applied for the same purpose as the mentioned circulation patterns and indices in Europe (STURMAN & WANNER 2001; WINKLER 2004b; CHINN et al. 2005). The conditions in the European and New Zealand Alps are comparable.

A negative SOI means a strengthened westerly circulation in summer, a southerly circulation in winter and south-westerly circulation in autumn and spring with lower than normal temperature for New Zealand (FITZHARRIS et al. 1997; CHINN et al. 2005). In advance phases, the SOI is negative, especially during the accumulation season (FITZHARRIS et al. 1997). A change from retreat to advance is associated with a westward shift of the positive sea level pressure anomalies and, therefore, cool sea surface anomalies near New Zealand (FITZHARRIS et al. 1997; CHINN et al. 2005). El Niño events are anomalies in sea surface temperature and correlated to a negative SOI. Many El Niño events are concurrent with a positive mass balance (FITZHARRIS et al. 1997).

TONIAZZO & SCAIFE (2006) postulate a connection between the El Niño/Southern Oscillation (ENSO) and NAO. Moderate and strong ENSO events influence the NAO. A teleconnection between NAO and SO was also found by ROGERS (1984).

4.3 Glacier monitoring

The importance of glacier monitoring and the relation between glaciers and climate has been widely accepted for several years (e.g. IPCC (2001)). A global terrestrial network for glaciers (GTN-G) was established in recent years within the framework of the global terrestrial and climate-related observing systems (GTOS/GCOS) (Figure 12) (HAEBERLI et al. 2002).

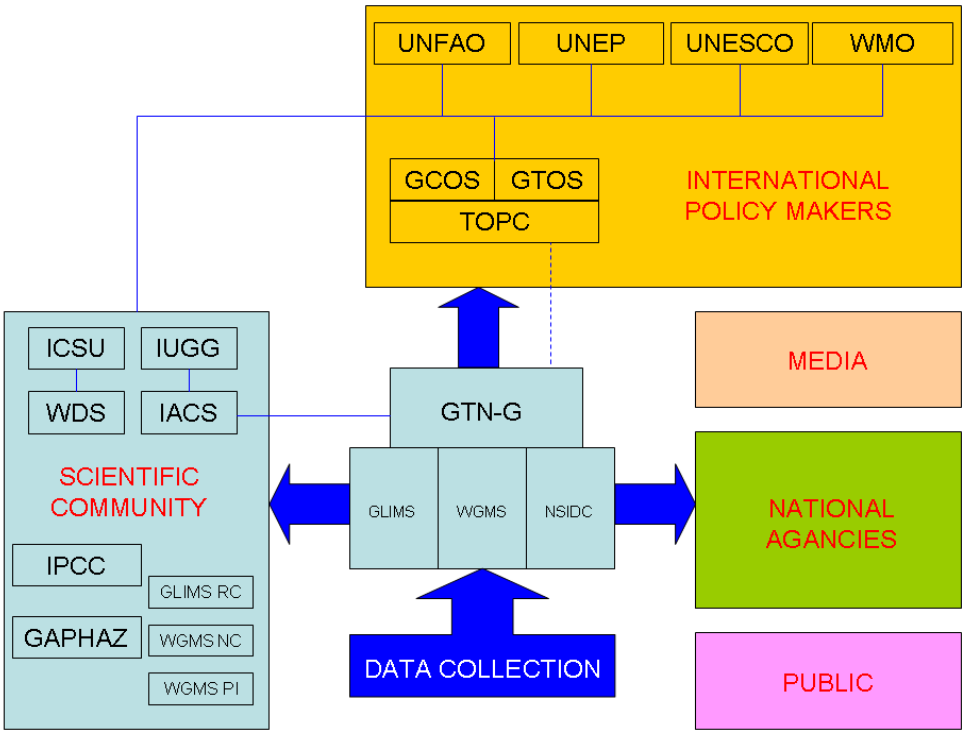

Figure 12: Organigram of GTN-G. Abbreviations important for this study are listed in the text and in the abbreviation list (Figure modified after GÄRTNER-ROER et al. (2009)).

Following a global hierarchical observing strategy (GHOST), five tiers were established to organize global and regional analyses of glacier changes, especially for detection of long-term climate changes (HAEBERLI 2004). The network is operated by the world glacier monitoring service (WGMS) (HAEBERLI et al. 2002). The global land ice measurements from space (GLIMS) were established to map and monitor a global glacier inventory from optical satellite instruments, e.g. ASTER (GLIMS 2009a). The project contributes e.g. to GCOS and collaborates e.g. with WGMS (GLIMS 2009b). Within GTN-G, the use of satellite data is recommended for compilation of glacier inventory data (PAUL 2009).

4.3.1 Glacier monitoring methods

Glacier monitoring can be done by ground, air, and space on a regional scale, e.g. by analyzing satellite images or vertical aerial photos, or on single glaciers. Analysis of remote sensing products or from topographical maps results in detection of the glacier outlines and, hence, glacier area (PAUL 2009). Combined with a digital elevation/terrain model (DEM/DTM), further glacier inventory data can be established, e.g. minimum and maximum elevation (PAUL 2009).

Glacier monitoring by field-work is mostly used for measuring mass balance and glacier length changes. Measurements of the glacier length changes are easier to make than mass balance measurements. The distance between glacier

terminus and a fixed mark, e.g. a big rock, is measured. This repeated measurement should at best be parallel to the glacier flowline and normal to the glacier perimeter (ANDREASSEN et al. 2005). Timing of the measurements is at the end of the ablation season (ANDREASSEN et al. 2005).

KASER et al. (2003) describe different methods of mass balance measurements. The most correct method, the glaciological method, uses in-situ measurements, but is most time and money consuming (ØSTREM & BRUGMAN 1991; WINKLER et al. submitted). Stakes, distributed over the whole glacier, are drilled into the glacier surface at the end of the accumulation season. Snow pits are dug to measure the snow density and the height of snow related to a reference surface, e.g. to the previous summer's layer. At the end of the ablation season, when snow and ice have melted away at most, the stakes are no longer covered completely. By measuring the visible stake length, the volume of melted snow and ice can be calculated. To calculate the mass change, the measured snow and ice (constant value) densities have to be used. This gives the mass balance data at one point. To obtain the mass balance over the whole glacier surface, these single values have to be extrapolated. Another very common method is the geodetic method. A change in elevation of the glacier surface is calculated by subtracting the glacier elevations of the glacier extent at two different times. This gives the volume change for this period. To convert this value into a mass change, densities of snow and ice have to be known. Some other methods still exist for calculating mass change, e.g. the hydrological method or index methods. Best measuring results are achieved by a combination of the glaciological and the geodetic method (WINKLER et al. submitted).

4.3.2 Glacier monitoring in Norway

The first reports about glaciers in Norway date from the mid-17th century. The occasions for these reports were damage or complete destruction of farms and farm land by glacier advances or other natural catastrophes caused by glaciers (HOEL & WERENSKIOLD 1962). Glacier monitoring was, therefore, not the reason for documentation but e.g. reporting of damages. Hence, these reports only exist from the populated western coast of Norway and not from remote areas as e.g. Jotunheimen.

In Jotunheimen, the first documents of glaciers do not exist as early and detailed as in other Norwegian areas. In contrast to Jostedalsbreen, there are no historical documents or images of the glacier area that would allow a distinct timing of the LIA maximum. ØYEN (1893) and HOEL & WERENSKIOLD (1962) report only a vague eyewitness story about the maximum extent of Storbreen. The precise date is not known and therefore gives no evidence about the distinct

timing of LIA maximum. The first historical photo-record exists from around 1900 (ØSTREM & HAAKENSEN 1993). First measurements on glaciers in Norway started at the beginning of the 20th century (ØSTREM & HAAKENSEN 1993).

Glacier length changes were measured at Jostedalsbreen, Folgefonna, Okstindane, Svartisen, Skjomen and Jotunheimen since about 1900 (HOEL & WERENSKIOLD 1962; ANDREASSEN et al. 2005). Until today, eleven glaciers have a relatively continuous length change record since then (ANDREASSEN et al. 2005). In 2008, glacier length changes were measured on 32 glaciers in Norway including five in Jotunheimen (KJØLLMOEN 2009). In total, length changes have been measured on 58 glaciers in Norway (ANDREASSEN et al. 2005).

First mass balance measurements took place in 1949 on Storbreen in Jotunheimen (LIESTØL 1967) and last until today. This record is one of the longest mass balance series of the world (NESJE et al. 2008a; NESJE 2009). In the 1960s, NVE started a mass balance program on several glaciers in Norway (ANDREASSEN et al. 2005). In 2008, mass balance was measured on 14 glaciers in Norway and in the whole period on 42 glaciers in Norway including seven in Jotunheimen (KJØLLMOEN 2009). The current glaciers with mass balance measurements in Jotunheimen are STO, HEL, and GRA (KJØLLMOEN 2009), all measured by the glaciological method.

4.4 Holocene glacier chronology and 'Little Ice Age' in Jotunheimen

The LIA is only one of several phases of glacier advances during the Holocene (GROVE 1988; MATTHEWS & BRIFFA 2005; GROVE 2008; MATTHEWS & DRESSER 2008). These advances are also called neoglacial events (MATTHEWS & DRESSER 2008), 'Little Ice Age'-type events (WANNER et al. 2000; MATTHEWS & BRIFFA 2005) or neoglaciations (ANIYA 1995). Causes of these events are solar irradiance, volcanic eruptions, and, during the earliest period in the Northern Hemisphere, freshwater outbursts into the North Atlantic and Arctic Ocean (GROVE 2008; MATTHEWS & DRESSER 2008; NESJE 2009). The causes of regional patterns are differences in glacier size and geometry, topography, and atmospheric circulation patterns (NESJE & DAHL 2003; RASMUSSEN et al. 2007; MATTHEWS & DRESSER 2008).

On a global scale, the best and most historical sources of as well as number of research on Holocene glaciers are found in Europe (GROVE 1988; MATTHEWS & DRESSER 2008). The most detailed records are related to the European Alps and

Scandinavia (MATTHEWS & DRESSER 2008). Methods used for Holocene research are moraine stratigraphy, dendrology, and glaciolacustrine and glaciofluvial approaches (e.g. SHAKESBY et al. (2007); MATTHEWS & DRESSER (2008)). Investigations on LIA glaciers are done by e.g. analysis of historical documents, lichenometry, Schmidt-Hammer measurements, dendrology, radiocarbon dating (^{14}C), analysis of isotopes, and remote sensing (e.g. MATTHEWS (1977, 1991, 2005); ERIKSTAD & SOLLID (1986); RÖTHLISBERGER (1986); GROVE (1988); WINKLER (2002, 2004b); PAUL (2007); NESJE et al. (2008b); BAUMANN et al. (2009); SVOBODA & PAUL (2009)). In Scandinavia, the most detailed and reliable data on LIA glaciation is given for Jostedalsbreen (NESJE et al. 2008b; BAUMANN et al. 2009).

4.4.1 Holocene glacier chronology

The glacier history of Norwegian glaciers during the Holocene has been observed for several decades. An overview of these studies is given in NESJE et al. (2008a) and NESJE (2009) for both maritime and continental glaciers. Studies on Holocene glacier variations in Jotunheimen have been made by KARLÉN & MATTHEWS (1992, 2005), MATTHEWS & KARLEN (1992), MATTHEWS et al. (2000), LIE et al. (2004). In Jotunheimen, as well as in all of Norway, the outlet glaciers from the Scandinavian ice sheet retreated in the early part of the Holocene (NESJE et al. 2008b). In western and central Jotunheimen, as well as in other areas, this retreat was followed by a glacier advance during the Finse Event at about 8200 cal. BP (MATTHEWS et al. 2000; MATTHEWS & DRESSER 2008; NESJE 2009). At a present high-altitude polythermal glacier in eastern Norway, an advance at this time was not visible, but later at about 7500 cal. BP (LIE et al. 2004) as well as in central Jotunheimen (MATTHEWS et al. 2005). After the Finse event, all studied glaciers in Jotunheimen as well as in all of Norway disappeared completely, approximately between 6600 and 6000 cal. BP in Jotunheimen (NESJE et al. 2008a; NESJE 2009). Four periods of glacier expansion followed this disappearance in central Jotunheimen: a first event between 4800 and 3900 cal. BP, a second event between about 3200 and 2550 cal. BP, a third event between 2350 and 1700 cal. BP, and a fourth event between 1400 and 750 cal. BP (MATTHEWS et al. 2000, 2005; MATTHEWS & DRESSER 2008), partly also visible in western Jotunheimen (NESJE 2009). At the high-altitude glacier in East Jotunheimen, glacier size increased also after the disappearance, but at about 3800 cal. BP, the glacier reached similar size as today (LIE et al. 2004). During the Mediaeval Warm Period, the glaciers in Jotunheimen retreated again before advancing during the 'Little Ice Age' as the most extensive Neoglacial maximum (GROVE 1988; MATTHEWS 1991; MATTHEWS et al. 2000; GROVE 2004).

4.4.2 'Little Ice Age'

The period between mid-14th century until the beginning of the 20th century is called 'Little Ice Age' (GROVE 1988; MATTHEWS & BRIFFA 2005). Discussions about the term 'Little Ice Age' occurred for several reasons. First, the term is misleading concerning the described circumstances (GROVE 1988; WINKLER 2002). Second, the first definition of the term referred to earlier periods during the Holocene (GROVE 1988; WINKLER 2002; MATTHEWS & BRIFFA 2005). Third, it is to its use in glaciology as well as in climatology dependent on different definitions and time intervals, respectively (GROVE 1988; WINKLER 2004a; MATTHEWS & BRIFFA 2005; NESJE et al. 2008b). In this study, the term is used according to the time interval defined above.

Lower temperatures during the LIA occurred over most if not all of the globe (GROVE 1988). The mean value of temperature rise for land areas in the Northern Hemisphere between 1850 and 2005 was 0.98 ± 0.23 °C compared with 1961 – 1990 and was 0.65 ± 0.19 °C globally (IPCC 2007). The temperature depression in mountain regions was about 1 or 2 °C during LIA compared with the 20th century mean (GROVE 2008). A temperature depression of 0.5 – 1°C was indicated by the ELA depression at Jostedalsbreen since LIA until today [1991] (NESJE et al. 1991). RASMUSSEN et al. (submitted) assumed a temperature difference during LIA and today [2003] of 0.5 °C for Jotunheimen. Mountain areas were and are more affected by changes of climate factors, e.g. air temperature, and exhibit(ed) higher changes compared to the global mean (WINKLER et al. submitted). Without any increase in precipitation, the temperature anomaly would be about -1.1 °C in Jotunheimen to cause the glacier advances to the LIA maximum extent, but proxy data indicate a temperature anomaly of about half this value (RASMUSSEN et al. submitted). Higher positive glacier net balances during LIA were therefore not only caused by lower temperatures but also by regional higher precipitation (GROVE 1988; GROVE 2001; NESJE & DAHL 2003; HOLZHAUSER et al. 2005; MATTHEWS & BRIFFA 2005; NESJE et al. 2008a; STEINER et al. 2008; RASMUSSEN et al. submitted). Precipitation was about 20 – 28% larger during LIA than today [2003] (RASMUSSEN et al. submitted).

Despite the global distribution of the LIA phenomenon, culminations, advances, and maxima of the glaciers did not show a uniform global pattern (GROVE 1988; WINKLER 2004a; GROVE 2008; MATTHEWS & DRESSER 2008; NESJE 2009).

In previous studies, the timing of the LIA maximum in Jotunheimen was dated mainly by lichenometry (MATTHEWS 1974, 2005; ERIKSTAD & SOLLID 1986;

WINKLER 2001, 2002). Therefore, the reconstructions of glacial chronology in Jotunheimen prior to the first scientific measurements and historical photographs are based mainly on this technique (e.g. MATTHEWS (1974, 1975, 1977, 2005); INNES (1985); ERIKSTAD & SOLLID (1986); WINKLER (2001); NESJE (2009)). These studies have a comparably high temporal resolution and relatively reliable results due to good ecological-methodological conditions in the area (MATTHEWS 2005). The accuracy of lichenometry in dating the LIA maximum in this region is assumed to be within ± 20 years for the more recent, sophisticated studies using regional lichen growth curves (e.g. MATTHEWS (2005)). As moraines formed during LIA maximum have not been overridden by any subsequent advance, they can be used for the reconstruction of LIA maximum glacier outlines.

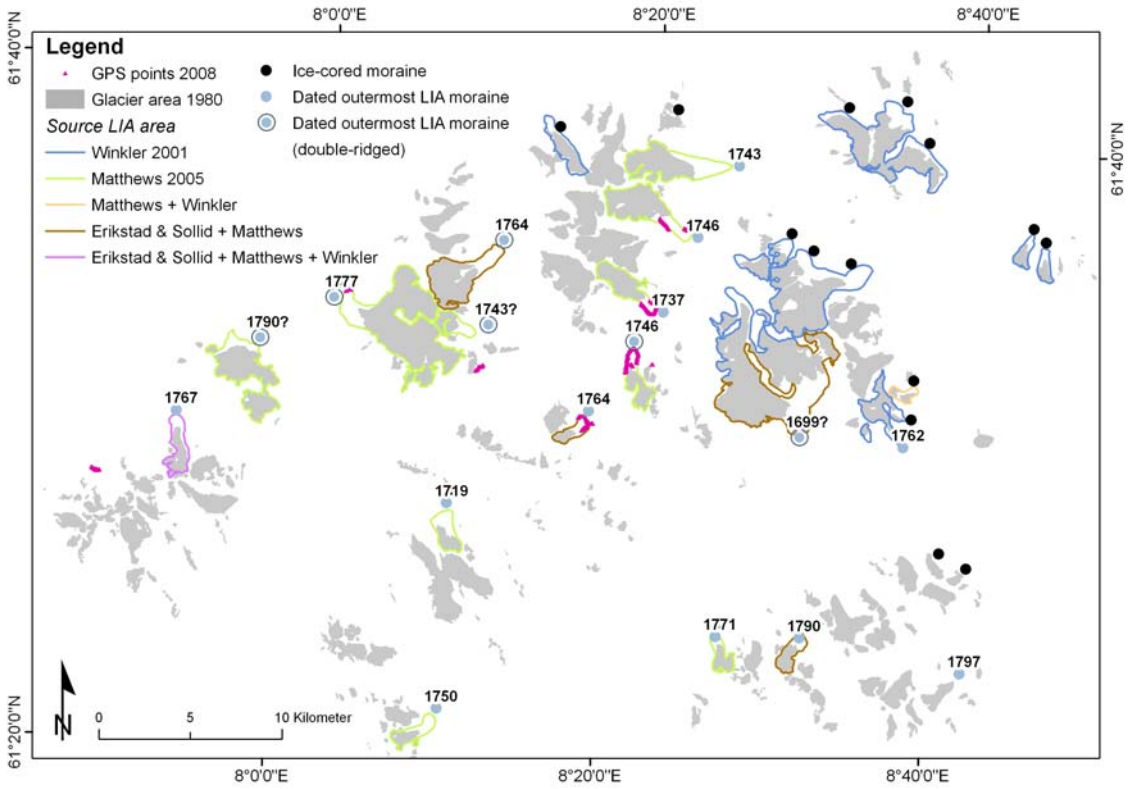

Figure 13: Available LIA glacier outlines from the geomorphological maps, divided after source, and GPS points of moraine walls measured 2008. Moraine type and timing of LIA maximum are marked. Glacier areas in the 1980s are shown in grey (Glacier outline 1980s: Statens Kartverk N50; LIA maximum outlines and timing: ERIKSTAD & SOLLID 1986; WINKLER 2001; MATTHEWS 2005).

The existing lichenometric analyses for Jotunheimen allow a general statement about the LIA maximum patterns in this region. The timing of the culmination of the LIA falls roughly between 1750 and 1800 (WINKLER 2002; NESJE & DAHL 2003; MATTHEWS 2005). In West and Central Jotunheimen, the outermost moraines of the LIA maximum mainly date from around 1750, whereas in East Jotunheimen, the related moraines are a few decades younger, i.e. date from

around 1780/1800 (Figure 13) (WINKLER 2002; MATTHEWS 2005; BAUMANN et al. 2009). Differences in timing of LIA maximum between individual glaciers or glacier regions may be explained by differences in glacier hypsometry, frontal lag times, and responses to winter precipitation and summer temperature (NESJE 2009).

Several glaciers, especially in West and Central Jotunheimen (e.g. Stor-, Visbreen) have formed so-called 'doubled' terminal moraines, i.e. the outermost position of the glacier during the 'Little Ice Age' is represented by a double-ridged moraine. At the glaciers with such a phenomenon, the outer ridge dates from the mid-, and the inner ridge from the late 18th century (WINKLER 2001). Terminal moraines with double ridged outermost moraine walls are found only in West and central Jotunheimen (see Figure 13) (WINKLER 2001, 2002, 2004a; BAUMANN et al. 2009). As far as known, double-ridged terminal moraines do not occur in East Jotunheimen (WINKLER 2001). A small number of ice-cored moraines, mainly in front of small high-lying cirque glaciers, can be found, most of them in eastern Jotunheimen (ØSTREM 1964; ØSTREM et al. 1988).

This spatial pattern and its glaciochronological interpretation was connected to a West-East gradient of the glaciological regime in Jotunheimen by WINKLER (2002), i.e. with a decline of the maritime influence eastwards within the mountainous region. The maximum around 1750 in West and Central Jotunheimen has therefore been interpreted as parallel to the maximum of the western outlet glaciers of Jostedalsbreen (GROVE 1988; KARLÉN & MATTHEWS 1992; NESJE & DAHL 1993, 2003; NESJE 2005; NESJE et al. 2008a, b). Analogously, the climatic causes are assumed mainly to have been in highly increased winter precipitation (NESJE & DAHL 2003; NESJE et al. 2008a; DE JONG et al. 2009; NESJE 2009). Climate reconstructions have shown that the second half of the 18th century was dominated by below-average summer temperatures (WINKLER 2001; NORDLI et al. 2005). The reduction in temperature slowed down the glacier retreat of Jostedalsbreen since LIA maximum (BICKERTON & MATTHEWS 1993). It had not enough impact to initiate a new maximum because of low winter precipitation (BICKERTON & MATTHEWS 1993). In Jotunheimen, especially at the most continental glaciers to the East, these climatic conditions were favourable for glacier growth (WINKLER 2002). The related advance culminated around 1800 in East Jotunheimen and overrode all earlier LIA moraines (WINKLER 2002). In the western and central part of Jotunheimen, glaciers advanced parallel to and near to the previous 1750 maximum position (WINKLER 2002). They did not override and destroy the existing outermost terminal moraines and, hence, formed the

double-ridged terminal moraines (ERIKSTAD & SOLLID 1986; WINKLER 2002; MATTHEWS & DRESSER 2008).

Even if the extent of Jotunheimen glaciers at 1750 and 1800 is only slightly different, the existing differences in the detailed timing of LIA maximum and its regional pattern have to be pointed out. Especially concerning the search of climatic causes of LIA and spatial differentiation of glacial behaviour, this information has to be kept in mind. In this study a uniform LIA maximum at 1750 was taken to be the basis of comparison.

5 Methodology

Remote sensing techniques play an important role in acquisition of the data. Methods of mapping glacier inventory and inventory data of LIA maximum are described in the following. For analyzing the inventory data of the three regions, a simple parameterization scheme developed by HAEBERLI & HOELZLE (1995) is used.

5.1 Remote sensing

The number of satellites in space increased since the first satellite Sputnik by the former Soviet Union was launched in 1957 (GARBER 2007). In 2007, there have been about 3000 satellites in the orbit (OBERRIGHT 2004).

5.1.1 Spaceborne data

The satellite type used for Jotunheimen in this study is Landsat 5 Thematic Mapper (TM) and for Nigardsbreen Landsat 7 Enhanced Thematic Mapper Plus (ETM+). The first Landsat (Landsat 1) was launched 1972, Landsat 5 in 1984, and the latest one (Landsat 7) in 1999 (U.S. DEPARTMENT OF THE INTERIOR 2009b). Landsat 5 has a circular, sun-synchronous, near-polar orbit at an altitude of 705 km (U.S. DEPARTMENT OF THE INTERIOR 2009a). The repeat cycle is 16 days, image size 170 km x 185 km (U.S. DEPARTMENT OF THE INTERIOR 2009a). The TM has seven bands from visible to mid-infrared, and a thermal one (Table 1).

Table 1: Spectral bandwidths of reflective and thermal bands of Landsat TM 5 (data from U.S. DEPARTMENT OF THE INTERIOR (2009a)).

TM Band	Spectral bandwidths [µm]
1 (blue)	0.45 – 0.52
2 (green)	0.52 – 0.60
3 (red)	0.63 – 0.69
4 (NIR)	0.76 – 0.90
5 (NIR)	1.55 – 1.75
6 (Thermal)	10.40 – 12.50
7 (MID)	2.08 – 2.35

The pixel size is 30 m for the reflective and 120 m for the thermal band (U.S. DEPARTMENT OF THE INTERIOR 2009b). As described in ALBERTZ (2007), passive systems such as Landsat 5 TM use the electro-magnetic radiation of nature. This is sunlight reflected at the earth surface (reflective bands) and intrinsic radiation absorbed by every body according to its surface temperature (thermal band). Electro-magnetic radiation depends on the intensity of radiation and the spectral

composition. The latter one is determined by the illumination of the surface and the properties of reflectance for reflective bands, and by surface temperature and the emission coefficient of the material for thermal bands. Due to the diversity of these factors, visibility and differentiation of surfaces and objects is possible. The main advantages of spaceborne derived data are the large covered area, the possibility of automatic classification, and low costs concerning data and man-power (PAUL 2007).

5.1.2 Airborne data

Additionally to spaceborne remote sensing products, airborne derived data is used in remote sensing. An overview is given by DAVIDSON (2008). In most cases, the film or digital camera is mounted at the snout or on the underside of air-planes. Special cameras have been developed, e.g. multispectral cameras or aerial cameras. Ordinary cameras can also be used but they are more common for occasional acquisitions. Vertical and oblique photos are aerial photos that differ concerning the attitude of the camera with respect to the earth's surface when the photograph is taken. Vertical aerial photos are taken pointing as straight downward as possible. For oblique aerial photos, the camera is inclined in a certain angle from the vertical. Different types of film generally used in aerial photography include panchromatic, infrared, colour, and camouflage. To obtain stereo-images, the acquisition of vertical stereo-pairs takes place in overlapping parallel tracks (ALBERTZ 2007). Main advantages of airborne derived data are a high spatial resolution and choice of date of image acquisition especially concern-ing weather, day time, and snow conditions (PAUL 2007).

Requirements for spaceborne as well as airborne image acquisition concern-ing glacier monitoring are cloud-free conditions near the end of the ablation season, a minimum snow cover, especially close to the glaciers, and accurate georeferencing and orthorectification (PAUL 2007). Restrictions for both cases are debris-covered glaciers and cast shadow. Data with these possible sources of error need manual post-processing when using automatic glacier classification (PAUL 2007).

5.1.3 Processing of data

All raw remote sensing data have to be pre-processed. This is necessary because of radiometric and geometric errors, described by RICHARD & XIUPING (2006). Radiometric distortion can occur due to e.g. the wavelength dependence of solar radiation on effects of the atmosphere, which affects the measured brightness values of the image pixels. Two characteristically types of radiometric

distortion are (i) a difference of the relative distribution of brightness over an image in a given band compared with the ground scene and (ii) a distortion of the relative brightness of a single pixel from band to band compared with the spectral reflectance character of the corresponding ground region.

Geometric errors occur due to a number of factors, e.g. panoramic effects related to the image geometry, rotation of the earth during image acquisition or uncontrolled variations and motion in the position and attitude of the remote sensing platform. Effects of geometric distortion are more severe than of radiometric distortion. They result e.g. in displacement of pixels or enlargement of the effective pixel size at the borders of the satellite image compared with nadir.

The big advantage in the actual case was the delivering of the satellite image already corrected concerning radiometric and geometric distortion. The vertical aerial photos were neither orthorectified nor georeferenced, but in most cases available as stereo-pairs.

5.2 Available data sources

Several data sources were needed for the compilation of the glacier inventory and the performance of the parameterization. To generate glacier outlines at LIA maximum, different data sources have been used:

- A satellite image: Landsat 5 TM, Path 199, Row 17, 09/08/2003; cell size 30 m x 30 m; cloud cover 0%, with little seasonal snow remaining (cf. PAUL (2009)) (see parts in Figure 2). The orthorectified Landsat image was supplied by Norsk Satellittdataarkivet and the orthorectification was tested with 14 check points by NVE (ANDREASSEN et al. 2008a);
- 26 vertical aerial photographs in 1:40000 taken in 1966, 1976 and 1981 by Fjellanger Widerøe (see Figure 15); cell size 0.4 m x 0.4 m (personal communication, J. Borgeraas, TerraTec AS (The Central archives for Vertical Photographs), 12/2008). All photos are cloud-free and taken at the end of the ablation season (August/September). In this study, the difference in date was unimportant, because these photos were used only for the purpose of mapping LIA maximum glacier extent. All photos were original black/white contact copies and had to be orthorectified and georeferenced;
- Geomorphological maps containing LIA maximum outlines of 25 glaciers, partially including detailed moraine ages (ERIKSTAD & SOLLID 1986; WINKLER 2001; MATTHEWS 2005) (see Figure 13). These maps have no

coordinate system, so some have to be classified as sketches rather than as accurate maps. They also had to be orthorectified and georeferenced;
- GPS points of LIA maximum moraine ridges on eight glaciers. This data were collected 2008 during field-work using a Garmin eTrex Summit (accuracy < 15 m; barometric altimeter (GARMIN 2005)) (see Figure 13);
- Digital topographic map in 1:50000 (called 'N50') with glacier outlines from the 1980s by Statens Kartverk (Norwegian mapping authorities);
- Digital terrain model with 25 m resolution (DTM25) by Statens Kartverk derived from the N50 maps with a root mean square error (RMSE) of 3 – 5 m;
- Digital glacier outlines from 2003 with defined identification numbers (IDs) of the glaciers and basins (ANDREASSEN et al. 2008a);
- Borders of hydrologic basins (called 'Regine' watershed). The Regine watersheds have been manually mapped by NVE with N50 as basis;

The digital glacier outlines from 2003 and the 1980s were transferred to glacier areas in GIS (ArcGIS 9.2 and 9.3 by *ESRI*). Digitization and calculation were also done using GIS. ERDAS IMAGINE 9.1 (by *Leica Geosystems*) was used for orthorectification and georeferencing (and classification). All material was converted into the same projection, using Universal Transverse Mercator projection in World Geodetic System 1984 European datum. Jotunheimen lies in zone 32N.

For the application of the parameterization and the applied sensitivity analysis, the data needed have been:
- Description of the scheme and specification of the calculations by HOELZLE (1994) and HAEBERLI & HOELZLE (1995);
- Inventory data of LIA maximum (BAUMANN et al. 2009), the 1980s (ØSTREM et al. 1988), and 2003 (ANDREASSEN et al. 2008a);
- A satellite image: Landsat 7 ETM+, Path 201, Row 17, 21/07/2000 (p201r017_7dt20000721_z31_40.tif.gz) (see parts in Figure 2). The Landsat image was downloaded from the Global Land Cover Facility (GLCF 2008);
- Digital glacier outlines from Jostedalsbreen at 1984 by Statens Kartverk.

5.3 Mapping glaciers at 'Little Ice Age' maximum

Mapping of the glacier area at LIA maximum was the first step in compilation of the glacier inventory. This data set was taken as basis for the mapping of the glacier length and other glacier properties.

5.3.1 Glacier area

The glacier outlines at LIA maximum were digitized manually on screen using three sources: the satellite image, the vertical aerial photographs, and the geomorphologic maps. Glacier outlines from the 1980s and 2003 served as basis for the minimum LIA maximum glacier extent. Hence, no glacier area at LIA maximum was smaller than the corresponding area in the later inventories.

5.3.1.1 Landsat image

On a glacier foreland relatively recently deglacierized, vegetation cover is absent or remains sparse (HOEL & WERENSKIOLD 1962). Therefore, the spectral signal is different between the glacier foreland and the area beyond (GAO & LIU 2001; CSATHO et al. 2005; RICHARD & XIUPING 2006; ALBERTZ 2007). This spatial pattern can be used for identifying the former glacier covered areas at LIA maximum on a satellite image.

The Landsat image was displayed as a band 543 composite as red, green, and blue, respectively (see parts in Figure 2) (cf. PAUL et al. (2004b); ANDREASSEN et al. (2008a)). The terminal moraine of LIA maximum was digitized. The outermost moraine wall was set as LIA maximum due to the absence of older Holocene moraines predating the LIA on the glacier forelands in this region (e.g. MATTHEWS (1991, 2005); SHAKESBY et al. (2008)). The former LIA maximum glacier area was in most cases adequate for manual mapping (BAUMANN et al. 2008).

(Semi-)Automatic classifications of the glacier foreland were also tested. Testing was done with different numbers of classes (3 – 50 classes). The spectral differences between ice, snow, vegetation, and bare rock were identified very well and classified correctly. But overlapping spectral signals between forelands and ubiquitous bare rock surfaces in the area made it very difficult to use such classification for glacier forelands. To separate these, several methods were applied: different class sizes, inclusion of elevation, slope, combination of different bands, and an object based classification using the image analysis software Definiens Developer 7 (by *Definiens*). Some of these methods enhanced the results to a certain, but not to a convincing degree (Figure 14). Therefore, a (semi-)automatic

classification was not applied in this case and the LIA maximum extent was digitized manually.

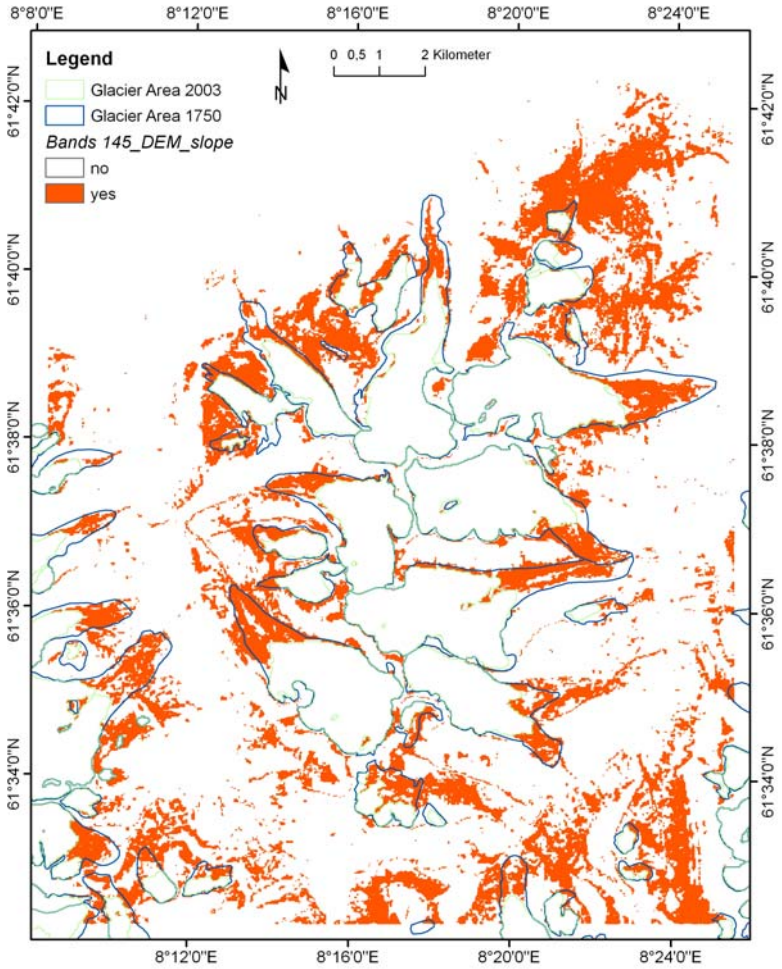

Figure 14: Result of the classification of the glacier foreland using bands 145, the DTM, and slope in the inquiry on the Landsat 5 TM image with band 1 > 60 digital numbers, band 4 < 50 digital numbers, band 5 in the interval (30; 85) digital numbers, DTM25 in the interval (1050; 2000) m a.s.l., and slope in the interval (8; 32)° (Raw data satellite image: Norsk Satellittdataarkivet; glacier outlines 2003: ANDREASSEN et al. 2008).

5.3.1.2 Vertical aerial photographs

The aerial photos, most of them available in stereo pairs, cover about 50% of the study area and 86% of the glacierized area (basis is glacier extent in the 1980s; Figure 15). They were georeferenced using the digital topographical map and orthorectified in ERDAS IMAGINE using the DTM25 as altitude reference, following the procedure for orthorectification as described in the ERDAS manual (ERDAS IMAGINE 2006). For each photo, four to eight ground control points (GCPs) depending on the fitting of the resulting image were collected. Moraine ridges and the outline of the forelands were used to detect and map the LIA maximum extent of the glaciers. On most glacier forelands in Jotunheimen, the

outermost moraines could be mapped fairly well. Photos in stereo-pairs were additionally examined stereoscopically and analyzed.

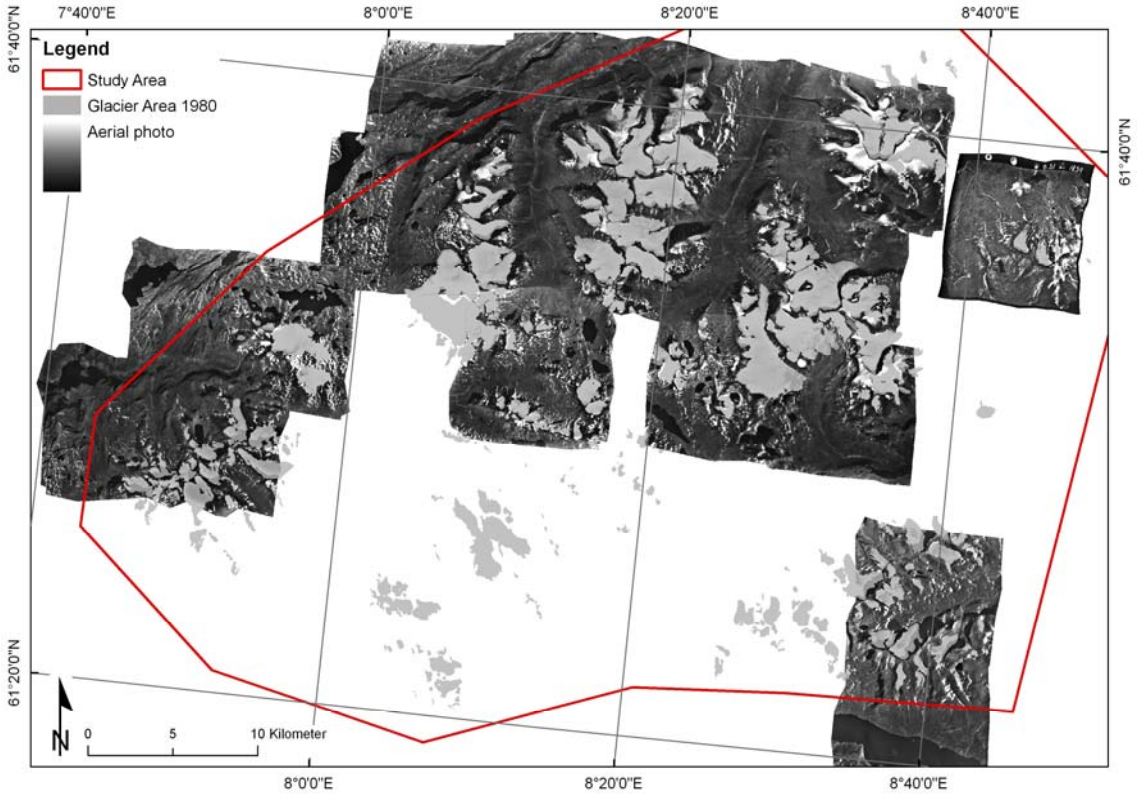

Figure 15: Coverage of vertical aerial photos available for the study. Glacier area from the 1980s (Aerial photos: Fjellanger Widerøe, 21.07.1966, 1834 B21; 22.08.1976, 5245 J6–8; 29.08.1981, 7084 17–8 44–46; 18–1 4–5, 9, 12–14; 18–2 6–7, 9–13; 18–3 7, 9–11, 13–14; glacier outlines 1980s: Statens Kartverk N50).

5.3.1.3 Geomorphological maps

On the geomorphological maps used in this study, detailed topo-graphical information was sparse, apart from the moraine ridges themselves. Consequently aerial photos were used to georeference and orthorectify them. In spite of minor problems in orthorectification, the results were considered good enough to make a digitization possible. LIA maximum extent was manually digitized. In addition to the position, timing of the moraine ridges was partly given on the geomorphological maps and in the respective studies.

5.3.1.4 Selection of 'Little Ice Age' maximum outline

To derive one final outline per LIA maximum glacier, the different outlines were compared. The outlines of the geomorphological maps were assumed to be the most correct and were chosen as the final outline where available (i.e. at 25 glaciers). For all other glaciers, the visibility of the LIA maximum area in the satellite image and aerial photo was compared and the one with the clearest

visible boundary was chosen. In cases with substantial deviation between the two outlines, a closer re-check of the sources was made to detect any mapping errors. By applying this method, inconsistency among possible multiple versions of the outline was resolved, and one outline for each glacier was finally derived. Only the final outlines were used to calculate the LIA maximum glacier area.

GPS points of the outermost moraine walls were collected in the field during summer 2008 at eight glaciers. They were collected from five glaciers where a geomorphological map was available and three unmapped glaciers. The accuracy of the projection of the map in a GIS system as well as the accuracy of the mapping itself could be tested using this information. The difference between the GPS data and the mapping ranged between 0 m and 250 m. The mean difference is 41 m with a standard deviation of 83 m. The difference at the unmapped glaciers was 83 m and was much less (16 m) at the mapped glaciers, probably because the mapped glaciers have better visible outermost moraine ridges. Nonetheless, georeferencing and mapping were considered to be satisfactory for all GPS-mapped glaciers with one exception.

Calculation of the glacier area was done using GIS. Since LIA maximum, a large number of the investigated glaciers separated due to glacier retreat and became individual glaciers. To reconstruct the glaciers at LIA maximum, the present basins were adjusted to fit the formerly larger glacier areas. The LIA basins had to include the transformation of separated glaciers into one basin if they constituted a single glacier during LIA maximum. Adjustments were especially needed at the lower parts of the glaciers. The boundary of single glacier units at LIA maximum was derived by clipping the LIA maximum extent with the LIA basins. The value of the glacier area was calculated automatically with GIS. Finally, all glaciers smaller than 0.01 km^2 were deleted from the inventory of the glaciers at LIA maximum. This was necessary, because at this scale, it is difficult to distinguish between glaciers and perennial snowfields (e.g. PAUL (2009)). Furthermore, the resolution and accuracy of mapping are limited by the pixel size of the satellite image. This has also been the reason why glaciers of this size class were not included in the inventory of 2003 (ANDREASSEN et al. 2008a).

5.3.2 Glacier centreline

To calculate glacier lengths during LIA maximum, centrelines were digitized manually using the glacier outlines at LIA maximum and the contour lines of N50 as basis. Flowlines were digitized perpendicular to the contour lines, preferably in

the middle of the glacier, and from its highest to its lowest points (PAUL 2009). On glaciers with different tributaries or wide accumulation areas, more than one flowline was digitized (e.g. Memurubreen in Figure 16). In branched cases, a mean of the flowlines was calculated and hereafter used as 'glacier length'. The number of flowlines varied between one and three at individual glaciers.

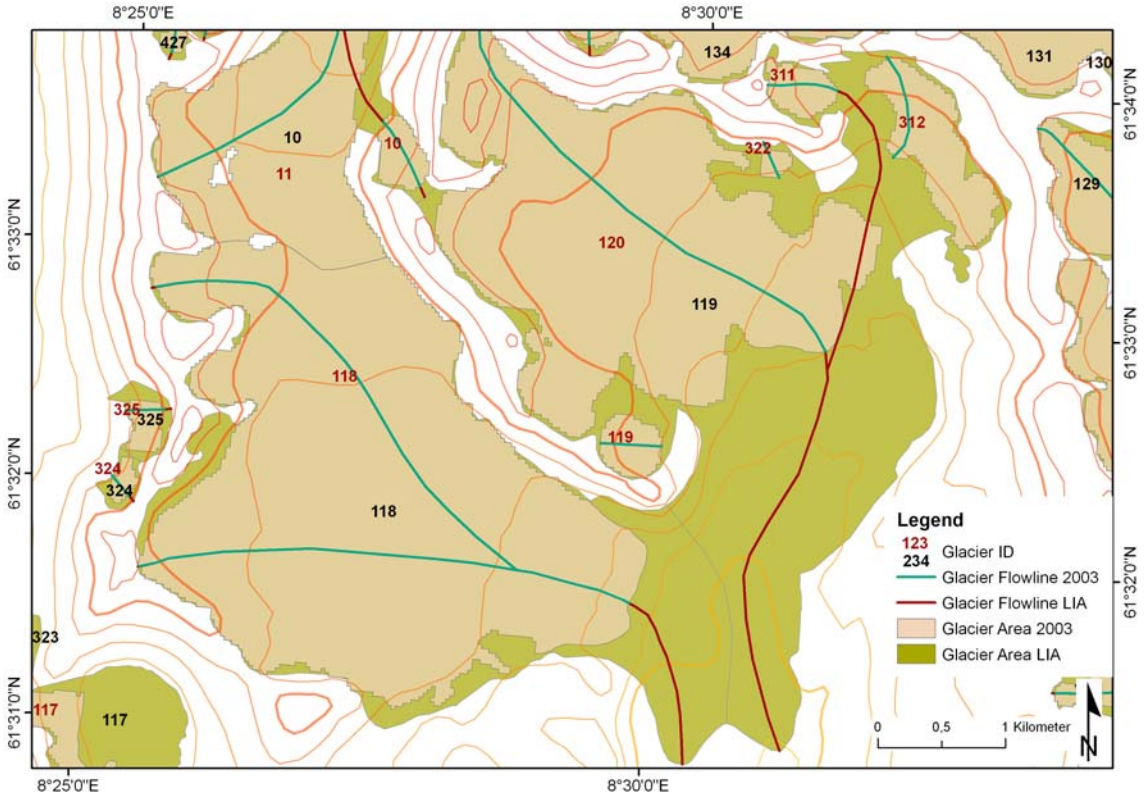

Figure 16: Vestre (LIA ID = 118; black number) and Austre Memurubreen (LIA ID = 119) with corresponding flowlines. The separation of Austre Memurubreen since LIA maximum in five single glacier units until 2003 (2003 IDs = 119, 120, 311, 312, 322; red numbers) is visible. The flowline on Vestre Memurubreen is divided in two branches. The mean of these branches (highest to lowest elevation) was used. For the comparison of glacier length in the parameterization of Austre Memurubreen, only the glacier lengths of the western branch of glacier ID 119 at LIA maximum and of glacier ID 120 in 2003 were chosen. These two lengths can be compared directly. The sum or mean of all glacier flowlines at each time cannot be compared because they do not rely on the same basis. The complete glacier flowline at LIA maximum is not visible because of coverage by the 2003 glacier flowline (directly over each other). Elevation contour interval is 100 m. The location of Vestre and Austre Memurubreen is seen in Figure 1 by letter code MEM (Glacier outlines 2003: ANDREASSEN et al., 2008; digital topo-graphic map: Statens Kartverk N50).

5.3.3 Glacier inventory data

Inventory data of the glaciers at LIA maximum were calculated automatically using GIS and the DTM25. The calculated inventory data included, among other variables, minimum, maximum, and mean altitude, slope, and aspect. Except for aspect, all variables were derived directly from GIS. The aspect was calculated using a routine described in PAUL (2007).

5.4 Parameterization

The simple parameterization scheme used for the analysis of glacier inventory data of Jotunheimen was developed for the European Alps by HAEBERLI & HOELZLE (1995). It has been applied to the Peruvian Andes (HUGGEL et al. 2003), the Southern Alps of New Zealand (HOELZLE et al. 2007), and the Swiss Alps (PAUL 2007).

5.4.1 Scheme

The parameterization scheme was first developed by HOELZLE (1994) and HAEBERLI & HOELZLE (1995). It is based on the concepts of glacier flow and glacier response by NYE (1960) and JÒHANNESSON et al. (1989b). All calculations of the variables and an overview of the parameters are listed in Appendix A.

The aim of the parameterization is the estimation of glacier behaviour based on (measured) inventory data (surface area, length, minimum and maximum altitude) caused by a postulated disturbance of a climate variable, i.e. air temperature or precipitation. Assumption is a glacier in steady-state that returns to a new steady-state after adaption to the new conditions by a step change of the equilibrium line altitude (ELA) and the mass balance disturbance (δb). This leads to a change in glacier length (δL) depending on the original length (L_0) and the ablation at the glacier tongue (b_t) (Figure 17).

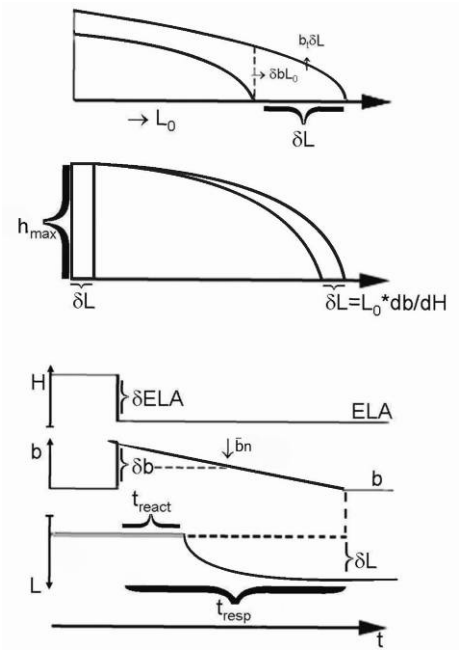

Figure 17: Glacier reaction after a step change of the equilibrium line altitude (δELA) and a there-after change in mass balance (δb). Terms see text and Appendix A (Figure modified after (HAEBERLI 1991)).

$$\delta b = b_t * \delta L / L_0 \quad (1)$$

The time needed is the dynamic response time (t_{resp}).

$$t_{resp} = h_{max} / b_t \quad (2)$$

The term h_{max} is the maximum ice thickness (see equation in Appendix A) and b_t the average annual ablation at the glacier tongue. The calculation of h_{max} is based on ice thickness measurements on various glaciers world-wide (HOELZLE et al. 2007) and was adopted from HAEBERLI & HOELZLE (1995). The ablation at the glacier tongue is calculated as:

$$b_t = (H_{mean} - H_{min}) * db/dH \quad (3)$$

db/dH is the mass-balance gradient and H_{mean} the mean glacier altitude (see equation in Appendix A), representing the ELA.

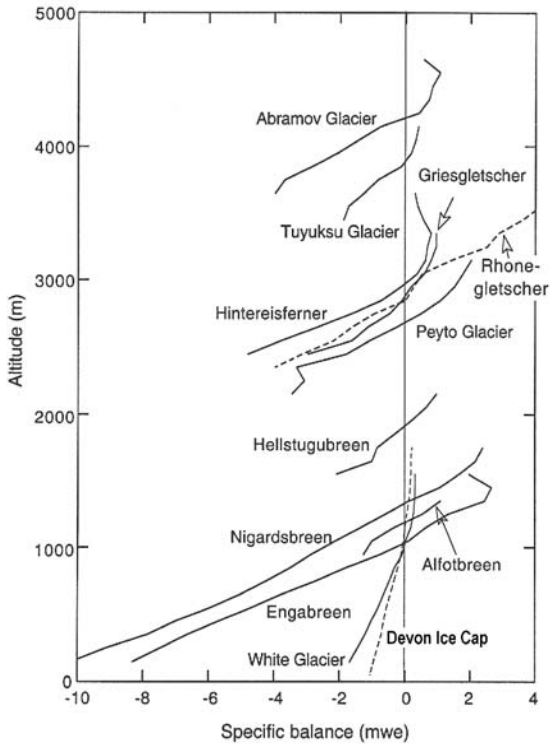

Figure 18: Examples of measured mass balance profiles. The curves are the mean of measurements over several years. Profiles of Rhone glacier and Devon Ice Cap dached lines (Figure modified after OERLEMANS (2001)).

Important for the parameterization is the selection of the mass balance gradient (HOELZLE et al. 2007). It is defined as the combination of accumulation and ablation gradient (NESJE et al. 2000). These two gradients are defined on

rates at which annual accumulation and ablation, respectively, change (NESJE et al. 2000). In this study, the ablation gradient is taken as mass balance gradient instead of the combination of accumulation and ablation gradient (cf. HAEBERLI & HOELZLE (1995)). This decision was made because of the significantly more homogeneous behaviour of the mass balance gradient below the ELA compared with the behaviour above the ELA (Figure 18) (OERLEMANS 2001). Therefore, the mean slope of the mass balance profile in the ablation area is defined as mass balance gradient in this study.

In the parameterization, only glaciers larger than 0.2 km² are used because of their more distinct reaction to changes in climate dynamics (HOELZLE et al. 2007). Additionally, large glaciers have a predominant influence on regional total mass changes and represent the largest part of the glacier area (HAEBERLI & HOELZLE 1995).

5.4.2 Compilation of the Jotunheimen data

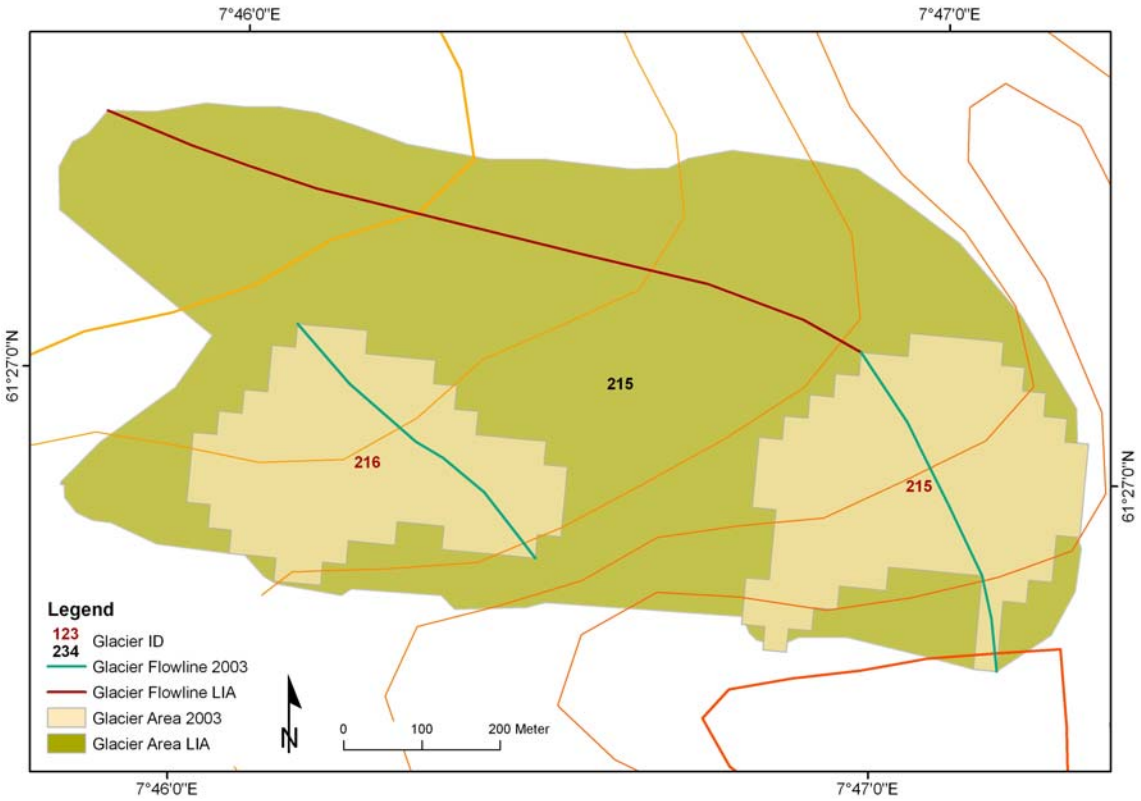

Figure 19: Soleibotnbreen (LIA ID = 216; black number) with corresponding flowline. The separation of Soleibotnbreen since LIA maximum in two single glacier units until 2003 (2003 IDs = 215 (Austre Soleibotnbreen), 216 (Vestre Soleibotnbreen); red numbers) is visible. The glacier flowline at LIA maximum could not only be shortened for the later areas, but had to be created new. Therefore, these lengths are not comparable, because they were not drawn on the same length as basis. The location of Soleibotnbreen is seen in Figure 1 by letter code SOL (Glacier outlines 2003: ANDREASSEN et al., 2008; digital topographic map: Statens Kartverk N50).

The inventory data of the 1970s was the basis for the parameterization in the European (HAEBERLI & HOELZLE 1995) and New Zealand Alps (HOELZLE et al. 2007). Therefore, the inventory data of the 1980s in Jotunheimen was chosen as the basis for selecting glaciers usable for the parameterization. To begin, all glaciers > 0.2 km² are chosen. Second, the comparability of these remaining glaciers is examined concerning glacier length in all three years used in the parameterization. The comparability of the glacier length can disappear due to separation of the glacier area between LIA maximum and 2003 depending on glacier retreat. An example of a rejected glacier for the parameterization is seen in Figure 19, an example of a glacier only usable with modifications in Figure 16. From the total number of 218 glaciers covering 208 km² in the 1980s, there remained 125 glaciers (57%) with a total area of 183 km² (88%) to be used for parameterization.

A couple of other input values had to be defined. As a first estimate, the mass balance data of all glaciers with mass balance measurements in the area were analyzed (data source: KJØLLMOEN (2006, 2008, 2009), and WGMS data-base). These measurements were done on three glaciers: Stor-, Hellstugu-, and Gråsubreen (see location in Figure 1). First all years with an annual net mass balance of 0 ± 0.19 m w.e. (net mass balance averaged over the whole glacier surface) were chosen to calculate (i) the mass balance gradient and (ii) the mean accumulation area ratio (AAR_0). The value of the annual net mass balance was chosen arbitrarily to limit the more or less balanced years (hereinafter referred to as 'steady-state years'). Variables of steady-state years are chosen because they most likely represent glaciers during equilibrium. Only years with vertical profiles of the net balance and not just the glacier-averaged net balance could be taken. For calculating the mass balance gradient, the altitude vs. net mass balance in the ablation area was plotted. The line y = ax + b best fitting these points was calculated and the coefficient a of x was taken as the mass balance gradient for this specific year and glacier (cf. TRENHAILE (2004)). The mean of all these values of each glacier was calculated and set as mass balance gradient. The calculated values corresponded quite well with the results of RASMUSSEN & ANDREASSEN (2005) (Table 2) and other studies (HOELZLE et al. 2003; RASMUSSEN 2004). They varied between 0.2 m w.e./100m/a for Gråsubreen in the East and around 0.6 m w.e./100m/a for Stor- and Hellstugubreen in the central part. Because of Gråsubreen not being a temperate glacier with an ice-cored moraine (see section 3.3), the resulting gradient was taken with care and not used for estimating a mass balance gradient in the parameterization. Also in another study (RASMUSSEN & ANDREASSEN 2005), the gradient for the winter mass balance of Gråsubreen showed unusual results and confirmed this decision of exclusion.

Nonetheless, these results point towards a difference in the gradient between the western/central and the eastern part. Hence, the area is divided in two sub-regions West and East depending on the calculated mean elevation during LIA (BAUMANN et al. 2009) and the occurrence of ice-cored moraines (Figure 20).

Table 2: Mass balance gradient db/dH of all years with an annual net mass balance of 0 ± 0.19 m w.e. (steady-state years) and vertical profiles of net balance available (not just glacier-average net balance). Mean value is resulting net mass balance gradient. Glac. = Glacier. *Year not used for calculation (Sources: (1) (RASMUSSEN & ANDREASSEN 2005); raw data db/dH: WGMS database).

Year / Glac.	1968	1971	1979	1991	1992	1994	1995	1998	2000	2005	2008	Mean	(1)
db/dH [m w.e./100m/a]													
STO	–	–	–	1.18	0.77	–	–	–	–	0.72	0.71	0.85	0.61
HEL	0.58	0.67	0.70	–	0.52	0.68	0.65	0.61	0.71	–	0.74	0.65	0.57
GRA	0.17	–	–	–	–	0.18	-0.09*	–	–	–	–	0.18	0.20

The calculated values of the mass balance gradient were not used in the parameterization, but taken as indicator. Thus for the selection of a certain value of the mass balance gradient, additional analyses were made.

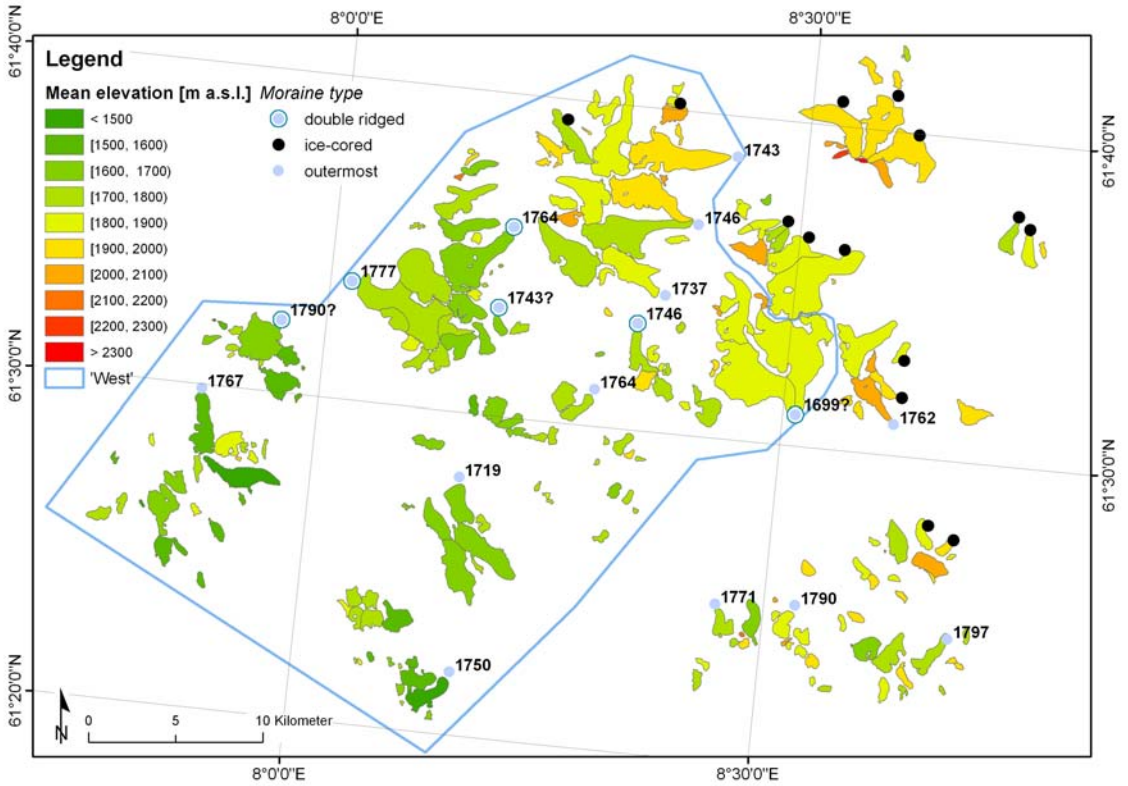

Figure 20: Colour-coded mean altitude at LIA maximum for each single glacier. Blue outline denotes western part of Jotunheimen, remaining glaciers build the eastern part. Moraine type and timing of LIA maximum are marked (LIA maximum timing: WINKLER 2001; MATTHEWS 2005).

First, the annual net mass balance from the years 1980 to 2003 was taken to calculate the mean annual mass balance $\bar{b}_n$. The data from these years have been selected despite a data set reaching much further back in time (until 1949 for STO) because of the direct comparability between measured data from the field and calculated values by the parameterization (1980s – 2003). Second, the mass balance at the glacier tongue b_t was derived from measurements of steady-state years. Also in this case, only years with vertical profiles of the net balance and not just the glacier-averaged net balance were taken. For calculation, the net mass balance at the very tongue was used (i.e. value of lowest measured interval).

Table 3: Ablation at the glacier tongue in the ablation area, measured from steady-state years in different time-periods and calculated by the parameterization with different values of mass balance gradient. Explanation of calculation in the text. b_t [m/a], db/dH [m w.e./100m/a] (Raw data measured b_t: WGMS database).

	measured				**calculated**				
Period [a]	*1991-2008*	*1991/92*		**Period [a]**	*1980-2003*				
b_t STO	-2.9	-3.4			-2.9	-6.3	-2.4	-1.6	-0.6
Period [a]	*1968-2008*	*1979-2008*	*1979-2000*	**db/dH (STO, HEL)**	**0.9**	**2.0**	**0.75**	**0.5**	**0.2**
b_t HEL	-2.5	-2.6	-2.5		-3.1	-7.0	-2.6	-1.7	-0.7
Period [a]	*1968-1995*	*1994/95*		**db/dH (GRA)**	**0.3**	**2.0**	**0.75**	**0.5**	**0.2**
b_t GRA	-0.3	-0.3			-1.0	-6.8	-2.5	-1.7	-0.7

The values of all chosen years were summarized again and divided by the number of years to gain an averaged value for the ablation at the glacier tongue over the chosen period for each glacier. These values were compared with calculated values of b_t resulted by using the parameterization (see Equ. (3)) (Table 3). These were calculated with different values of the mass balance gradient to achieve the best fitting correlation. According to this process, a mass balance gradient of 0.9 m w.e./100m/a for the West and of 0.3 m w.e./100m/a for the East were chosen. These values were only slightly higher than the calculated ones by using steady-state years. The ELA was estimated as the mean glacier elevation (setting of the parameterization).

Table 4: Overview of the parameterized values used in Jotunheimen, the European and New Zealand Alps, and sub-regions. *Data from (HOELZLE ET AL. 2007).

Region / **Parameter**	**European Alps***	**New Zealand Alps***		**Jotunheimen**	
		'wet'	**'dry'**	**West**	**East**
A	0.16				
n	3				
ρ	900			917	
g	9.81				
f	0.8			1	
db/dH	0.75	1.5	0.5	0.9	0.3
τ [bar]	$1.3*10^5$	$1.8*10^5$	$1.2*10^5$	calculated	

The geometry shape factor f was chosen according to PATERSON (1994). It is used for calculating shear stress based on glacier geometry. The half-width w, the ice thickness and the cross-section profile of the glacier must be known for the assessment of f. The value of f was estimated as 1 by a cross-profile of Hellstugubreen (HOEL & WERENSKIOLD 1962) as well as thickness (NVE 2006) and width assessments of Storbreen. An overview of the parameterized values used for all three regions is given in Table 4.

5.4.3 Overview input data 1970s/80s

Table 5: Statistics of the glacier area in 1970s/80s for Jotunheimen, the European and New Zealand Alps, and sub-regions.

Region / S [km²]	European Alps	New Zealand Alps	Jotunheimen	Jotunheimen	
				West	East
Mean	1.44	1.40	1.46	1.68	1.09
Max	86.76	98.34	8.90	8.90	7.62
Min	0.21	0.20	0.21	0.22	0.21
Std	3.69	4.81	1.75	1.89	1.39
Sum	2544.38	982.04	182.50	131.38	51.13
Number [n]	1763	702	125	78	47

Table 6: Classification of the glacier area in 1970s/80s into size intervals for Jotunheimen, and the European and New Zealand Alps.

Region / Area interval [km²]	European Alps		New Zealand Alps		Jotunheimen	
	Number		Number		Number	
	[n]	[%]	[n]	[%]	[n]	[%]
≤ 1	1241	70.4	544	77.5	70	56.0
1 – < 2	250	14.2	77	11.0	30	24.0
2 – < 3	103	5.8	25	3.6	4	3.2
3 – < 4	49	2.8	19	2.7	9	7.2
4 – < 5	21	1.2	7	1.0	4	3.2
5 – < 10	66	3.7	14	2.0	8	6.4
10 – < 15	14	0.8	7	1.0	-	-
15 – < 20	12	0.7	4	0.6	-	-
20 – < 25	2	0.1	-	-	-	-
25 – < 30	1	0.1	1	0.1	-	-
30 – < 35	2	0.1	2	0.3	-	-
35 –< 40	-	-	1	0.1	-	-
40 – < 45	-	-	-	-	-	-
45 – < 50	-	-	-	-	-	-
50 – < 55	-	-	-	-	-	-
55 – < 60	-	-	-	-	-	-
60 – < 65	-	-	-	-	-	-
65 – < 70	1	0.1	-	-	-	-
70 – < 75	-	-	-	-	-	-
75 – < 80	-	-	-	-	-	-
80 – < 85	-	-	-	-	-	-
85 – < 90	1	0.1	-	-	-	-
≥ 90	-	-	1	0.1	-	-
Total	1763	100	702	100	125	100

The input data of Jotunheimen, the European, and the New Zealand Alps consisted of area, length, and minimum and maximum altitude of the 1970s/80s. The total glacier area in each region varied quite a lot depending on the number of glaciers (Table 5). The largest glacier in Jotunheimen was only about a tenth of the largest glacier in the European and New Zealand Alps. The mean glacier area, however, was very similar, and in all regions more than 90% of the glaciers were < 5.0 km² (Table 6). The western and eastern part in Jotunheimen differed in area e.g. regarding mean and maximum value (Table 5).

Table 7: Statistics of the length of the glacier flowline in 1970s/80s for Jotunheimen, the European and New Zealand Alps, and sub-regions.

Region / L_0 [km]	European Alps	New Zealand Alps	Jotunheimen	Jotunheimen West	Jotunheimen East
Mean	1.63	1.58	1.64	1.73	1.50
Max	24.70	28.50	5.12	4.56	5.12
Min	0.30	0.05	0.33	0.33	0.53
Std	1.53	1.99	1.09	1.13	0.98
Number [n]	1763	702	125	78	47

The pattern of the distribution of the glacier length was comparable: the mean was nearly the same in all regions, but the maximum was only a fifth in Jotunheimen compared with the other two regions (Table 7). The mean of the mean elevation of the European Alps was ~ 1000 m higher compared to the value of the New Zealand Alps and Jotunheimen (Figure 21a). The range of the values was much smaller in Jotunheimen than in the other two regions.

a)

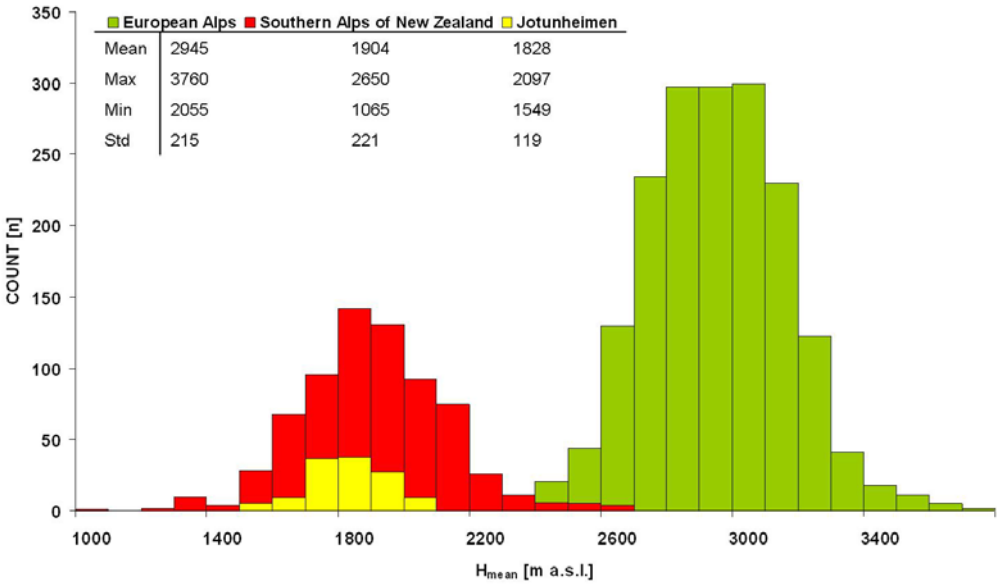

b)

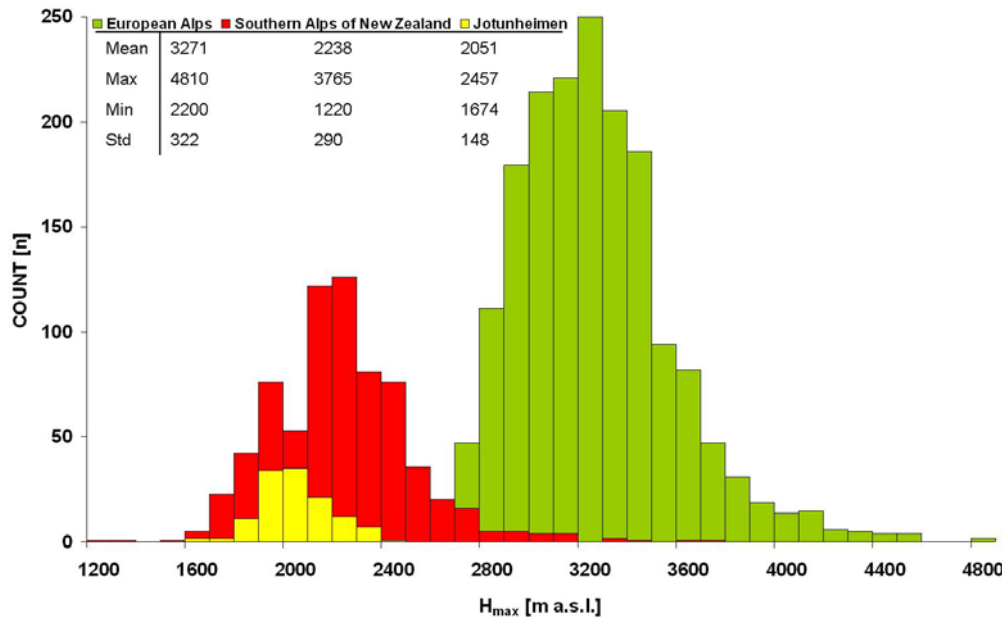

c)

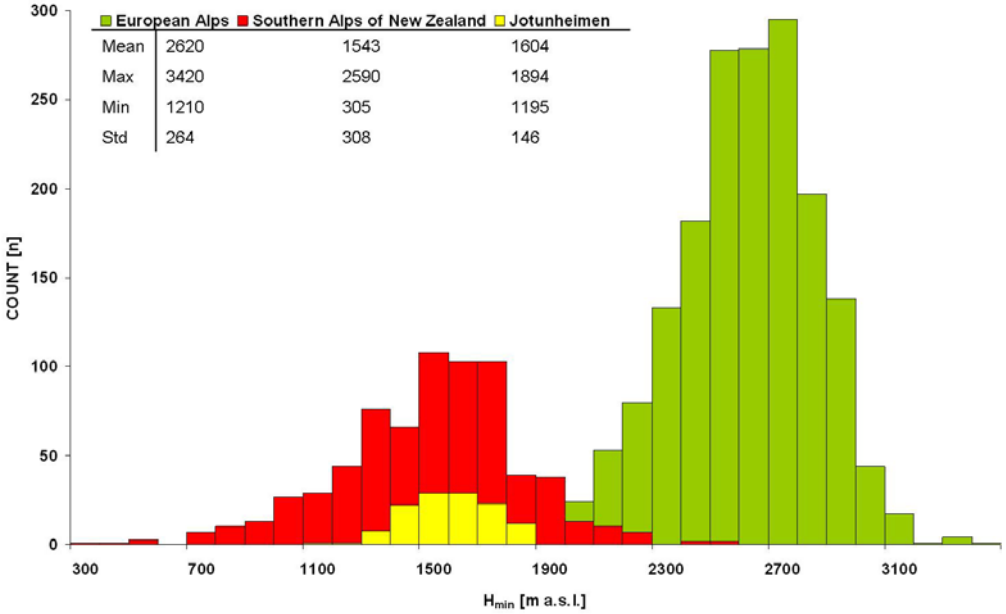

Figure 21: Distribution of glacier a) mean altitude (H_{mean}), b) maximum altitude (H_{max}), and c) minimum altitude (H_{min}) during the 1970s/80s in Jotunheimen, the European, and New Zealand Alps used in the parameterization.

The frequency distributions of the maximum elevation were very similar for the European and the New Zealand Alps, but the values for mean, maximum and minimum were ~1000 m higher in the European Alps (Figure 21b). The mean maximum elevation was also ~1000 m higher in the European Alps than in Jotunheimen. The range of the maximum altitude was much smaller in Jotunheimen compared with the other two regions. The mean maximum elevation was lower in the western (2025 ± 155 m a.s.l.) than in the eastern part (2096 ± 122 m a.s.l.) of Jotunheimen. The mean value of the minimum elevation was

pretty similar in the New Zealand Alps and Jotunheimen, but was again ~1000 m higher in the European Alps (Figure 21c). The lowest value of the minimum elevation was 305 m a.s.l. in the New Zealand Alps (Fox Glacier) and ~1200 m a.s.l. in the European Alps (Bossons Glacier) and Jotunheimen (Riingsbreen). Both the minimum (difference = 265 m) and the mean value (difference = 147 m) of minimum elevation were remarkably higher in the eastern compared with the western part of Jotunheimen.

6 Results

To narrow and estimate uncertainties during the compilation process or the further analyses of the results, different sensitivity analyses are performed. Afterwards, the results of mapping the LIA maximum and of the parameterization in Jotunheimen are shown.

6.1 Sensitivity analysis

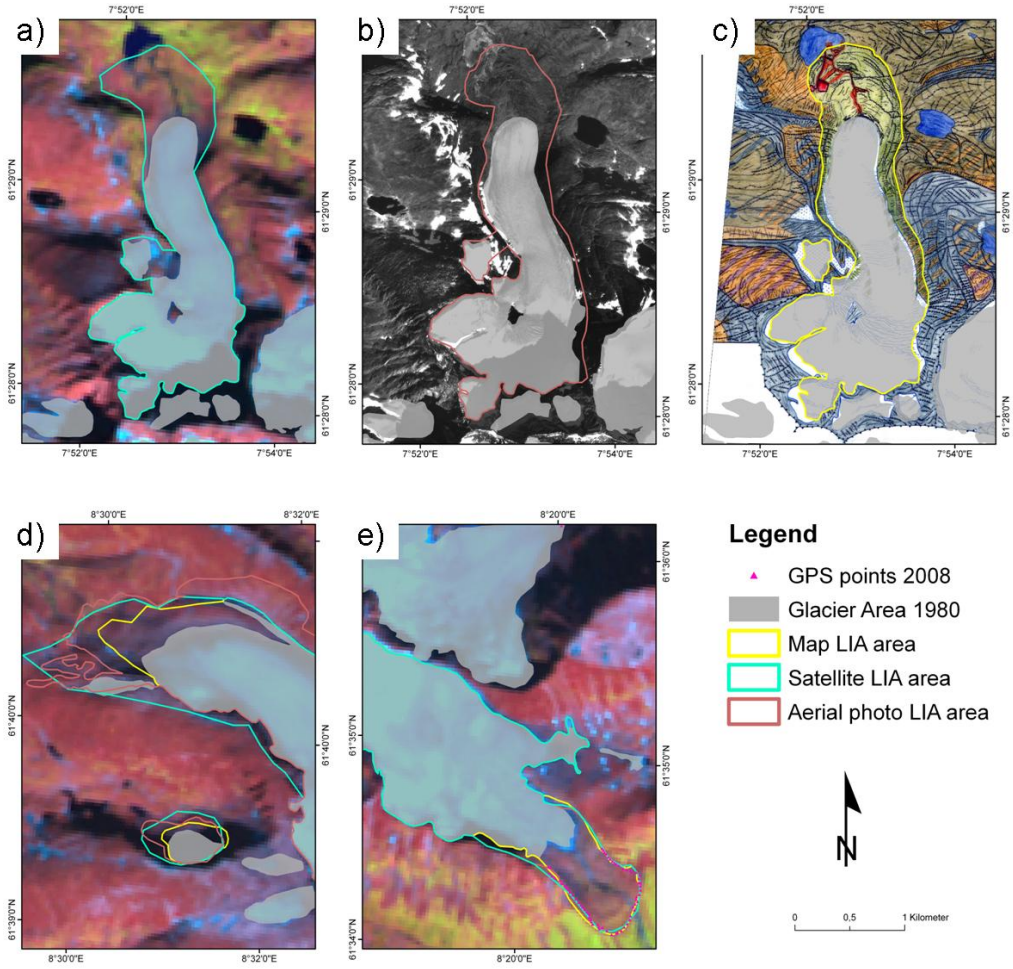

Figure 22: Mapping of the LIA maximum extent of Styggedalsbreen (STD) on a) the satellite image, b) an aerial photo, and c) a geomorphological map. Overlapping of all three sources for the sensitivity analysis with poor correspondence in d) at Grjotbreen (GRJ) and with good correspondence in e) at Bukkeholsbreen (BUK). Location of the glaciers in Figure 1 given by letter codes (Satellite image: Norsk Satellittdataarkivet; aerial photo: Fjellanger Widerøe, 29.08.1981, 7084 17–8 46; map: Winkler, 2001; glacier outline 1980s: Statens Kartverk N50).

Glacier outlines at LIA maximum were available from one or more of these sources: satellite image, aerial photographs, and geomorphological maps. For 18

of the glaciers, all three sources were available, and they were compared (examples in Figure 22).

Therefore, the glacier areas of each source were summarized and the mean and standard deviation was calculated. The coefficient of variation was 1.7%, and all areas were within the 95%-confidencel interval. Therefore, the resulting glacier outlines of LIA maximum were judged to be sufficiently accurate.

In addition, a comparison was made between the glacier areas from the satellite image and the aerial photos, each time with the geomorphological maps. The resulting differences were very small. But mapping using the satellite image showed a closer agreement with the geomorphological maps than mapping using aerial photos. In direct comparison between the 18 glaciers used for the sensitivity analysis, the resulting areas by the satellite image showed a plus of 1.3 km² (0.01%), whereas these results by the aerial photos showed a plus of 2.2 km² (0.02%).

A sensitivity study was applied to the parameterization to estimate the range of possible values of the variables (Table 8). The parameterization was calculated with extreme values of db/dH for each part of Jotunheimen:

- East: 0.1 and 1.0 m w.e./100m/a
- West: 0.5 and 1.5 m w.e./100m/a

Table 8: Four calculated variables with the parameterization using different values of the mass balance gradient (db/dH) for the sub-regions of Jotunheimen at different times, compared with the used values (Used). Chosen are extreme values for db/dH. Shown are the variables depending directly on the mass balance gradient (not shown: relaxation time (t_{relax})). b_t = balance at the glacier tongue, $u_{s,a}$ = surface flow velocity, $u_{b,a}$ = sliding velocity, t_{resp} = response time. db/dH [m w.e./100m/a], b_t [m/a], $u_{s,a}$ and $u_{b,a}$ [m/s], t_{resp} [a].

Area/ (db/dH) \ Variable/ time		b_t			$u_{s,a}$			$u_{b,a}$			t_{resp}		
		LIA	**'80s**	**2003**	**LIA**	**'80s**	**2003**	**LIA**	**'80s**	**2003**	**LIA**	**'80s**	**2003**
East	**0.1**	0.2	0.2	0.2	2.6	2.3	2.0	1.6	1.6	1.5	393.5	341.2	353.6
	1.0	2.2	2.0	1.8	26.1	22.8	20.1	25.1	22.2	19.6	39.4	34.1	35.4
Used	**0.3**	0.7	0.6	0.5	7.8	6.7	6.0	6.8	6.1	5.5	131.2	118.7	117.9
West	**0.5**	1.5	1.2	1.5	19.3	13.8	13.1	16.8	12.8	12.1	75.2	70.0	70.5
	1.5	4.6	3.6	3.4	57.8	41.5	39.3	55.3	40.2	38.4	25.1	23.3	23.5
Used	**0.9**	2.8	2.1	2.1	34.7	25.0	23.6	32.2	23.9	22.6	41.8	39.0	39.2

Not all variables were influenced by the mass balance gradient. Thus, the analysis was only performed with a selection of all and compared with the chosen values for the parameterization (Table 9).

Table 9: Selection of results by the parameterization applied on inventory data from Jotunheimen at LIA maximum, the 1980s, and 2003. Differences between two times (at δL, δELA, δb, and $\bar{b}n$) are indicated as follows: LIA = 1750 – 2003, 1980s = 1750 – 1980, 2003 = 1980 – 2003. δL = length change, α = surface slope, V = glacier volume, h_{max} = maximum ice thickness, b_t = balance at the glacier tongue, $u_{s,a}$ = surface flow velocity, t_{resp} = response time, δELA = change in ELA, δb = mass balance disturbance, $\bar{b}n$ = mean mass balance.

Statistics/time \ Variable		δL [km]	α [°]	V [km³]	h_{max} [m]	b_t [m/a]	$u_{s.a}$ [m/a]	t_{resp} [a]	δELA [m]	δb [m/a]	$\bar{b}n$ [m/a]
Mean	**LIA**	0.669	16.46	0.085	109.9	1.97	24.58	75.40	-55.3	-0.42	-0.04
	1980s	0.577	18.26	0.049	81.8	1.56	18.11	67.01	-46.0	-0.38	-0.04
	2003	0.081	18.14	0.044	77.8	1.50	17.08	68.38	-9.4	-0.02	-0.08
Std	**LIA**	0.672	6.31	0.155	81.1	1.34	19.53	61.28	53.7	0.50	-0.05
	1980s	0.623	7.40	0.087	63.8	0.99	12.74	52.87	54.7	0.49	-0.05
	2003	0.178	9.55	0.080	62.0	0.98	12.52	52.79	24.2	0.15	-0.16
Min	**LIA**	0.000	7.00	0.002	24.2	0.25	2.68	14.02	-309.5	-2.79	-0.26
	1980s	-0.102	7.97	0.001	18.5	0.22	2.30	12.61	-300.5	-2.70	-0.24
	2003	-0.325	7.87	0.001	20.4	0.17	0.15	8.36	-156.0	-0.76	-0.76
Max	**LIA**	3.799	39.64	0.967	372.3	6.28	105.02	321.67	0.0	0.00	0.00
	1980s	3.157	44.76	0.462	272.8	4.50	63.23	298.95	115.5	0.35	0.07
	2003	0.932	89.74	0.441	256.0	4.35	59.69	254.15	59.0	-0.05	0.33
Sum	**LIA**	–	–	10.672	–	–	–	–	–	–	–
	1980s	–	–	6.084	–	–	–	–	–	–	–
	2003	–	–	5.465	–	–	–	–	–	–	–

Table 10: a) Input data for the parameterization of the glaciers NIG, STO, HEL, GRA, and of total Jotunheimen (Jot) at LIA maximum and during the 1980s. The maximum altitude (H_{max}) and the mass balance gradient (db/dH) were chosen similarly for both years. The input data for NIG are taken from the digital sources and not taken from the literature. Therefore, differences occurred compared with the published values (e.g. (KJØLLMOEN 2004)). H_{min} = minimum elevation, Δ [%] = difference between LIA maximum and the 1980s. b) Calculated variables by the parameterization for the four glaciers of Table 10a) and total Jotunheimen (Jot). t_{resp} = response time, t_{relax} = relaxation time, α = surface slope, V = volume, $u_{s,a}$ = surface flow velocity, $u_{d,a}$ = velocity by ice deformation, VR = velocity ratio, b_t = balance at the glacier tongue, б̄n = mean net mass balance.

a)

Glacier \ Variable/time		H_{max} [m a.s.l]	H_{min} [m a.s.l]			Area [km²]			Length [km]			db/dH [m w.e./100m/a]
			LIA	1980s	Δ [%]	LIA	1980s	Δ [%]	LIA	1980s	Δ [%]	
NIG		1955	249	349	40	46.6	42.3	-9	14.4	9.8	-32	1.25
STO		2084	1125	1385	23	7.0	5.2	-26	4.7	3.0	-36	0.9
HEL		2240	1401	1473	5	4.9	3.7	-24	4.5	3.4	-24	0.9
GRA		2393	1689	1710	1	4.8	4.7	-2	4.5	4.1	-9	0.3
Jot	Min	1674	1044	1195	–	0.2	0.2	–	0.5	0.3	–	–
	Max	2457	1876	1894	–	12.3	8.9	–	7.3	5.1	–	–
	Mean	2062	1512	1607	6	2.0	1.5	-26.9	2.2	1.6	-26.1	–

b)

Glacier \ Variable/time		t_{resp} [a]		t_{react} [a]		α [°]		V [km³]		$u_{s,a}$ [m/a]		$u_{d,a}$ [m/a]		VR		b_t [m/a]		б̄n m/a] (1750-1980s)
		LIA	1980s	LIA	1980s	LIA	1980s	LIA	1980s	LIA	1980s	LIA	1980s	LIA	1980s	LIA	1980s	
NIG		62.2	47.8	0.017	0.013	6.7	9.3	6.51	4.28	163.1	144.2	47.9	34.8	0.706	0.759	10.7	10.0	-6.38
STO		16.2	15.8	0.004	0.004	11.6	13.1	0.37	0.18	202.1	133.9	7.4	2.7	0.963	0.980	14.4	10.5	-0.14
HEL		18.6	16.2	0.005	0.004	10.6	12.5	0.24	0.14	169.5	147.4	5.7	3.5	0.967	0.976	12.6	11.3	-0.04
GRA		65.8	66.7	0.018	0.018	9.4	9.4	0.23	0.22	45.3	43.6	3.8	3.5	0.993	0.920	3.5	3.4	-0.02
Jot	Min	14.0	12.8	0.004	0.003	7.0	5.7	0.00	0.00	2.7	1.5	0.0	0.0	0.496	0.640	0.3	0.1	-0.24
	Max	321.7	302.8	0.086	0.081	39.6	44.8	0.97	0.46	105.0	63.2	14.8	6.4	0.997	0.997	6.3	4.5	0.00
	Mean	75.4	68.9	0.020	0.018	16.5	18.0	0.09	0.05	24.6	18.1	1.9	0.9	0.933	0.955	2.0	1.6	-0.04

The lower limit of the mass balance gradient for the eastern region was chosen slightly lower than the lowest value found in the literature for GRA (db/dH = 0.2 m w.e./100m/a by RASMUSSEN & ANDREASSEN (2005)). The upper one was chosen according to the assumption that the mass balance gradient of 50 of the annual measured glaciers was between 0.7 and 1.0 m w.e./100m/a (MACHGUTH 2003) and the higher value was taken. In the western region, the lower and upper limit was chosen according to the values for the sub-regions of New Zealand (HOELZLE et al. 2007). The values used in the parameterization lay quite well in the middle of the chosen intervals. Therefore, the calculated values seemed to represent the possible range very well and the sensitivity analysis was successfully performed.

Additionally, a testing regarding glacier size was performed. The parameterization was applied to the data of Nigardsbreen (NIG) and compared with the values of STO, HEL, and GRA (Table 10). Nigardsbreen, an outlet glacier form the neighbouring Jostedalsbreen, was chosen because of the larger size compared with the Jotunheimen glaciers. The parameterization was constructed for larger glaciers (HAEBERLI & HOELZLE 1995; HOELZLE et al. 2007), and therefore it had to be tested, if the results fit better for Nigardsbreen than for the other (smaller) glaciers. Input data for NIG (surface area, length, minimum and maximum elevation) were mapped manually. The digital glacier outline of 1984 was used as minimum for the LIA maximum extent. For LIA maximum, the glacier outline was not changed in the upper part, but the lower part was enlarged by mapping on the satellite image (Landsat 7 ETM+). The balance at the glacier tongue and the mass balance gradient were determined in the same way as for the Jotunheimen glaciers. The value of 1.25 m w.e./100m/a was higher than the value calculated by RASMUSSEN & ANDREASSEN (2005) (0.78 m w.e./100m/a), but lay at the upper limit of the range of maritime glaciers, including western Norway (HOELZLE et al. 2003). The variables depending directly on the mass balance gradient (see Table 8) have unfortunately not been measured. Therefore, the fitting could not be tested. But remarkably differences were seen for the velocity ratio and the mean net balance between the NIG values and the values of the Jotunheimen glaciers. Only using larger glaciers for Jotunheimen and therefore deleting of the smallest ones from the parameterization (as partly already done by choosing glaciers > 0.2 km²) would however not mirror the region as a whole.

All results, from the glacier inventories as well as from the parameterizations, were in several cases only used as single values of indivi-dual glaciers, but taken as mean of the total data set. In the comparison of different regions, the statistic

population differed widely. Therefore, an analysis of significance was performed with these mean values by using a t-test. The t-test is a method to compare two means of independent probes and to test them for significance (BORTZ 2005). The test could not be performed with the inventory data, because the values of the individual glaciers were only available for Jotunheimen in this study. There were three tests in total, each run with two regions. Two-tailed significant levels of 1, 5, and 10% were used. The test between Jotunheimen and the European Alps in the 1970s/80s showed significance on the 5% level for 14 variables and no significance for six. During LIA maximum, only the volume was significant on a 10% level. Area and length did not show any significance. The test between Jotunheimen and the New Zealand Alps in the 1970s/80s was significant on the 5% level for 15 variables and not significant for seven. Neither area nor length was significant at LIA maximum. The t-test between the European and the New Zealand Alps in the 1970s was significant on the 5% level for 14 variables and not significant for four. During LIA maximum, only glacier length was significant. Regarding the input variables of the parameterization, the glacier area was not significant, neither in the 1970s/80s nor during LIA maximum in no region. The same result was seen for glacier length in the 1970s/80s, but it was significant on the 1% level for the European and New Zealand Alps during LIA maximum. All results from the t-test are shown in Appendix B.

6.2 Mapping glaciers at 'Little Ice Age' maximum

Table 11: Classification of the glacier area during LIA maximum into size intervals and comparison with 2003.

Area Interval	Number [n]		Number [%]		Mean area [km]		Cumulative Area [%]	
[km²]	LIA	2003	LIA	2003	LIA	2003	LIA	2003
< 0.1	26	75	11.16	28.63	0.06	0.06	0.56	2.29
[0.1, 0.5)	96	101	41.20	38.55	0.26	0.24	9.09	14.32
[0.5, 1.0)	37	36	15.88	13.74	0.73	0.72	18.42	27.71
[1.0, 5.0)	63	43	27.04	16.41	2.35	2.20	69.47	76.95
[5.0, 10.0)	8	7	3.43	2.67	6.87	6.40	88.42	100.00
≥ 10.0	3	–	1.29	–	11.19	–	100.00	100.00
Total	233	262	100	100	1.24	0.87	–	–

The LIA maximum extent of 233 glaciers in Jotunheimen was mapped with a total area of about 290 km² (see Figure 1). The indivi-dual parts of composite glaciers and ice caps were here referred to as single glaciers and further analyses were also made with the individual parts. The mean glacier area was 1.24 km² (Table 11). Most of the glaciers fell within the interval [0.1, 0.5) km², whereas the glaciers in the interval [1.0, 5.0) km² exhibited the largest contribution to the total area. Despite a large percentage of the overall number of glaciers

(68%), the group of smallest glaciers represented only a minor part of the total glacier area (18%). By contrast, less than 5% of all glaciers (area > 5.0 km²) constituted more than 30% of the total glacier area. Only three glaciers were larger than 10 km² at LIA maximum. The largest glacier in Jotunheimen was Østre Memurubreen with an area of 12.4 km². The maximum altitude of the glaciers ranged between 1500 and 2500 m a.s.l. with a mean of 2010 m a.s.l. (σ = 170 m a.s.l.) (Figure 23a), the minimum altitude between 1000 and 2400 m a.s.l. with a mean of 1590 m a.s.l. (σ = 206 m a.s.l.) (Figure 23b). The highest elevation range was found on Styggebreen with a range of 1396 m.

The minimum, maximum, mean, and median altitude showed a spatial differentiation, and all generally increased from West to East (see Figure 20 for mean altitude). Connection to glacier size was only visible for the minimum altitude.

a)

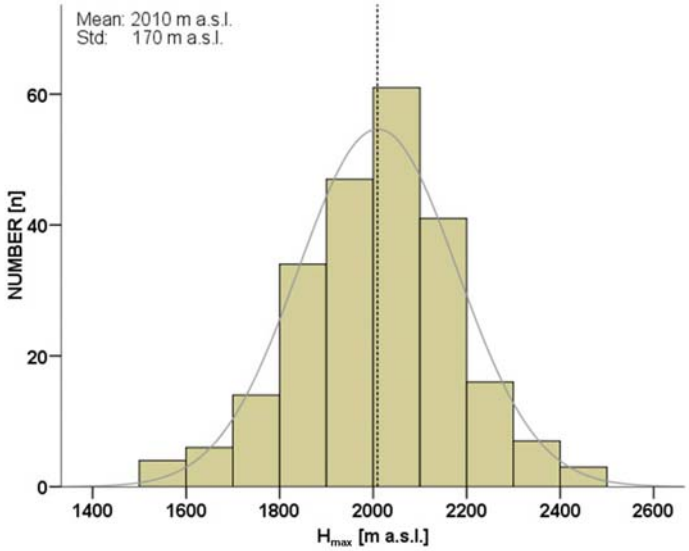

b)

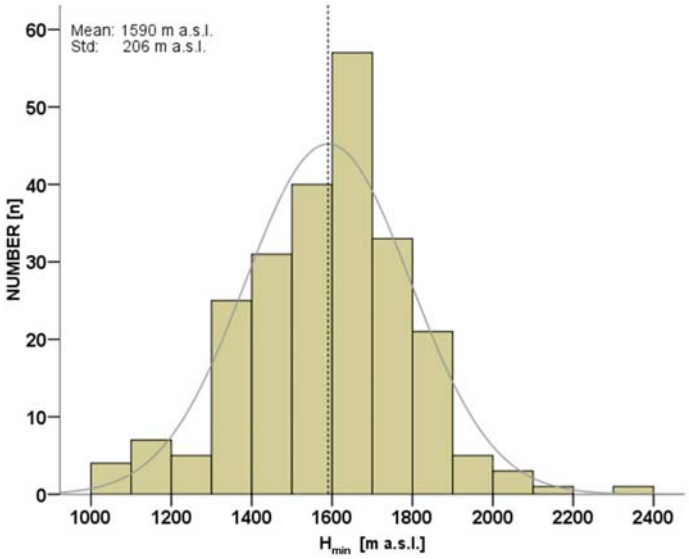

c)

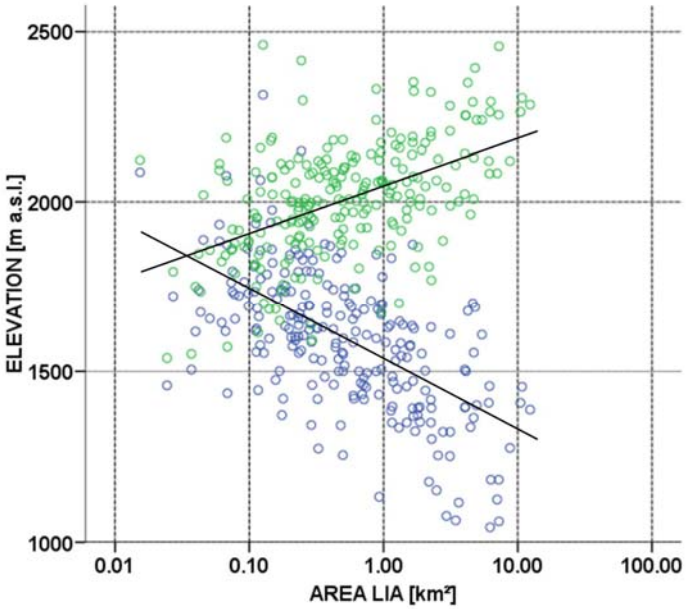

Figure 23: Distribution of glacier a) maximum altitude (H_{max}) and b) minimum altitude (H_{min}) at LIA maximum in Jotunheimen in the glacier inventory. Dashed line indicates mean, grey line normal distribution curve (Std = standard deviation). c) Scatter plot of minimum (blue dots) and maximum (green dots) elevation vs. LIA glacier area. The solid lines give the best fitting straight line of minimum and maximum elevation, respectively. Note logarithmic horizontal scale in c).

The plot of minimum glacier altitude vs. area (Figure 23c) revealed a lower minimum altitude for larger glaciers than for smaller ones. The coefficient of determination of the best fitting straight line through all points is 0.36. The coefficient of determination for the mean maximum glacier altitudes, shown in the same plot (Figure 23c), is 0.26.

a)

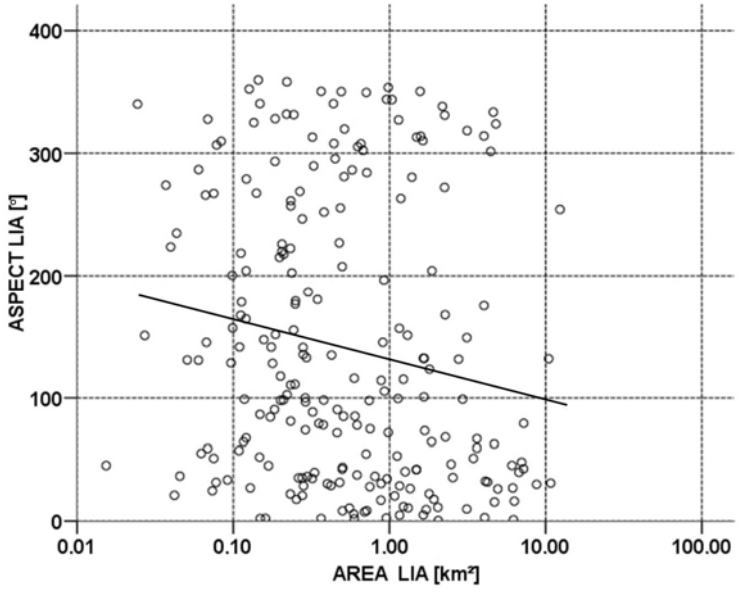

b)

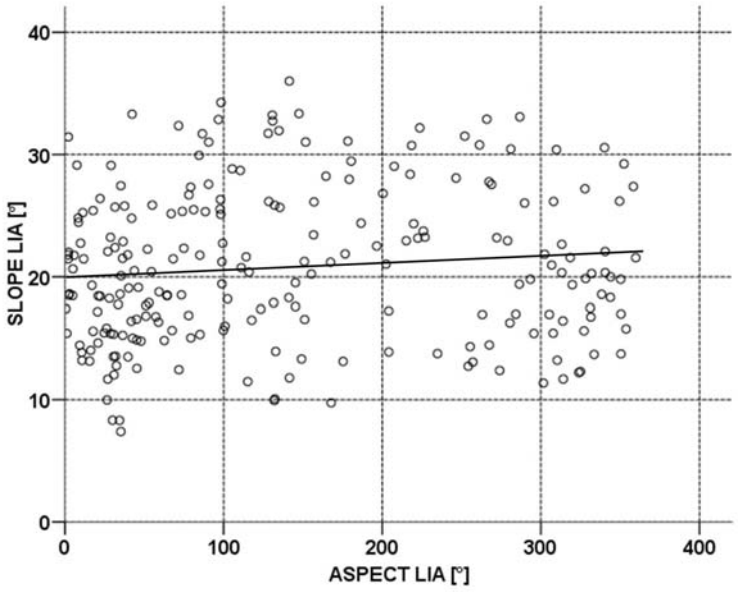

Figure 24: Scatter plot of a) mean aspect and b) mean slope of glaciers at LIA maximum vs. area at LIA maximum. The coefficient of determination of the best fitting straight line through all points is 0.03 in a) and 0.01 in b). Note logarithmic horizontal scale in a).

Scatter plots of mean aspect vs. glacier size (Figure 24a) and of mean slope vs. aspect (Figure 24b) showed no distinct pattern. Furthermore, no relationship was found between the four calculated altitudes (minimum, maximum, mean, and median) and mean aspect (Figure 25a) or slope (Figure 25b).

a)

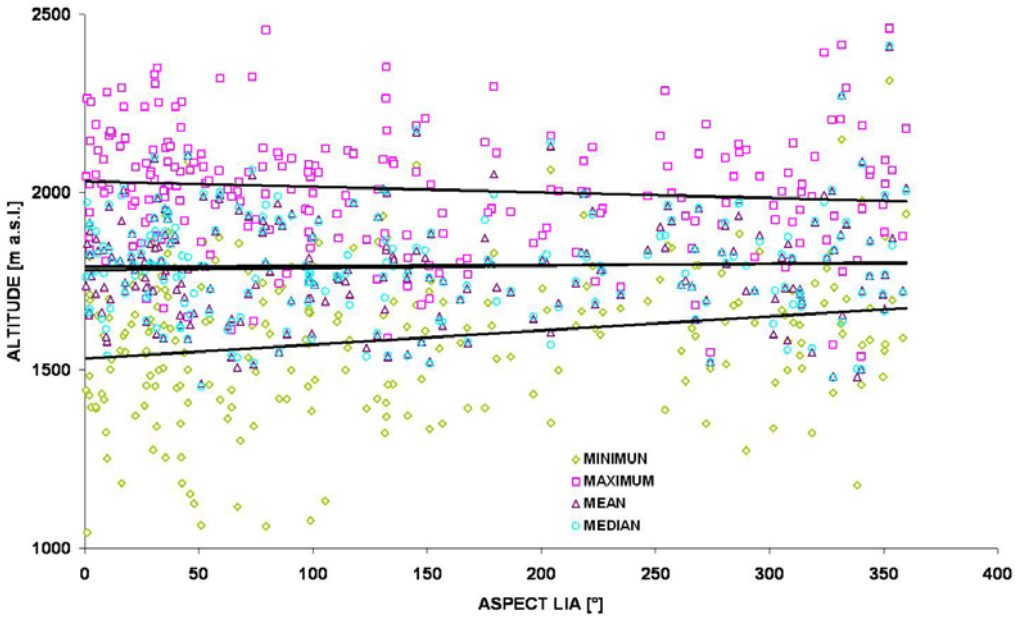

b)

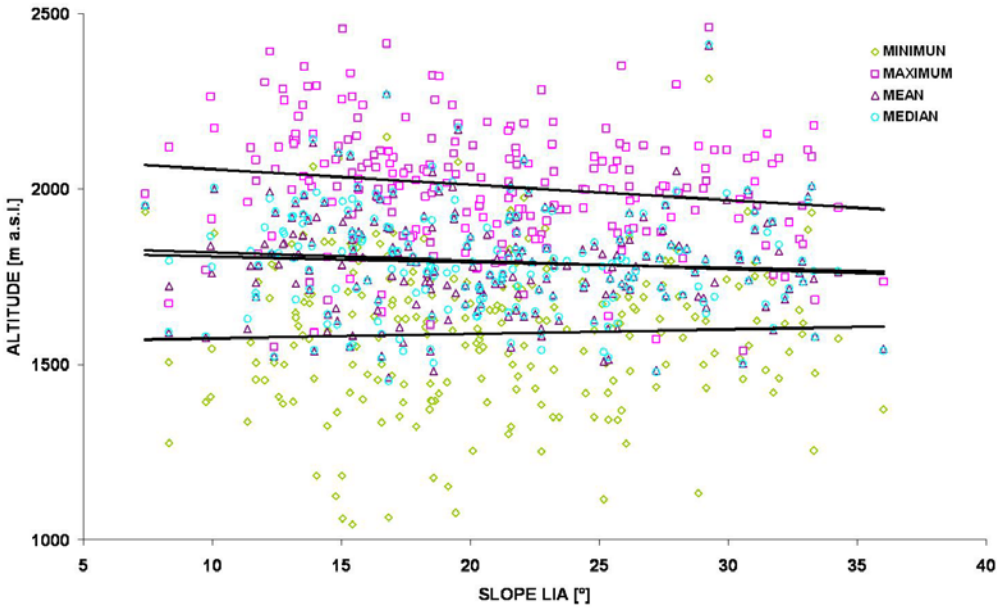

Figure 25: Scatter plot of minimum, maximum, mean, and median altitude of glaciers at LIA maximum vs. a) mean aspect and b) mean slope of glaciers at LIA maximum. The coefficient of determination of the best fitting straight line through all points is in a) for minimum altitude 0.05, for maximum altitude 0.01, for mean altitude -0.002, and for median altitude 0.0004, and in b) for minimum altitude 0.001, for maximum altitude 0.03, for mean altitude 0.005, and for median altitude 0.01.

The flowline lengths of the glaciers varied between 134 and 6818 m with a mean of 1554 m. Two thirds of the glaciers had lengths shorter than the mean. The median value was 1064 m. More than half of the lengths (50%) were in the interval [1.0, 5.0) km (Table 12). Only eight glaciers had a length exceeding 5.0 km. Søre Veobreen had the longest flowline with a length of 6818 m. 41 glaciers (18%) had more than one flowline.

Table 12: Classification of the glacier length during LIA maximum into length intervals and comparison with 2003.

Length interval [km]	Number [n]		Number [%]		Mean length [km]	
	LIA	2003	LIA	2003	LIA	2003
< 0.5	38	92	16.31	35.11	0.33	0.33
[0.5, 1.0)	70	85	30.04	32.44	0.73	0.71
[1.0, 5.0)	117	85	50.21	32.44	2.13	2.08
≥ 5.0	8	–	3.43	–	6.16	–
Total	233	262	100	100	1.55	1.02

6.3 Parameterization

The parameterization has been applied to the inventory data of Jotunheimen at LIA maximum (BAUMANN et al. 2009), the 1980s (ØSTREM et al. 1988), and 2003 (ANDREASSEN et al. 2008a). The inventory data was used as a complete

data set, but was also split in the two areas East and West with different mass balance gradients.

Some results of the total data set are presented in Table 9. Due to the area and length decrease between LIA maximum and 2003, the mean glacier length changed in all three times. It is visible by the minimum value, that some flowlines were longer in the 1980s than at LIA maximum and in 2003 than in the 1980s. This resulted from the partly problematic data-set of the 1980s, where some snow-covered areas have been included into the glacier area (ANDREASSEN et al. 2008a). The only small reduction between the 1980s and 2003 compared with the reduction since LIA maximum is visible in the mean and the maximum values. The mean slope of the glacier surface became steeper from LIA maximum over the 1980s until 2003. The difference between the 1980s and 2003, however, is only slightly. According to the reduction in glacier area, the reduction in glacier volume is visible for all three times. The calculation of the volume is based on the inverse ice-flow-law. In 2003, only about half of the volume (51%) of LIA maximum is left. The mean maximum ice thickness ranged between ~110 m at LIA maximum, ~82 m in the 1980s, and ~78 m in 2003. The maximum value is about 100 m higher at LIA maximum compared with the 1980s and more than this compared with 2003. The mean value of the balance at the glacier tongue reduced by ~25% between LIA maximum and the other two times. The value of the standard deviation is quite high, also visible at the large differences between the minimum and the maximum values of b_t. The depth-averaged mean flow velocity along the central flowline in the ablation area was taken as an assumption of the mean surface flow velocity along the central flowline in the ablation area. The mean surface flow velocity ($u_{s,a}$) slowed down between LIA maximum, the 1980s, and 2003. This variable also shows the great differences between individual glaciers by its minimum and maximum values and the standard deviation. The mean sliding velocity is very similar to the $u_{s,a}$. The velocity ratio of sliding and surface flow velocity in the ablation area is a measure of glacier dynamics and gives information about the proportion between sliding and total velocity (HOELZLE 1994). Its value is close to 100% (> 93% at all three time steps). The velocity due to ice deformation is nearly negligible (mean value 1.9 m/a at LIA maximum and 0.79 m/a in 2003). In the data analyses, the three velocities were plotted vs. several variables.

A relationship was found between the three velocities and the glacier area at LIA maximum (Figure 26a). All velocities, but especially the velocity of ice deformation increased with glacier size.There is a strong correlation between the three velocities and glacier length at LIA maximum (Figure 26b). The correlation

between the three velocities and mean slope at LIA maximum is negligible (Figure 26c).

a)

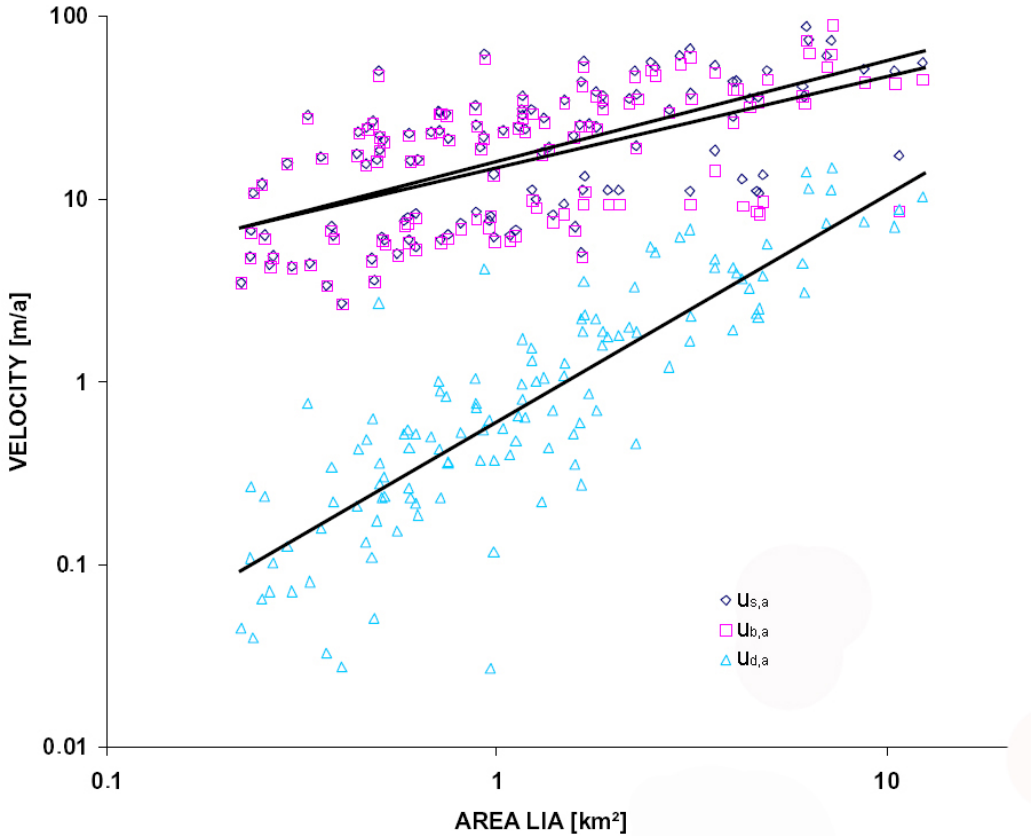

b)

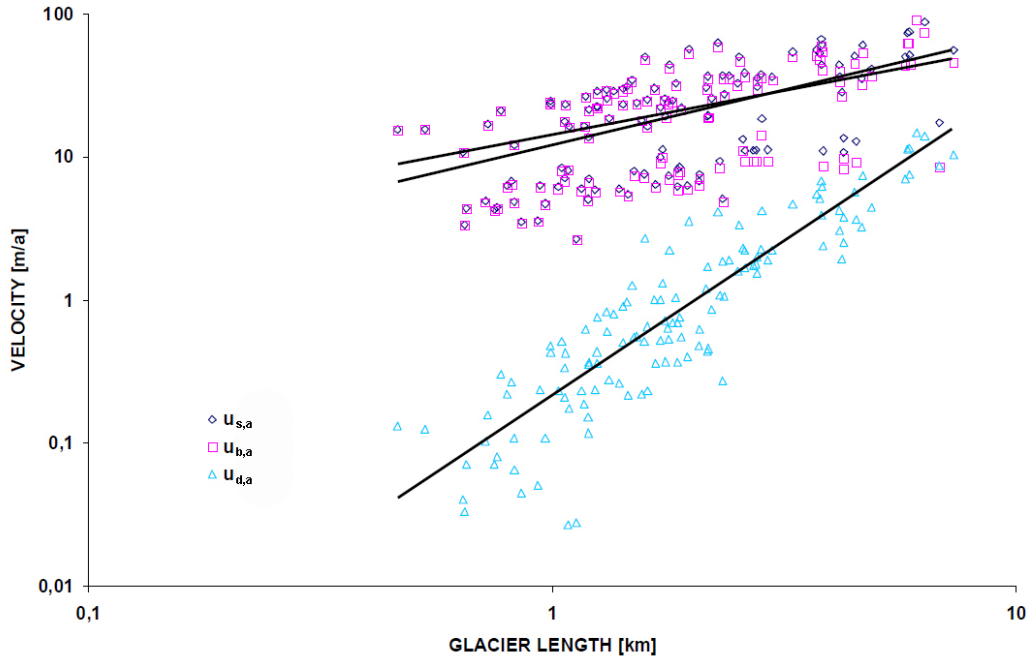

c)

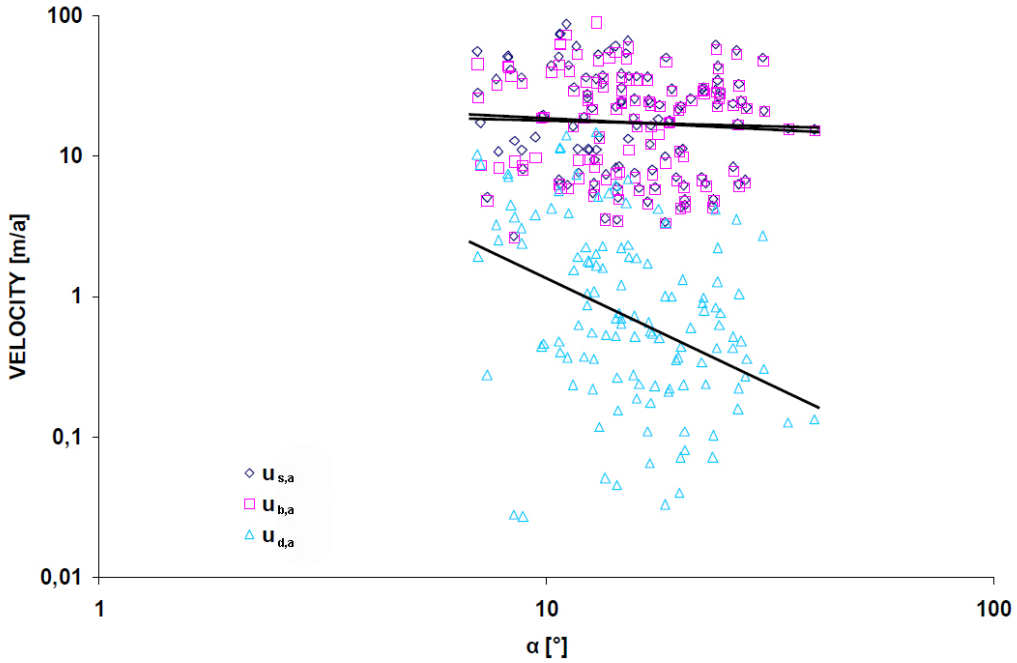

Figure 26: Scatter plot of surface flow velocity ($u_{s,a}$), velocity of ice deformation ($u_{d,a}$), and sliding velocity ($u_{b,a}$) vs. a) glacier area, b) glacier length, and c) glacier slope (α) at LIA maximum. The coefficient of determination of the best fitting straight line through all points is in a) for $u_{s,a}$ 0.41, for $u_{d,a}$ 0.75, and for $u_{b,a}$ 0.34, in b) for $u_{s,a}$ 0.41, for $u_{d,a}$ 0.81, and for $u_{b,a}$ 0.34, and in c) for $u_{s,a}$ and $u_{b,a}$ < 0.01 and for $u_{d,a}$ 0.14. Note logarithmic scale at both axes in all plots.

The response time was calculated by Equation (2). The mean response time reduced from LIA maximum until the 1980s by ~11% and increased by ~2% between the 1980s and 2003. Again, σ is very large and also the difference between minimum and maximum values. The mean value of the ELA shows an ascending of this value at all three times. Between LIA maximum and the 1980s and between the 1980s and 2003, descending values of ELA are estimated as seen at the maximum value. The mean values of the mass balance disturbance were much more negative between LIA maximum and 2003 and LIA maximum and the 1980s compared with the 1980s and 2003 (~5% remaining compared with both earlier inventories). The maximum value shows, that δb in the 1980s was larger at some glaciers than at LIA maximum. The mean value of the mean net balance halved between the 1980s and 2003 compared with both earlier time intervals. The maximum values showed a positive balance for some glaciers between LIA maximum and the 1980s and the 1980s and 2003.

The data-set of the western and eastern part of Jotunheimen has been analyzed, and a selection of results is shown in Table 13 and Table 9. The mean elevation is (H_{max} + H_{min}) / 2, and its value is taken as estimation of the ELA. The mean value rose 61 m in the western and 24 m in the easterm part between LIA maximum and 2003. The mean value differed ~100 m between the eastern and the western part in the 1980s. This is the greatest difference at all three times.

Table 13: Selection of results by the parameterization applied on inventory data from the sub-regions of Jotunheimen (W = West, E = East) at LIA maximum, the 1980s, and 2003. Differences between two times (at $\bar{b}n$) are indicated as follows: LIA = 1750 – 2003, 1980s = 1750 – 1980, 2003 = 1980 – 2003. H_{mean} = mean altitude, α = surface slope, τ = mean basal shear-stress, h_{max} = maximum ice thickness, $\bar{b}n$ = mean mass balance.

Variable/ Sta- area tistics/time		H_{mean} [m a.s.l]		α [°]		τ [bar]		h_{max} [m]		$\bar{b}n$ [m/a]	
		W	E	W	E	W	E	W	E	W	E
Mean	**LIA**	1728	1885	16.7	15.6	0.79	0.62	120.7	93.1	-0.05	-0.03
	1980s	1787	1899	18.7	16.8	0.65	0.56	88.1	71.9	-0.05	-0.02
	2003	1789	1909	18.2	16.3	0.63	0.51	86.1	66.6	-0.06	-0.11
Std	**LIA**	100	86	6.6	5.3	0.24	0.19	84.3	71.3	0.06	0.03
	1980s	113	90	8.3	5.7	0.20	0.20	66.5	57.5	0.06	0.03
	2003	110	96	7.9	5.1	0.20	0.18	65.0	55.0	0.15	0.17
Min	**LIA**	1493	1716	7.0	7.1	0.26	0.26	24.2	29.0	-0.26	-0.10
	1980s	1549	1726	8.3	5.7	0.26	0.15	18.5	25.5	-0.24	-0.08
	2003	1551	1745	7.9	7.8	0.23	0.18	20.4	24.5	-0.49	-0.76
Max	**LIA**	2010	2088	39.6	27.8	1.39	1.09	372.3	353.0	0.00	0.00
	1980s	2061	2097	44.8	31.3	1.17	0.98	248.9	272.8	0.00	0.07
	2003	2060	2202	42.1	27.5	1.14	0.93	251.7	260.0	0.33	0.03

The minimum value differed 223 m at LIA maximum, 177 m in the 1980s, and 194 m in 2003, with the higher value at all three times in the eastern part. The maximum differed between ~2 (1980s) and ~6% (2003). A difference was recognisable in mean slope: the eastern part was gentler than the western part at all three times. The mean basal shear stress is calculated by a formula connected to the altitude range (see Appendix A). If this range reaches a maximum of 1.6 km, τ is set to 1.5 bar. But this limit was not reached in Jotunheimen and the shear stress has always been calculated with the formula. It was higher in the West than in the East at all three times. The difference between West and East Jotunheimen was large for the balance at the glacier tongue, as also seen in the statistics from the 1980s in Table 14. The shown differences were about the same order at the other points of time. The mean surface flow velocity is roughly four times higher in the western compared with the eastern part at all time steps. The mean value decreased in both parts from LIA maximum until 2003. Glaciers in the western part of Jotunheimen reached equilibrium faster than the ones in the East: the response time is about three times higher in the East than in the West. The maximum value was 105 years at LIA maximum, 94 years in the 1980s, and 95 years in 2003 in the West, and 322, 302, and 254 years, respectively, in the East. In terms of the mean, the glaciers in the western part had a higher glacier thickness compared with the eastern part. But regarding the maximum values, higher glacier thicknesses are estimated for the East in the 1980s and 2003. The minimum is always lower in the western part. The mean net mass balance is lower between LIA maximum and 2003 and between LIA maximum and the 1980s in the West, and lower between the 1980s and 2003 in the East. This low value

results from the very low minimum value in 2003 (estimated for Glitterbreen, see section 8.5).

7 Comparison and interpretation

The results of the glacier inventory data at LIA maximum in Jotunheimen and the data of the parameterization of Jotunheimen were compared with data from other inventories of Norway and with other glacier regions. A connection to climate was also established on this data.

7.1 Comparison with other glacier inventories of Jotunheimen

The LIA inventory data were compared with the glacier data from 2003. To compare both points of time, each glacier of the LIA inventory was considered and not the composite ice caps. The total area declined from about 290 km^2 during LIA maximum to 190 km^2 in 2003 (-35%).

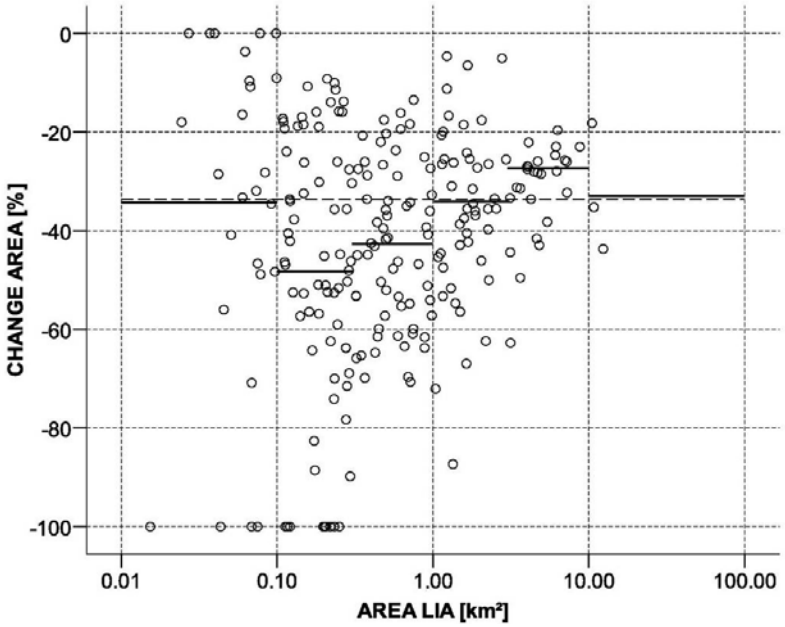

Figure 27: Scatter plot of relative area change of glacier area between 2003 and LIA maximum vs. glacier area at LIA maximum. The solid lines give mean values per size class, the bold dashed line shows the mean for all glaciers (raw data glacier outlines 2003: ANDREASSEN et al. (2008a)).

The relative area reduction between LIA maximum and 2003 is slightly higher for smaller glaciers than for larger ones, but without indicating any clear pattern (Figure 27). However, the range of change at the smaller glaciers is very large (0% – -100%). The highest reduction (-47%) is found in the interval [0.1, 0.5) km², the smallest (-28%) in the interval [5.0, 10.0) km² (see Table 11). No notable spatial pattern in area reduction could be detected between LIA maximum and 2003 (Figure 28). The spatial pattern of higher relative area reduction in the north-eastern and eastern part of Jotunheimen between the 1980s and 2003

detected by ANDREASSEN et al. (2008a) is not visible between LIA maximum and 2003.

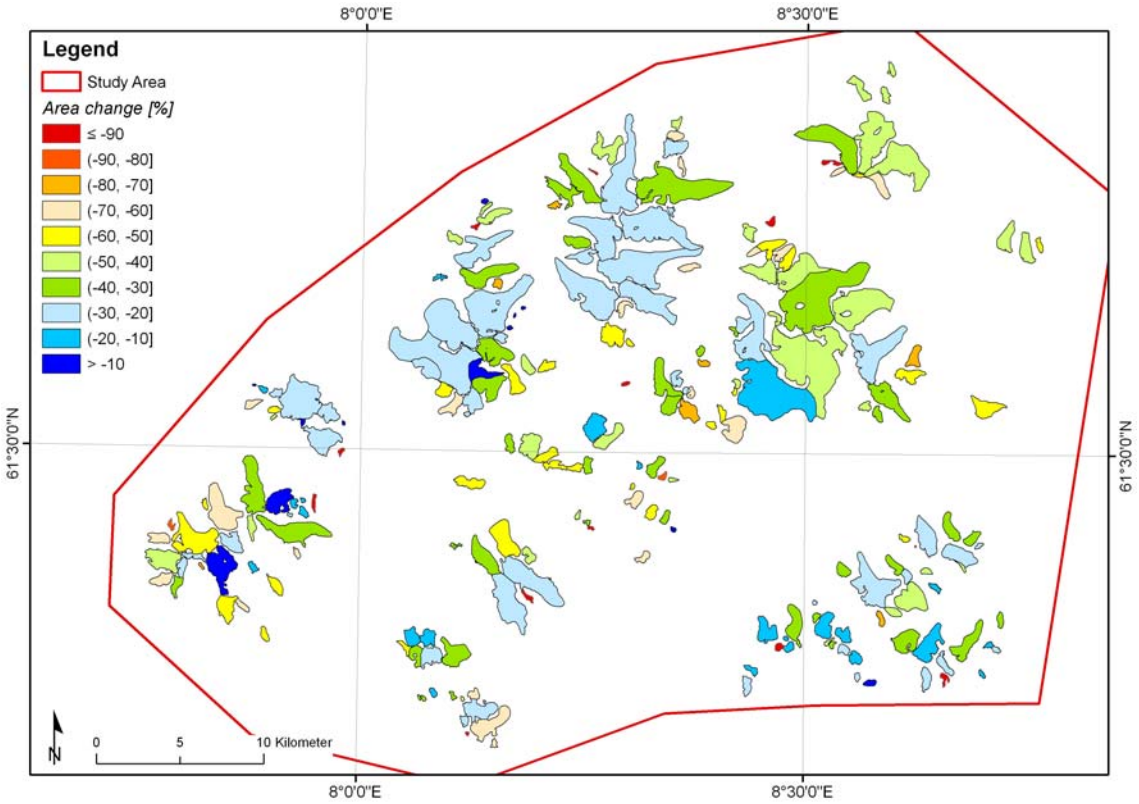

Figure 28: Colour-coded relative area change between LIA maximum and 2003 for each single glacier. Shown are glacier extents of LIA maximum (raw data glacier outlines 2003: ANDREASSEN et al. (2008a)).

The calculated hypsography in 100 m intervals of LIA maximum and 2003 (Figure 29) showed a higher absolute area loss in the lower elevations (cf. RASMUSSEN et al. submitted). The area loss in the higher elevations is only marginal. The highest absolute loss occurred at an elevation range of 1500 – 1700 m a.s.l. The increase in mean elevation (+61 m) is slightly higher than for median elevation (+55 m). As shown on Figure 30, a higher number of glaciers smaller than 0.1 km^2 existed in 2003 but non larger than 10.0 km^2. Except for these two intervals, the relative distribution of glaciers and glacier area was similar at both points of time. In total, 13 glaciers disappeared between LIA maximum and 2003, and 34 glaciers separated into two or more parts.

The mean length was reduced by 34% from LIA maximum (1.6 km) to 2003 (1.0 km). The number of glaciers with lengths in the interval < 0.5 km decreased from LIA maximum to 2003 (see Table 12). The relative number of glacier length stayed nearly the same in the size interval [0.5, 1.0) km, but declined from 50% to 32% in the interval [1.0, 0.5) km.

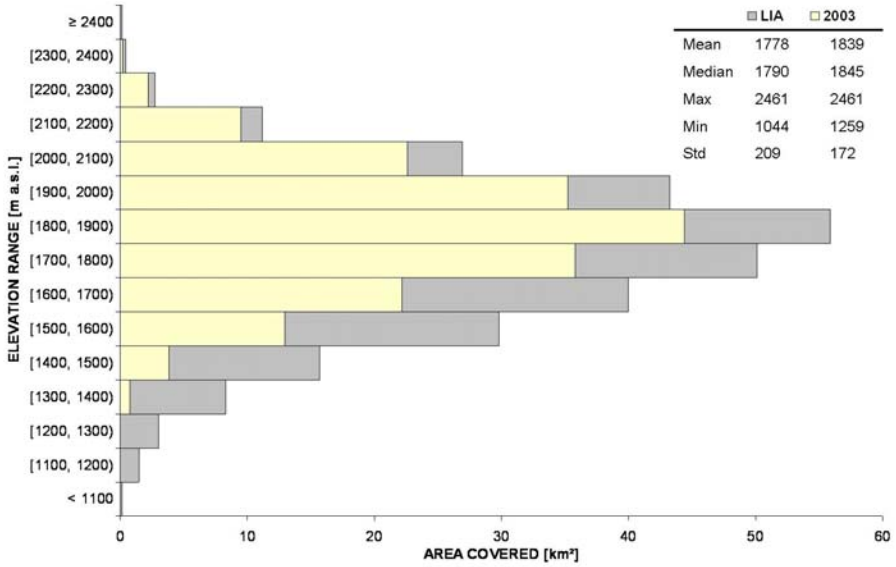

Figure 29: Glacier hypsography with 100 m contour interval for LIA maximum (grey) and 2003 (yellow) including statistical data. LIA maximum area-altitude distribution is an assumption based on the topographic map of the 1980s (raw data glacier outlines 2003: ANDREASSEN et al. (2008a)).

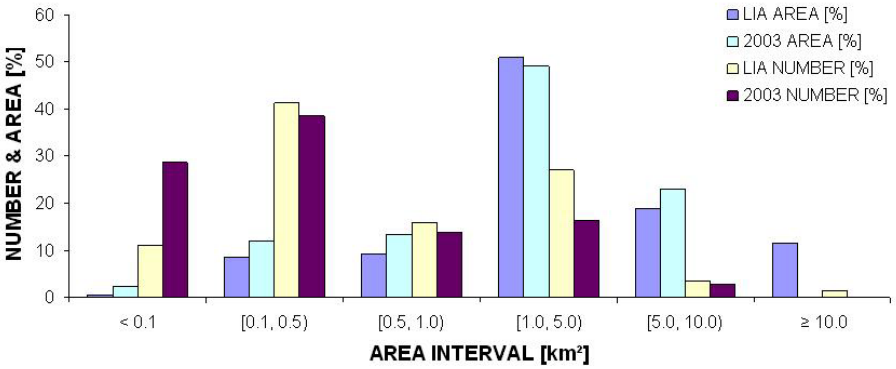

Figure 30: Comparison of area intervals between LIA maximum and 2003. Both number and area sum are compared (raw data 2003: ANDREASSEN et al. (2008a)).

7.2 Comparison with other regions

In the following, the LIA maximum results obtained for Jotunheimen are compared with similar inventories from the European Alps, the New Zealand Alps, and the Canadian Arctic. Unfortunately, no LIA inventory on a regional scale for other glacier regions of Norway is available. The parameterization data of Jotunheimen was compared with the parameterization data of the European and the New Zealand Alps.

7.2.1 Inventory data

The inventory data of the European Alps consist of input data from different alpine countries (ZEMP et al. 2008). Two examples from Switzerland and Austria are presented first before showing the total data of the European Alps.

The glacier inventory of LIA maximum in Switzerland was compiled by MAISCH et al. (2000). The area decrease from 1850 (regional LIA maximum) until 1999 is 3.4% per decade (PAUL et al. 2004b), or 51% in total. This decrease is higher than the corresponding one between LIA maximum (1750) and 2003 in Jotunheimen (~35%; ~1.3% per decade). A higher relative loss at small glaciers also occurred in Switzerland (PAUL et al. 2007). Such a difference in relative area decrease depending on glacier size was not detected in Jotunheimen. Whereas 69% of the glacier area in Jotunheimen is due to glaciers < 5 km², the corresponding number for the Swiss Alps is only 55% (ZEMP et al. 2008). At LIA maximum, a considerably higher amount of glacier area was due to glaciers > 10 km² in Switzerland (33%) than in Jotunheimen (12%).

A glacier inventory for LIA maximum (1850) exists for the Austrian Alps (GROSS 1987). It is based on moraine mapping, maps, written documents, and specific knowledge of the area (GROSS 1987). A second inventory was compiled for 1969 (ROTT et al. 1993). The glacier area decrease between 1850 and 1969 was 46% (GROSS 1987). This area loss is much higher than calculated for the Swiss Alps (27%) in a comparable period (1850 – 1973) (ZEMP et al. 2008) and for Jotunheimen in the period 1750 – 2003 (35%). The relative area loss is higher for small glaciers and glaciers in South and West exposition (GROSS 1987). Glaciers in the Austrian Alps exhibit relatively smaller sizes compared with Jotunheimen, though the maximum extent is higher. The glacier size is possibly the reason for the higher decrease in glacier area as small glaciers respond more sensitively to changes in climate (JÒHANNESSON et al. 1989a; HAEBERLI 1995; KUHN 1995; BÖHM et al. 2007).

The LIA maximum extent as well as the extent at 2000 of the glaciers in the European Alps was extrapolated from the glacier inventory of Switzerland (1850, 1973, and 2000) and the inventory data of the 1970s for the European Alps (ZEMP et al. 2008). The European Alps are a prominent mountain system with a higher number of glaciers and a larger glacier area compared with Jotunheimen. As in Jotunheimen, most of the glacier area is found in the glacier size interval [1.0, 5.0) km², but with a lower total amount of glacier area in this size class (European Alps: 29%; Jotunheimen: 51%). 7.5% of the glaciers in the European Alps are > 20 km². Here, the glacier area decreased from 1850 (regional LIA maximum) until 2000 by 49% (3.2% per decade) (ZEMP et al. 2008), a higher decrease compared with Jotunheimen between LIA maximum (1750) and 2003 (~35%; ~1.3% per decade). A strong trend of higher relative loss at small glaciers was noticed, less pronounced in Jotunheimen (see Figure 27). As described in section 4.2, glaciers in Jotunheimen and the European Alps show an asynchronous pattern due to the influence of the NAO modes (NESJE & DAHL 2003) and there-

fore poorly correlating annual net balances (GÜNTHER & WIDLEWSKI 1986; STEINER et al. 2008). Higher summer temperatures correlate well with negative mass balances in the Alps, but there is no obvious correlation with winter precipitation (ZEMP et al. 2008). Mass balance in southern Norway is, by contrast, stronger correlated with winter precipitation (NESJE & DAHL 2003; MATTHEWS & BRIFFA 2005). As a consequence, the increase in temperature affected the European Alps more strongly than Jotunheimen and caused the differences in glacier behaviour and glacier area development.

The glacier inventory data for LIA maximum in New Zealand (between ~1600 – 1900, maybe 1750) were compiled by detection of moraines on vertical aerial photos (CHINN 1996). A second inventory of the whole region exists for 1978. Many of the larger valley glaciers are debris-covered and recently formed glacier fronts calving into pro-glacial lakes (CHINN 1996). During LIA maximum, 67% of the glaciers were in the area class [1, 5) km² (in total 98% < 5 km²) (M. Hoelzle, personal communication, 07/2009). In 1978, 90% of the glaciers were smaller than 0.5 km², a shift towards smaller area intervals compared with LIA maximum (M Hoelzle, personal communication 07/2009). The area decrease from LIA maximum until 1978 is 49% (3.9% per decade) (HOELZLE et al. 2007). The relative area distribution in the New Zealand Alps and Jotunheimen is similar for LIA maximum. The reduction in glacier area since regional LIA maximum is smaller in Jotunheimen (until 2003) than in the Southern Alps of New Zealand (until 1978).

The difference in the mean minimum altitude at LIA maximum between the glaciers of Jotunheimen (1590 m a.s.l.) and the measured glaciers of the New Zealand Alps (1203 m a.s.l.) was ~400 m a.s.l. at LIA maximum (raw data New Zealand: CHINN (1996)). The difference was still more pronounced at the minimum value, showing lower reaching glacier tongues in New Zealand (range of minimum glacier elevation in the New Zealand Alps: 220 – 1951 m a.s.l. and Jotunheimen: 1000 – 2400 m a.s.l.). These data emphasize the location of Jotunheimen in a more continental and the New Zealand Alps in a maritime climatic regime. Maritime glaciers are regarded as highly sensitive to climate (KUHN 1984; LAUMANN & REEH 1993; DYURGEROV & MEIER 1999). This might mainly explain the differences between the two regions.

LIA maximum glacier extent on Baffin Island in the Canadian Arctic (occurring about 1920s (PAUL & KÄÄB 2005)) was mapped by a trimline and moraine survey using remote sensing (PAUL & KÄÄB 2005; PAUL & SVOBODA 2009). The glaciers at LIA maximum were larger compared with Jotunheimen, and only 19% were < 5 km² (PAUL & SVOBODA 2009). On Cumberland Peninsula,

a part of Baffin Island, there is no scatter towards smaller glaciers as in Jotunheimen and a dependency of relative area change on glacier size (PAUL & KÄÄB 2005). Since LIA maximum, the glaciers on Baffin Island have lost 13% (1.6% per decade) (PAUL & SVOBODA 2009), on Cumberland Peninsula 11% (1.4% per decade) (PAUL & KÄÄB 2005). The difference in glacier sizes and in climate setting compared with Jotunheimen limit, however, the value of this comparison.

7.2.2 Parameterization data

In recent studies, the parameterization was already applied to the inventory data of the European and New Zealand Alps (HAEBERLI & HOELZLE 1995; HOELZLE et al. 2007). The parameterization data of Jotunheimen was compared with the results of these studies. The three regions suited very well for comparison. The time of compiling the glacier inventories used as main basis is very similar, and the inventories show the same high level of accuracy. The inventories used as basis are:

- European Alps: early 1970s (HAEBERLI & HOELZLE 1995);
- New Zealand Alps: 1978 (HOELZLE et al. 2007);
- Jotunheimen: 1980s (ØSTREM et al. 1988).

For their parameterization, HOELZLE et al. (2007) set the date of LIA maximum extent of the New Zealand Alps arbitrarily to 1850 (owing to the lack of reliable widespread datings set to 1850, when many glaciers remained close to their LIA maximum position; see section 3.5) to perform the comparison with the European Alps at similar time scales.

Differences between the published values by HOELZLE et al. (2007) and the values presented in section 7.2 depend on rounding errors.

7.2.2.1 1970s/80s

The calculated total volume was 126 km³ in the European, 60 km³ in the New Zealand Alps, and 6 km³ in Jotunheimen. These volumes corresponded to a potential sea-level rise of 0.40 mm for the European, 0.18 mm for the New Zealand Alps, and 0.02 mm for Jotunheimen (calculated after IPCC (2007)). The mean slopes in Jotunheimen were much gentler (18.3°) than in the European (24.3°) and the New Zealand Alps (28.6°) as well as the maximum values (Figure 31a).

a)

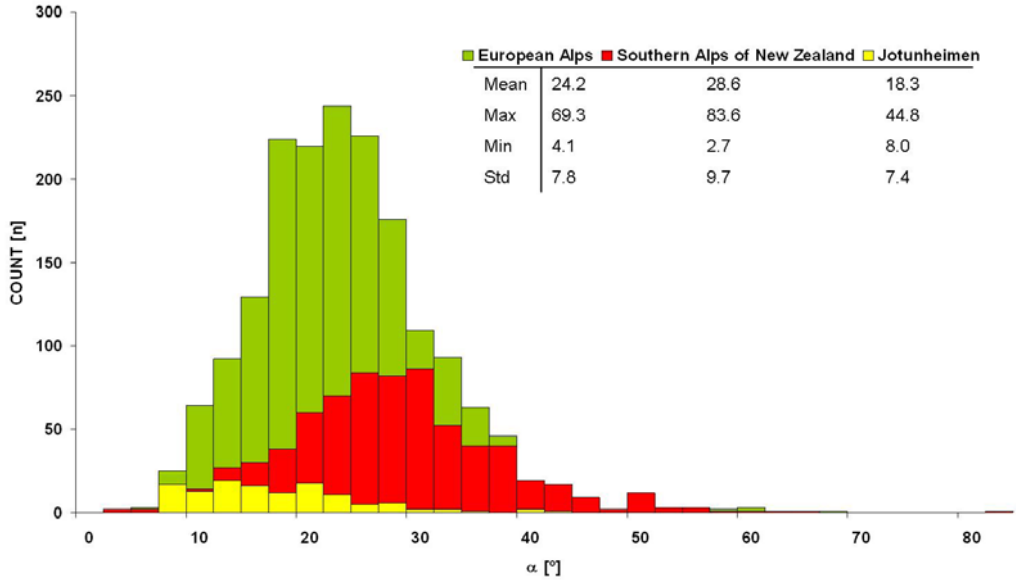

b)

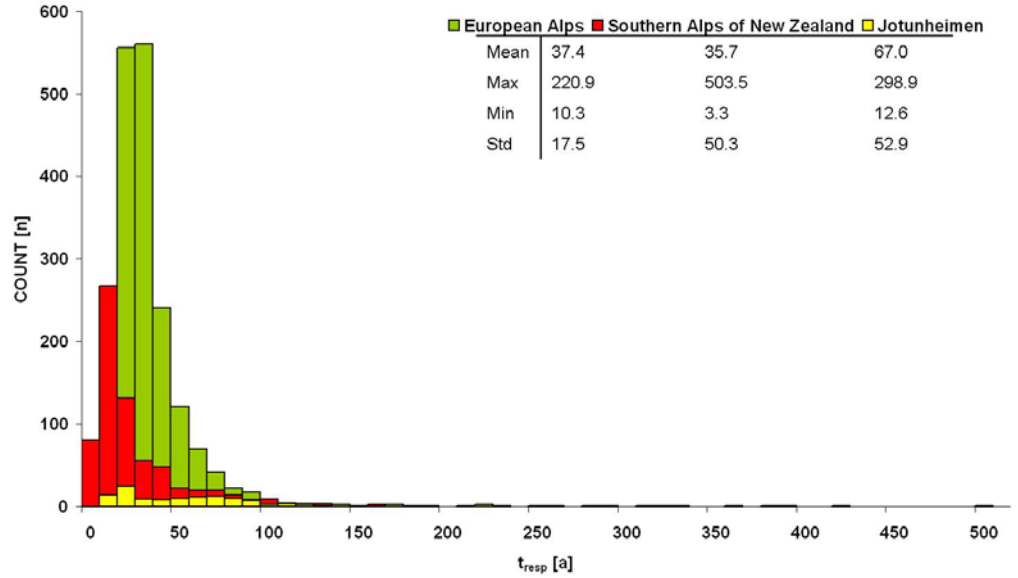

Figure 31: Distribution of glacier a) surface slope (α) and b) response time (t_{resp}) during 1970s/80s in Jotunheimen, the European, and New Zealand Alps.

The calculated ablation at the tongue (Table 14) showed the lowest mean value in Jotunheimen (1.6 m/a). It was higher in the European Alps (2.4 m/a) and twice of this in New Zealand. The maximum value was highest in the New Zealand Alps (23.9 m/a; Fox glacier), less in the European Alps (13.5 m/a; Bossons Glacier) and lowest in Jotunheimen (4.5 m/a; Styggedalsbreen). The theoretically mean time needed to reach equilibrium after a step climate change (i.e. response time) was 37.4 years in the European, 35.7 years in the New Zealand Alps, and 67.0 years in Jotunheimen (Figure 31b). The mean flow velocity varied between 15.7 m/a in the European Alps, 18.1 m/a in Jotunheimen, and 36.9 m/a in the

New Zealand Alps. The mean value of the velocity ratio ranged between 0.89 in the European, 0.95 in the New Zealand Alps, and 0.96 in Jotunheimen.

Table 14: Statistics for the parameterization results of the ablation at the glacier tongue in the ablation area (b_t) in 1970s/80s for Jotunheimen, the European and New Zealand Alps, and sub-regions.

Region / b_t [m/a]	European Alps	New Zealand Alps	Jotunheimen	Jotunheimen	
				West	East
Mean	2.4	4.8	1.6	2.1	0.6
Max	13.5	23.9	4.5	4.5	1.2
Min	0.2	0.2	0.2	0.7	0.2
Std	1.5	3.6	1.0	0.8	0.2
Number [n]	1763	702	125	78	47

7.2.2.2 Reconstruction of 'Little Ice Age' maximum

The difference between Jotunheimen and both other regions is the existence of glacier inventory data for the whole region at LIA maximum. Therefore the parameterization could be applied in Jotunheimen in the same way as for the 1980s (see section 6.3). For the European and the New Zealand Alps, no comparable inventory data set was available; only selected parts of the European Alps have LIA inventories (e.g. Switzerland).

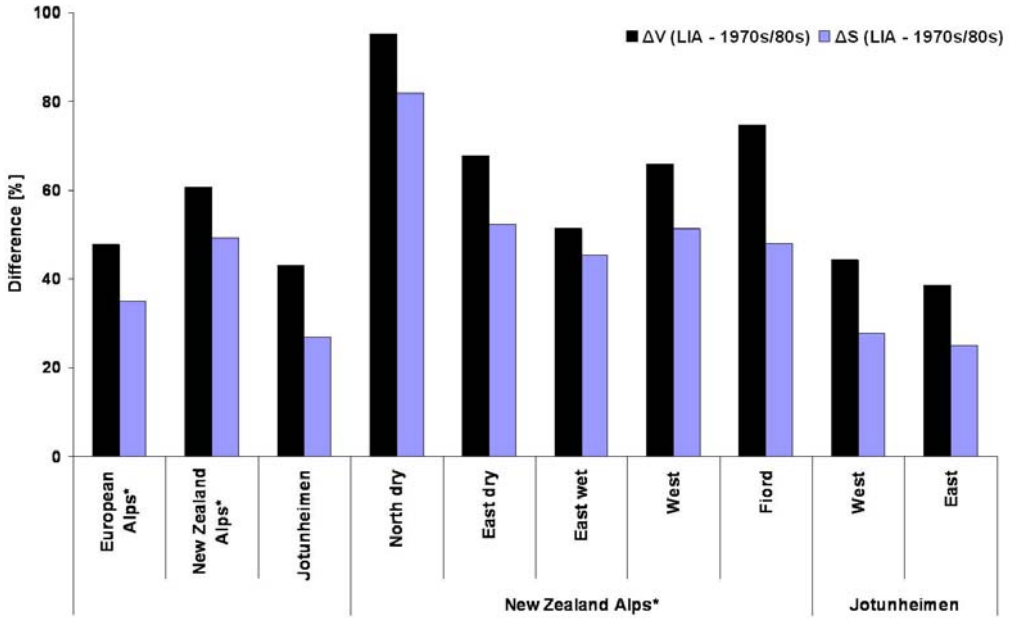

Figure 32: Development of the glacier surface area and volume between LIA maximum and 1970s/80s in Jotunheimen, the European and New Zealand Alps, and sub-regions. Difference between two points of time in [%]. *Data from HOELZLE ET AL. (2007).

Surface area, length, volume, and mean specific mass balance were reconstructed for the European Alps by HAEBERLI & HOELZLE (1995) and for the New Zealand Alps by HOELZLE et al. (2007), calculated slightly different than shown in

Appendix A. In their reconstruction, the mean mass balance of the 1970s was used to calculate glacier length at LIA maximum, using Equ. (1). The area at LIA maximum was calculated using an area/length relationship. The volume was calculated with these values. Measured area and length values were used to verify and correct the chosen net mass balance values. The comparison of Jotunheimen was performed with the four variables mentioned above.

An overview of the development of the glacier surface area between LIA maximum and the 1970s/80s is given in Table 15 and Figure 32. The relative area loss between LIA maximum and the 1970s/80s was highest in the New Zealand Alps and lowest in Jotunheimen. The comparison between the more maritime and more continental sub-regions of the New Zealand Alps and Jotunheimen showed no large difference. All 'dry' glacier regions in New Zealand (North dry, East dry) had an extent of 261 km² at LIA maximum and reduced to 123 km² (- 53%) in 1978. The 'wet' glacier regions (East wet, West, Fjord) decreased by about 49% during the same period. In Jotunheimen, the reduction of area in the more maritime West was about the same as in the eastern part and showed therefore a smaller difference (1.5%) than between the sub-regions of the New Zealand Alps (36.6%).

Table 15: Development of a) the glacier surface area and b) the glacier volume between the LIA maximum and the 1970s/80s in Jotunheimen, the European and New Zealand Alps, and sub-regions. ΔS, ΔV = Difference of surface area and glacier volume, respectively, between two points of time, EU = European, NZ = New Zealand, Jot = Jotunheimen. *Data from HOELZLE et al. (2007).

a)

Area S [km²]	EU Alps*	NZ Alps*	Jot	NZ Alps*					Jot	
				North dry	East dry	East wet	West	Fiord	West	East
LIA	3914.61	1931.66	249.83	3.81	257.39	640.43	951.67	78.36	181.56	68.27
'70s/'80s	2544.38	978.75	182.50	0.69	122.80	350.26	464.20	40.80	131.38	51.13
ΔS [km²]	1370.23	952.91	67.33	3.12	134.59	290.17	487.47	37.56	50.18	17.15
ΔS [%]	35.0	49.3	26.9	81.9	52.3	45.3	51.2	47.9	27.6	25.1

b)

Area V [km³]	EU Alps*	NZ Alps*	Jot	NZ Alps*					Jot	
				North dry	East dry	East wet	West	Fiord	West	East
LIA	241.35	170.10	10.67	0.16	16.71	66.4	80.98	5.82	8.00	2.67
'70s/'80s	126.00	66.77	6.08	0.01	5.38	32.37	27.56	1.48	4.44	1.64
ΔV [km³]	115.35	103.33	4.59	0.15	11.34	34.03	53.42	4.35	3.56	1.03
ΔV [%]	47.8	60.7	43.0	95.1	67.9	51.3	66.0	74.8	44.5	38.6

The pattern of volume change between LIA maximum and the 1970s/80s was slightly different from the area development (Table 15b and Figure 32). Most of the relative volume was lost in the New Zealand Alps. The relative loss in the

European Alps and Jotunheimen was quite similar. In the sub-regions, a difference was visible in the New Zealand Alps. The volume declined from 153 km³ during LIA maximum to 61 km³ (- 60%) in 1978 in the 'wet' glacier regions, and from 17 km³ to 5 km³ (- 68%) in the 'dry' regions. The difference between the eastern and the western regions in Jotunheimen (6%) was smaller compared with the sub-regions of New Zealand (43.8%).

During LIA maximum, most glacier lengths in all regions lay in the interval [1.0, 5.0) km (Table 16a). In the 1970s/80s, most of the lengths of the flowlines were found in this interval, but relatively less than before. The flowlines decreased between these two points of time, and relatively more were found in the interval [0.5, 1.0) km. The maximum length decreased in the European Alps from 27.2 to 24.7 km (both Aletsch Glacier), in the New Zealand Alps from 29.8 to 28.5 km (both Tasman glacier), and in Jotunheimen from 7.3 (Østre Memurubreen) to 5.1 km (Søndre Veobreen). An overview of all length intervals in the sub-regions is given in Table 16b.

Table 16: a) Classification of the length of the glacier flowline during LIA maximum and in the 1970s/80s into size intervals for Jotunheimen, the European, and New Zealand Alps, and b) for sub-regions of Jotunheimen and the New Zealand Alps. EU = European, NZ = New Zealand, Jot = Jotunheimen. Numbers in [%] at a) and in [n] at b), length interval in [km].

a)

Region / Length interval	EU Alps		NZ Alps		Jot	
	LIA	'70s	LIA	'78	LIA	'80s
Number [%]						
< 0.5	0.1	1.5	1.7	7.1	0.8	3.2
[0.5, 1.0)	3.6	32.7	21.8	38.3	16.0	35.2
[1.0, 5.0)	91.3	62.0	71.7	49.9	76.8	60.8
[5.0, 10.0)	4.1	3.5	3.6	3.6	6.4	0.8
≥ 10.0	0.9	0.3	1.3	1.1	-	-

b)

Region / Length interval	NZ Alps								Jot			
	North dry		East dry		West		Fjord		West		East	
	LIA	'78	LIA	'78	LIA	'78	LIA	'78	LIA	'80s	LIA	'80s
Number [n]												
< 0.5	-	-	-	5	8	24	4	14	1	4	-	-
[0.5, 1.0)	-	-	6	55	62	88	30	30	8	23	12	21
[1.0, 5.0)	2	2	122	68	210	169	29	19	62	51	34	25
[5.0, 10.0)	-	-	-	-	17	17	-	-	7	-	1	1
≥ 10.0	-	-	1	1	5	4	-	-	-	-	-	-

The mean specific net mass balance for the time period between LIA maximum and the 1970s/80s was calculated in all three regions. A value of -0.33 m w.e./a was taken for the European Alps. In the New Zealand Alps, the

values varied between -1.25 m w.e./a in the 'wet' areas and -0.54 in the 'dry' areas. In Jotunheimen, a mean value of -0.05 m w.e./a for the western part was calculated, and -0.03 m w.e./a for the eastern part.

7.3 Relationship to climate

The connection between glacier behaviour and climate and climate change has already been addressed in previous sections. On the smallest scale, a climate gradient was visible in Jotunheimen between the two sub-regions. The lower mean elevation in the West is a sign of maritime regime (WINKLER 2009). Reasons for the same assumption concerning climate regime gave the higher values of the balance at the glacier tongue, the faster surface flow, ice deformation, and sliding velocities, and the shorter response time in the West. But the steeper slopes and the higher shear stresses in the West pointed towards more continentality compared with the East. The net balance gave no clear signal. In the first two periods, the western part is more maritime, in the last one the eastern part. These results gave no unambiguous picture, but a tendency of the relation West – maritime and East – continental. These first conclusions were combined with the knowledge about the occurrence of double-ridged moraine walls mostly in the western part and of ice-cored moraines as well as of high-altitude polythermal glaciers in the East. Therefore, the assumption of a more maritime western and a more continental eastern part seems consistent with the resulted assumptions of the inventory and parameterization data.

Regarding southern Norway, the connection between glacier and climate is analyzed on a larger scale than before. The influence of the NAO was explained in sections 3.3 and 4.2 and also the stronger impact on maritime than on continental glaciers in Norway. The difference of this influence is seen in comparing area and volume development between LIA maximum and the 1980s of NIG, STO, and HEL (see Table 10 a and b). GRA cannot be used for this comparison because of its different behaviour due to its ice-cored moraine (see section 3.4). The glacier area of NIG decreased by 9% during the indicated time interval, the area of STO by 26%, the area of HEL by 24%, and the total area of Jotunheimen by 27%. The higher loss at the more continental glaciers showed the higher influence of precipitation on the more maritime glaciers and the higher influence of temperature on the continental ones. The difference in volume loss is not as pronounced as for the glacier area. NIG lost 34%, STO 51%, HEL 42%, and total Jotunheimen 43%. However, this indicates the lowest volume reduction on NIG,

caused by the same reasons as for the area reduction. The minimum altitude is lower at NIG as on all glaciers in Jotunheimen and the surface slope of NIG is about half of the mean value in Jotunheimen at LIA maximum and the 1980s. The calculated mean net balance by the parameterization for STO and HEL between the 1980s and 2003 is -0.24 and -0.35 m/a, respectively and for NIG and Ålfotbreen 0.46 and 0.26 m/a, respectively (raw data NIG and Ålfotbreen: KJØLLMOEN (2004)). This shows the continental influence mirrored in the mass balance data of the Jotunheimen glaciers, resulting in a mass loss due to temperature and a lower influence of precipitation. This is underlined by the circumstance, that the increase in volume since the 1990s in maritime Norway was only slightly visible in Jotunheimen. The reversed effect is seen at the two maritime glaciers NIG and Ålfotbreen.

On a large scale, by comparing Jotunheimen, the European, and the New Zealand Alps, a connection with climate was made. Arctic Canada was not included in this interpretation. Results of the comparisons are found in the previous section. The highest area and volume loss of all three regions was calculated for the New Zealand Alps. Because of the very sensitive reaction of maritime glaciers to climate changes, the New Zealand Alps were categorized as the most maritime region in this comparison. The stated minimum of the minimum elevation in the inventory data and the calculated value of the same variable by the parameterization (see Figure 21c) had the lowest value in the New Zealand Alps. It is about 300 m a.s.l. and combined with the very high precipitation and the latitude of the area showed a very maritime climate. Regarding the ablation at the glacier tongue in all three regions, the lowest mean values were calculated in Jotunheimen and, therefore, would implicit a lower mass turnover. That is a sign of a more continental regime (WINKLER 2009). The estimation of the response time was highest in Jotunheimen, and glaciers with longer response times are common in more continental regions. The highest mean surface velocity of all three regions was calculated in the New Zealand Alps, also a signal of maritime influenced glaciers. Jotunheimen and the European Alps showed only about half of that. The gentle slopes and the very low mean net balance in Jotunheimen implicated a more continental regime (WINKLER & NESJE 2009). All these results would imply Jotunheimen as the most continental region in this comparison. Beyond the parameterization results, the high correlation coefficient between net and summer balance (see section 4.1.4) would also indicate a more continental regime for the glaciers in Jotunheimen. Therefore, the results from the inventory and from the parameterization data show a clear order. The New Zealand Alps

are the most maritime region, the European Alps have a transient regime, and Jotunheimen exhibit the most continental one in this comparison.

The NAO index implies an antiphase relationship between the European Alps and South Norway (HAEBERLI 2004): a positive NAO index results in lower summer temperatures and especially high winter precipitation in southern Norway (NESJE et al. 2001; MATTHEWS & BRIFFA 2005; NESJE 2005), whereas a temperature rise and low precipitation over the European Alps is recorded (HURRELL 1995; NESJE & DAHL 2003; HOLZHAUSER et al. 2005; FEALY & SWEENEY 2007; MATTHEWS & DRESSER 2008). A negative NAO index is related to the reversed situation with dry conditions in northern Europe and wet conditions in central and southern Europe. This circumstance may also explain the different LIA advances in Scandinavia and the European Alps (SOLOMINA et al. 2008). Therefore, the glacier maxima in the European Alps during the LIA and more recently the readvances during the 20th century did not occur at the same time in southern Norway (GÜNTHER & WIDLEWSKI 1986; GROVE 2004; MATTHEWS & BRIFFA 2005).

8 Discussion

The discussion focuses on a detailed view of critical topics, not or only slightly addressed in the preceding sections.

8.1 Uncertainties in mapping

When mapping the LIA maximum outlines, the outermost moraine was assumed to represent the glacier maximum during LIA. An analysis of the age of moraines is not possible via remote sensing, but dating was based on extensive previous studies (see section 4.4.2). The outermost moraine represents the LIA maximum, and pre-LIA moraines in close vicinity were absent. Exceptions are ice-cored moraine systems at some high-altitude cirque glaciers in East Jotunheimen, e.g. at Gråsubreen (ØSTREM 1964). Their outermost ridges could well pre-date the LIA, although evidence is sparse (e.g. ØSTREM (1964); WINKLER (2001); SHAKESBY et al. (2004, 2008)).

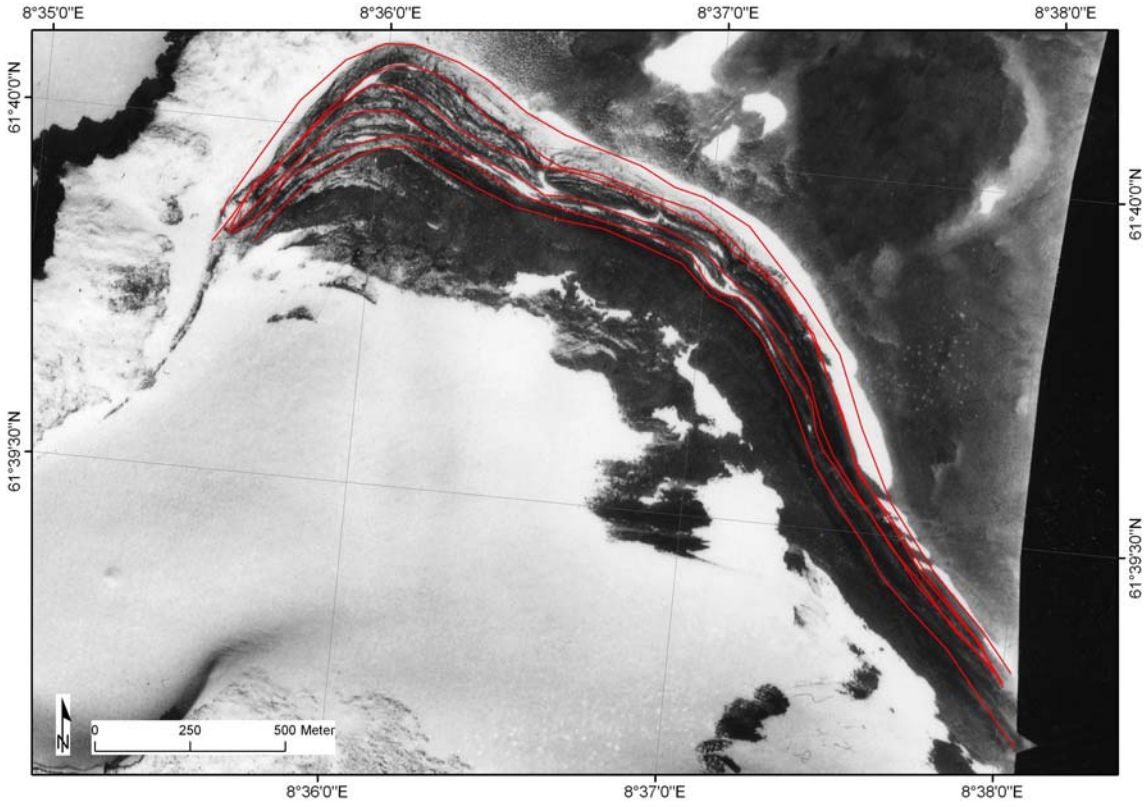

Figure 33: Front section of Gråsubreen (GRA) with six indicated moraine walls. See Figure 1 for location (Aerial photo: Fjellanger Widerøe, 29.08.1981, 7084 18–3 14).

Due to short distances between the individual ridges, the possible error by non-exact location of the ridge representing the maximum LIA position within these complex moraine systems are considered to be small. At Gråsubreen, a comparison of the LIA maximum glacier area using six different moraine walls as LIA maximum glacier limit (Figure 33) showed a coefficient of variance of 4.5%. Hence, the uncertainty resulting from not knowing the precise position of the LIA maximum moraine at undated ice-cored moraine systems can be neglected.

Another uncertainty is the unknown LIA maximum topography which affects the accuracy of the inventory parameters. For example, the slope calculation using the present deglaciated glacier foreland differs from the slope of the former glacier tongue. Estimations of mean, median and maximum altitude are also influenced by the lack of known LIA maximum glacier surface topography. The drainage basins might also be different at the LIA maximum, but this is difficult to account for in the analyses. The dimension of the uncertainty concerning topography is hard to estimate though. Reconstructions of surfaces at LIA maximum could be possible, but will nevertheless be an estimate as no reliable maps are available for validation.

As mentioned in section 5.3.1.4, all glaciers smaller than 0.01 km^2 were removed from the inventory because of uncertainties in mapping. In particular, it is difficult to distinguish perennial snow patches from small glaciers at this size (PAUL & ANDREASSEN 2009). Using a larger glacier minimum size revealed that an exclusion of the smallest area interval would, indeed, alter the results concerning disappeared
glaciers. In the original dataset, 13 glaciers disappeared between LIA maximum and 2003. Nine glaciers disappeared between LIA maximum and 2003 if all glaciers < 0.1 km^2 at LIA maximum were excluded. These nine glaciers ranged between 0.11 and 0.25 km^2 at LIA maximum. In relative numbers concerning the total glacier number, 5.6% of the glaciers disappeared with the original dataset and 5.0% with LIA maximum and 2003 area > 0.1 km^2. If only the mapped glacier area at LIA maximum is changed, 4.3% of the glaciers disappeared with LIA maximum area > 0.1 km^2.

Mapping should preferably be an objective process with clear rules and a high degree of reproducibility independent of the analyst. In reality, however, different analysts will, as a result of subjective interpretation, never produce the exactly same results (cf. ANDREASSEN et al. (2008a); PAUL & ANDREASSEN (2009)). Therefore, including any kind of objective analysis would be desirable. Using

supervised or unsupervised image classification was unfortunately not successful in this study (see section 5.3.1.1). Thus, objectivity was sought by using a larger number of different sources of the same area, i.e. the comparison of different image sources and the verification with the ground truth data.

For the inventory, glacier length was derived by using the mean of all tributaries to compare lengths at LIA maximum and 2003. The results represented those glaciers as a whole, but the purely theoretical character of this value should be kept in mind. This is especially important, because the utilization of the mean glacier length is very critical by suppressing the individual signal of the glaciers (M. Hoelzle, personal communication, 09/2009). Additionally, the connection point of the flowlines of the different tributaries is only estimation. With different methods, e.g. by selecting the maximum flowline, a length that actually is measured on the glacier could have been chosen. But, contrary, by choosing this method, only a part of the glacier is taken into account. Regarding branched flowlines, the change in maximum value for two points of time might cause a change of the corresponding tributary. The flowlines would not longer be identical, and a comparison would be impossible. Changes in the mean value refer to all tributaries and remain, therefore, comparable. Generally, it is not evident, from which branch the largest mass flux is coming, if there have been no other measurements. Three glaciers with mass balance measurements (STO, HEL, and GRA) are available for Jotunheimen, but detailed data of stake readings were not published or available for this study. By not being the main purpose of this study to go into more detail on mass balance of individual glaciers, deeper research on this topic was not initiated. Theoretically, a coincidence of the largest mass flux with the maximum length does not necessarily occur because of higher dependency on glacier area and volume. Therefore, calculating the mean glacier length from the one to three flowlines for each glacier was considered to be an appropriate method for recording glacier centrelines at LIA maximum.

8.2 Methodological challenges in remote sensing methods

Mapping glacier outlines at LIA maximum using aerial photos had some limitations. As mentioned in section 5.3.1.2, only 86% of the glacierized area was covered by aerial photos (see Figure 15). Furthermore, due to distortion and displacement towards the edges of the individual photos, the effective working size was even smaller than the whole photo. Finally, it was sometimes difficult to detect the moraine ridges in cases where stereo pairs were missing. A general

disadvantage of using aerial photos is the time required for preparation. Each single photo had to be referenced separately. Depending on the number of photos needed to cover the study area, the process of orthorectification and geo-referencing of the aerial photos took much longer in total compared with processing the satellite image. Despite multiple use of some GCPs, the processing time was almost the same for each photo. The big advantage of the aerial photos, however, is their high resolution (0.4 m x 0.4 m). Objects could be identified very precisely, whereas the resolution of the satellite image (30 m x 30 m) is a limiting factor.

As already mentioned in section 5.1.3, possible sources of error in using remote sensing in high altitudes for glacier detection are cast shadow and debris-covered glaciers (SIDJAK & WHEATE 1999; PAUL 2001; KÄÄB et al. 2002; BOLCH & KAMP 2006; RAUP et al. 2007). Complications due to these features especially occur in mapping the actual glacier extent on the source image and by using automatic mapping methods. Nonetheless, possible problems caused by both in mapping glaciers at LIA maximum manually are shortly outlined here. Shadowed areas were mostly found in the high-altitude accumulation areas and not on the low-lying glacier forelands important for mapping LIA maximum. Furthermore, considering cast shadow is easier in manual mapping than in automatic classification. No systematic error is produced during the mapping process, and each single shadowed area is controlled manually. Therefore, cast shadow was not a problem for the calculation of the LIA maximum extent. Additionally, shadowed areas on the aerial photos were in many parts not totally black, and especially snow was still visible.

In the study area, there is only little debris cover on the glaciers. Because of not mapping the present glaciers on the image, this circumstance did not generate any problems. On the satellite image, the glacier foreland shows the same structural and spectral signal as debris-covered glaciers. Because of manual mapping, all glacier forelands were detected correctly. In remote sensing, there is an unsolved problem in (semi-)automatic mapping of debris-covered glaciers (PAUL et al. 2004a; BOLCH & KAMP 2006; BOLCH et al. 2008). Hopefully due to increasing effort on this topic, (semi-)automatic mapping methods will become possible for detection of glacier forelands. Altogether, neither cast shadow nor debris cover was a source of error.

A comparison of the inventory data would have been possible with the glacier inventories of the 1960s and 1980s of Jotunheimen. This data is available, although the digital glacier outlines from the 1980s exhibit large errors (doubled

compared with the inventories of LIA maximum and 2003 (ANDREASSEN et al. 2008a)) because of mapping glaciers and snow areas (ANDREASSEN et al. 2008a). Therefore, a comparison based on the printed glacier inventories by ØSTREM & ZIEGLER (1969) and ØSTREM et al. (1988) would be the more reliable solution. Unfortunately, only the variables recorded in these reports can be used, meaning a restriction concerning the variety of comparable variables. A comparison of glacier lengths would be not possible because of the unknown position and course of the flowline on the glacier. This was the reason why the digital glacier inventory of the 1980s was used for the parameterization despite these errors, because glacier length was one of the absolutely necessary input data.

Another restriction is the notation of the glaciers in these inventories, by IDs as well as by names. A unique ID was at last given to each glacier in the inventory of 2003. In the older volumes, glaciers are indicated differently from volume to volume. Therefore, a comparison with these inventories resulted in challenges of finding the correct glaciers. Because not all glaciers could be identified correctly, this would have resulted in a comparison of almost only the larger glaciers. Therefore, this comparison was not made due to representativity. Nonetheless, a splitting of the large time interval between LIA maximum and 2003 will bring more information about the distinct development and can then also be related more profoundly to climate parameters and climate changes.

8.3 Comparison of sources

For about one third of the aerial photos the accuracy of fitting was not satisfying. In those cases, close examination of the sources revealed differences between contour lines from the topographical map (N50) and the DTM25 (mean altitudinal error = 3.3 m, σ = 12.6 m) (Figure 34). Those were possibly related to interpolation errors because they were in the range of the RMSE (see section 5.2). To quantify the impact of this difference on mapping LIA maximum extents, several aerial photos were orthorectified again using only the DTM25. The areas at LIA maximum digitized with these orthophotos were compared with the first results. The coefficient of determination was close to 1 (r^2 = 0.9997). Thus, the error regarding the resulting LIA maximum areas could be ignored and errors in orthorectification of the aerial photos were assumed to be negligible. The reported difference in fitting might be caused by the altitude range on each aerial photo (often exceeding 1000 m). The determined deviation is in equal range compared with other studies (e.g. CSATHO et al. (2008)).

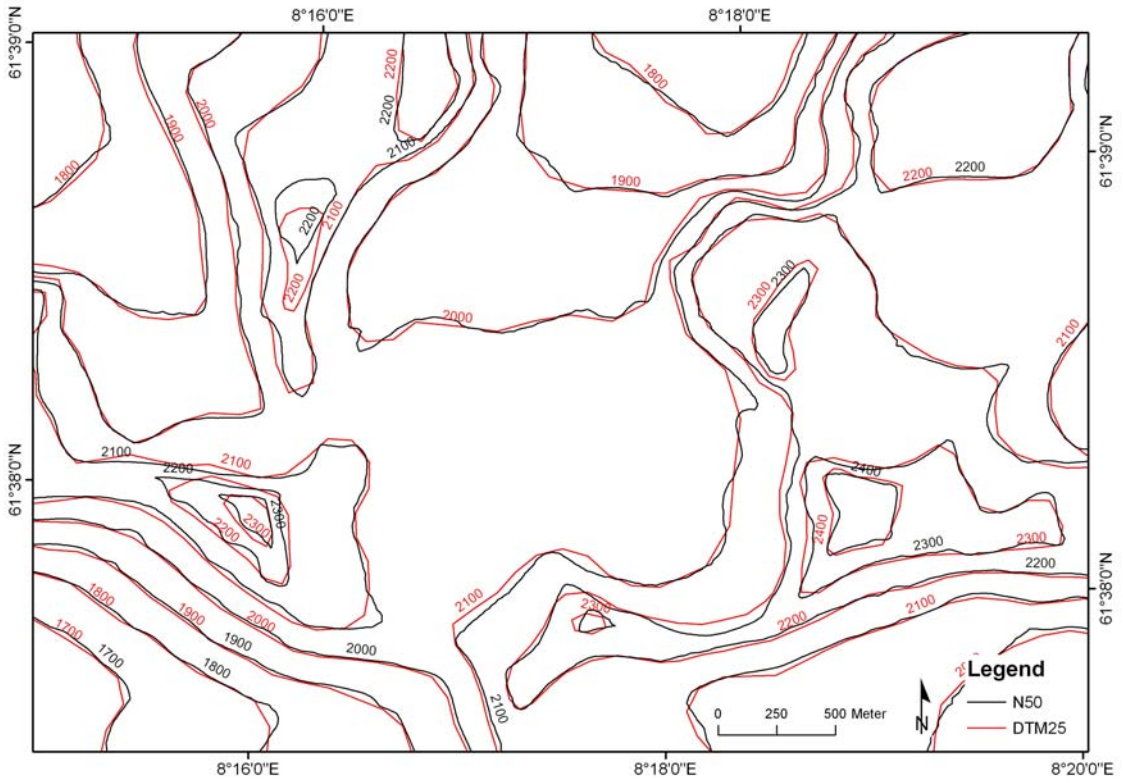

Figure 34: Differences between the altitude lines of N50 and the DTM25 (Digital topographic map and DTM25: Statens Kartverk N50).

In several cases, the geomorphological maps were obviously drawn using non-orthorectified aerial photos due to the too poor topographical information on the maps (see section 5.3.1.3). For georeferencing of these maps, aerial photos had to be used. Only on those, the precise position of the moraine ridges could be mapped if no other useful information was available on the maps. Therefore, the geomorphological maps cannot be regarded as an independent source. To determine the potential error emerging during this procedure, the GPS-data collected in field were used. Comparable data were available for five glaciers. The difference between these GPS-coordinates and the position of the outermost moraine on geomorphological maps was calculated without taking into account the error of the GPS-data themselves. The mean error of the resulting LIA area is about 28.2 m^2 (σ = 8.8 m^2). This error is smaller than the pixel size of the satellite image (30 m x 30 m). The RMSE of the georeferenced satellite image itself is about 0.65 pixels, which is about 20 m (ANDREASSEN et al. 2008a). The error resulting from topographical inaccuracy of the geomorphological maps is therefore too small to be taken into account and is acceptable for this purpose.

The general but also more theoretical question arises whether an error is already implemented by comparing sources of different resolutions. This means in particular, whether sources of different resolutions can be compared without

any restrictions or whether there is always a loss of information or accuracy, resulting in possible errors. In the actual case, the pixel size of the satellite image is coarse (30 m x 30 m) compared with the aerial photos (0.4 m x 0.4 m). Thus, the proportion in resolution between the satellite image and the aerial photo is about 75:1. PAUL et al. (2003) analyzed changes in glacier area with pixel size and detected errors depending on glacier size. Given σ = 3%, glaciers of 0.2 km² represent the minimum glacier size in mapping for a 30 m resolution (e.g. the satellite image in the present case). Mapping sources with a resolution of 5 m can be used for all glaciers, taking into account the same standard deviation. The study of PAUL et al. (2003) means for mapping the glacier extent in Jotunheimen at LIA maximum with sources of different resolutions, that an error is included when comparing glaciers smaller than 0.2 km².

Also other publications (e.g. WOLKEN (2006)) used sources of different resolution to map the glacier extent at LIA maximum. In these cases, those sources were taken as complementary products and used to compensate the disadvantages of each other (as also done in this study). Therefore, an error in comparing sources is existing according to PAUL et al. (2003), but it is not taken into account in the practical mapping process.

8.4 Usability of the parameterization

The main principle of the parameterization scheme is a step change in mass balance depending on a disturbance of temperature or precipitation (see section 5.4.1). No feed-back processes are involved and all other parameters and input variables (except area, minimum and maximum altitude, and length) stay the same over time (HOELZLE 1994). Influence of precipitation on the glaciers is included in the parameterization by the mass balance gradient (HOELZLE 1994). It is also implemented in the resulting net glacier mass balance, because changes in temperature and precipitation caused the value of this variable. But precipitation serves therefore only as a hidden variable of the output scheme, and not as forcing factor. Detailed studies about the individual impact of temperature and precipitation on the glacier behaviour are not possible by only using the parameterization. Changes in precipitation (patterns) can be included by changing the mass balance gradient for different time steps. The problem of this method is that the inventories are not always prepared at points of time when the state of glacier behaviour is changing from a gaining to a loosing mass period or vice versa. Therefore, this method is not suitable for the used parameterization. Additionally, the mass balance gradient is calculated by using steady-state years (see section

5.4.2) and e.g. does not vary much during selected years (see Table 2). One conclusion for the New Zealand Alps by HOELZLE et al. (2007) is the underestimation of the net annual mass balance for the 'wet' area by the parameterization. This result is possibly caused by a less pronounced effect of precipitation in the scheme.

As a further differentiation, seasonality is not included and maybe goes beyond the possibilities of this rather simple scheme. It only should be kept in mind that an averaged change of air temperature over the whole year, as used in the parameterization, is not significant (e.g. RASMUSSEN et al. (2007); STEINER et al. (2008); WINKLER (2009); WINKLER et al. (2009)). Depending on the season, a change in temperature can have quite different effects as already discussed before (see section 4.1.4).

The original calculations by JÒHANNESSON et al. (1989a) are based on the assumption of energy conservation and eliminate thereby potentially realistic behaviour that would affect ice dynamics through e.g. ice flow. These assumptions are strongly restricting for the parameterization, especially by using the scheme over such a long period of more than 250 years as for Norwegian glaciers. For example, temperatures of ice can change over time by climate changing and, therefore, the glacier regime can change. This process has a pronounced effect on the glacier behaviour, but in most cases, nothing is known about the temperature distribution in glaciers. Only assumptions can be made in e.g. using the altitude distribution of glaciers. Therefore, also if an inclusion of change of flow dynamics was possible in the parameterization scheme, the input data needed would not be more than a rough estimation.

Creation of future scenarios is also possible by using the parameterization. But no scenarios were simulated here with the parameterization because of recent down-wasting processes of several glaciers (see section 4.1.4). These processes cannot be described with the actual parameterization scheme. Down-wasting is also visible in Norway (KJØLLMOEN 2009; WINKLER & NESJE 2009; WINKLER in print), but has not been reported from Jotunheimen. A stronger debris-cover at some glaciers was visible during field-work in 2009, compared with the two previous years, e.g. at Visbreen. The reasons can be increased rock fall from the surrounding walls or enhanced melting processes leading to more rocks on the glacier surface, that have been incorporated in the ice before. However, the increase of summer temperatures over the last few decades gave evidence, that the anthropogenic signal has exceeded the natural background (MATTHEWS & BRIFFA 2005). Therefore, the glaciers of Jotunheimen will react to

this warming because of their strong relation to summer temperature. Concluding, it seems more useful to use other models to predict future behaviour and extents, e.g. by LAUMANN & NESJE (2009).

8.5 Selection of variables for the parameterization

Table 17: Calculations of the ELA_0, AAR and AAR_0 at the three glaciers in Jotunheimen with mass balance measurements (STO, HEL, GRA) (Raw data ELA: WGMS database).

Glacier	Year	ELA	AAR
Hellstugubreen	1964	1900	0.40
	1968	1875	0.43
	1971	1860	0.45
	1979	1820	0.47
	1992	1850	0.47
	1994	1850	0.47
	1995	1885	0.42
	1998	1870	0.45
	2000	1840	0.51
	2008	1880	0.45
	Mean	1863	0.45
Storbreen	1957	1680	0.56
	1958	1700	0.53
	1968	1700	0.53
	1973	1705	0.53
	1975	1760	0.43
	1976	1740	0.48
	1979	1700	0.53
	1981	1730	0.49
	1991	1740	0.48
	1992	1715	0.51
	2005	1795	0.43
	2008	1770	0.46
	Mean	1728	0.50
Gråsubreen	1968	2140	0.36
	1979	2025	0.61
	1983	2090	0.47
	1985	2100	0.44
	1994	2075	0.49
	1995	2180	0.25
	2001	2070	0.50
	Mean	2097	0.45

Several estimations had to be made for the setting of the parameterization. The estimation of ELA ~ H_{mean} was not changed. This means that no uniform AAR_0 was chosen for all glaciers, because this ratio depends on a uniform defined accumulation area vs. total glacier area relationship (KASER et al. 2003). The selection of the mean altitude seems to be the worst method in estimating the ELA, but more important is the assumption that the ratio stays the same over time (Hoelzle 1994). Calculations of the AAR_0 at glaciers with mass balance

measurements in Jotunheimen were done by using ELA, minimum and maximum altitude. The ratio of accumulation vs. total glacier area was calculated for all years where data was available (Table 17). The results showed an AAR_0 close to 0.5, i.e. AAR_0 of 0.5 for STO, and 0.45 for HEL and GRA, and no significant change during the available periods. Therefore, the selected method was chosen only because of practical and comparability reasons of the different parameterizations and possible larger errors in the assumption of staying the same ratio since LIA maximum.

To estimate the geometry factor f, some specifications and declarations about glacier geometry have to be known. The shape of the cross-section of the glaciers in the area was not established and, as far as known, has not been measured on any glacier in the area yet. HOEL & WERENSKIOLD (1962) have given a sketch of a cross-section of Hellstugubreen in the ablation area, estimating a parabolic or semi-elliptic profile. For the parameterization, a semi-elliptic geometry was chosen for all glaciers. NVE (2006) report a mean ice thickness of 115 m for Storbreen in 1997. The half-width of Storbreen was ~1065 m in 2003, estimated by measurements on the N50. Measured thicknesses of Styggedalsbreen at several points were reported by AHLMANN (1928) in 1923/24, but no width was given for this glacier in this specific year. Extrapolating the numbers of Storbreen to the total area resulted in a value of w = 9.3 and therefore f = 1.

The basal shear stress is calculated by a formula developed empirically for glaciers in the Upper Engadine (HOELZLE 1994), that is varying between maritime and continental regimes as the Jotunheimen area. But the transferability of this formula was not tested for glaciers in Jotunheimen (e.g. magnitude of variation) and, hence, can only serve as best assumption. The formula would then underestimate the basal shear stress for more maritime and overestimate it for more continental glaciers. This uncertainty also influences the net mass balance.

The chosen value of 0.9 m w.e./100m/a for the western and 0.3 m w.e./100m/a for the eastern part of Jotunheimen are only slightly higher than the calculated values from the steady-state years (see Table 2). Reasons for the selection of these values are implemented in the calculations of the parameterization, especially by the values of the ablation at the glacier tongue (see Equ. (3)). An overview of b_t-values calculated with different values of db/dH is given in Table 3. The value for the eastern part was chosen according to the ratio of the calculated values of the mass balance gradients of the three mass balance glaciers. db/dH of Gråsubreen is about one third of db/dH of Stor- and Hellstugubreen. This ratio was kept and transferred to the chosen values, although the

gradient of the potentially cold-based Gråsubreen itself seems not reliable enough to be taken for the parameterization (see section 3.4).

Other possibilities to adjust the mass balance gradient inherent in the parameterization do not exist in this case. db/dH is included in the calculation of the mass balance disturbance (see Appendix A), but no measurements are available for this variable. It is also included in the calculations of the response time, and the surface and the sliding velocity. But also for these variables, no measured values are available. Measurements are available for the mean net mass balance (see Table 18), but in the calculation, the mass balance gradient is included twice and, hence, is reduced.

A consideration concerning the mass balance gradient is the importance or validity of this variable. RASMUSSEN & ANDREASSEN (2005) found a weak correlation between the net mass balance gradient and the net mass balance on ten Norwegian glaciers (including STO, HEL, and GRA). This resulted from a generally positive correlation between winter net mass balance and its corresponding gradient, and a negative one between summer net balance and its gradient (see section 4.1.4).

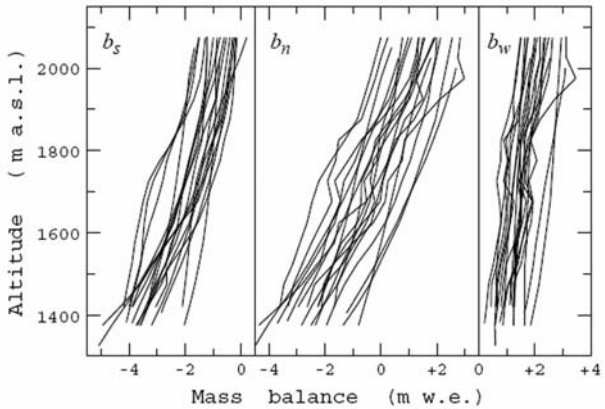

Figure 35: Balance profiles of Storbreen for 19 individual years (Figure after RASMUSSEN & ANDREASSEN (2005)).

The net mass balance gradient changes only little from year to year in Norway (example of Storbreen in Figure 35) (RASMUSSEN & ANDREASSEN 2005), and, therefore, the validity of the mass balance gradient concerning the mass balance is probably overestimated (cf. WINKLER et al. (2009)). Generally, the net gradient serves as index of glacier activity (HOELZLE 1994), but in Norway, the mass balance itself is the indicator of glacier activity (personal comment L.A. Rasmussen, 08/2009). To use mass balance gradients for Jotunheimen, it is probably more useful to use gradients split into winter and summer periods to make statements about the seasonal and then afterwards about the net mass balance. Regarding the use of db/dH in the parameterization,

MACHGUTH (2003) evaluates a reconstruction of the mass balance gradient to former climate as connected with large uncertainties.

The value of the mean net balance in Jotunheimen was much higher between LIA maximum and the 1980s compared with the European and New Zealand Alps in the corresponding period. $\bar{b}n$ in Jotunheimen had its lowest value between the 1980s and 2003, but still very high compared with the values of the other regions from the further periods. Nonetheless, the values for Stor- and Hellstugubreen fit very well to the measured values between the 1980s and 2003 (Table 18). The calculated value for Gråsubreen did not fit very well. The bad adjustment of Gråsubreen is probably based on the existence of the ice-cored moraine and a possible cold-based glacier type (see section 3.4). The parameterization is made for temperate glaciers (JÒHANNESSON et al. 1989a; HOELZLE 1994), and, therefore, has to be adjusted to cold-based or, at least, polythermal ones. Especially the response time is influenced by the glacier temperature. This may also explain the low values for the mean net mass balance in Jotunheimen, because t_{resp} is a main factor in the calculation of $\bar{b}_n$ (see this equation in Appendix A). Additionally, the response time is calculated in using the basal shear stress (see above).

Table 18: Comparison of the measured and calculated mean annual net mass balance from glaciers with mass balance measurements in Jotunheimen. Measured values from years 1980 – 2003, calculated values by the parameterization. Letter codes denote: STO = Storbreen, HEL = Hellstugubreen, GRA = Gråsubreen (Raw data measured $\bar{b}_n$: ANDREASSEN et al. (2009)).

Glacier / $\bar{b}n$ [m/a]	STO	HEL	GRA
measured	-0.24	-0.35	-0.29
calculated	-0.26	-0.28	-0.04
Difference	0.02	-0.07	-0.25

The very low values of the mean net balance in 2003 in the eastern part (see Table 13), especially the mean and the minimum value, resulted from the values of Glitterbreen. This glacier had a large glacier tongue at LIA maximum that split in the 1980s. The total disappearance of these remainings appeared until 2003. Therefore, the differences of H_{min} between the 1980s and 2003 have been extraordinary high and, correspondingly, the value of δELA. This value is needed for the calculation of the mean net mass balance and caused the very low value. This splitting of the glacier tongue may be due to the errors in the inventory of the 1980s (ANDREASSEN et al. 2008a) (see section 8.2). No differentiation was made between glaciers and snow, so possibly, these glacier remainings were snow patches and did not belong to the glacier any more. No analysis was made in detection of similar errors at other variables in the data-set. But it has to be kept

in mind, that the glacier inventory of the 1980s has a higher uncertainty concerning glacier area than the inventories of LIA maximum and 2003 and therefore the resulting data.

The adjustment of the parameterization in using the three mass balance glaciers, mainly depended on the ablation at the glacier tongue and the net mass balance, seems to be an appropriate method. As HOELZLE (1994) mentioned, the value of the ablation at the glacier tongue is critical for the parameterization, and, therefore, goodness of the parameterization can only benefit by tuning with this measured value. Hence, the difference between the periods LIA maximum – 1980s and 1980s – 2003 is probably not large enough so that the measured values can be transferred to this earlier period without adjustment (cf. WINKLER & NESJE (2009). Nonetheless, it has to be mentioned that the value for ablation at the glacier tongue derived from the conventional mass balance data might not in every case be reliable. Most recently, the decoupling of net mass balance and length variation at the short outlets of Jostedalsbreen in western Norway has partly been attributed to the underestimation of ablation at the lower part of the glacier by the traditional extrapolation procedure (WINKLER et al. 2009; WINKLER & NESJE 2009).

8.6 Analysis of mapping results

Unfortunately, no inventory on a regional scale at LIA maximum is available for any other glacier area of Norway than for Jotunheimen. Therefore, the data of STO, HEL, and GRA in Jotunheimen were compared with the estimated inventory data of NIG at Jostedalsbreen between LIA maximum and the 1980s (see section 6.1 and 7.3). The relative development of area and volume showed a more pronounced decrease at the glaciers in Jotunheimen (ΔV NIG = 34%, ΔV STO = 51%, ΔV HEL = 42%, ΔV GRA = 4%). This comparison might not give a convincing overview of the two glacier areas because of the small selection of glaciers (cf. section 2). A larger variety of outlet glaciers of Jostedalsbreen would be needed, including e.g. different sizes and expositions, to represent the total glacier area. Best would be, of course, a regional inventory data set at LIA maximum. Therefore, this data indicates differences concerning the three glaciers, but not concerning the whole glacier regions. A comparison between the whole Jotunheimen data and the data of NIG was also performed and showed the same results as the comparison with the three mass balance glaciers.

8.7 Comparison between glacier regions

Differences between the compared glacier areas and their respective data have already been visible in the description of the glacier areas. The results of the comparisons are regarded in this section enlightening these circumstances.

8.7.1 Inventory data

The sources of the inventory data at LIA maximum in the European Alps, the New Zealand Alps, and Baffin Island were based on different methods and on different accuracy in compilation and analysis. The glacier areas themselves are very different in extent, glacier size, and climate setting.

The inventory data at LIA maximum of Switzerland is based on very profound analyses (MAISCH et al. 2000), as well as the other two following inventories (1973 by MÜLLER et al. (1976) and 2000 by PAUL (2007)). Therefore, the Jotunheimen as well as the Swiss data revealed the same level of accuracy and nearly the same times of compilation. Only the timing of LIA maximum is different for the Swiss and European Alps compared with Jotunheimen. Therefore, the period between the first two inventories lasted 100 years longer in Jotunheimen. This difference in timing results from individual responses of each region to changes in climate and to the influence of the NAO. The same causes, relevant at LIA maximum, appeared in later times and are responsible for the glacier behaviour until today. Therefore, the different timing of LIA maximum is only an expression of processes still happening today. Hence, it is not a 'problem' of different timing by using these data in analyses, but an expression of different reactions on climate. This means, that these data sets fit very well for comparison.

The same reasons explained for the Swiss Alps, matter for the Austrian Alps. Their glacier inventory at LIA maximum is also based on profound analyses by GROSS (1987). Furthermore, the glacier size is smaller compared with Jotunheimen and serves as further reason for the differences in glacier behaviour.

As mentioned in section 7.2.1, the inventory data at LIA maximum for the European Alps are extrapolated from the Swiss inventory based on the national inventories during the 1970s (ZEMP et al. 2008). No description was found, that this data was verified with other mapped inventories at LIA maximum (e.g. from Austria). A differentiation in extrapolation was made concerning different size classes (ZEMP et al. 2008), but no differentiation concerning individual climate regimes – especially precipitation – due to the climate gradient in this region (see section 3.5). Therefore, some regions within the European Alps have been

underestimated while others have been overestimated by this method concerning their individual behaviour in comparison with the glacier behaviour of Switzerland. But, the results of this extrapolation fit quite well to the observed climate data, also in comparison with the Jotunheimen data set. Therefore, the stated judgement about their good quality in precision (e.g. HAEBERLI & HOELZLE (1995)) was not doubted.

The LIA maximum inventory of glaciers in New Zealand is based on moraine surveys using aerial photography (see section 7.2.1). A selection of 127 glaciers with large moraine walls well visible on the photos was chosen (CHINN 1996). This selection gave a bias towards glaciers favourable for moraine formation and preservation (CHINN 1996), but according to CHINN (1996), the sample was stated large enough to fairly represent the total magnitude and variety of glaciers in New Zealand. Additionally, some glaciers had been already observed before (CHINN 1996), so that supplementary material could be used for verification and correction.

Timing of LIA maximum in New Zealand is not indicated yet (see section 3.5) du to problems in methodology. Because of the more or less stagnant position of the glacier tongues close to their maximum extent between 1750 and 1900 (CHINN et al. 2005), 1750 could be chosen as possible date of LIA maximum because of its initial position of this phase. But also every date in between, as maybe done by HOELZLE et al. (2007), could serve as date of LIA maximum because of the close position to the maximum extent. Therefore, more research is needed to answer the question concerning timing of LIA maximum in New Zealand finally.

The comparison between Jotunheimen and Baffin Island was slightly unsatisfactory because of the great differences of these two areas in climate setting and glacier size. But even therefore, this comparison shows the large variety of glaciers and their locations and gives a better overview of glacier distribution worldwide, also during LIA maximum. An explanation of the different timing of LIA maximum in both areas would enhance the comparison and give more insight into the forcing climate factors on glaciers.

8.7.2 Parameterization

For some variables, the large difference between West and East Jotunheimen (see section 6.3 and 7.2.2) depended mainly on the different mass balance gradients (see Equ. (3)). Calculated with db/dH = 0.3 m w.e./100m/a (mass balance gradient of East Jotunheimen) the ablation at the glacier tongue

was still higher in the western part. West Jotunheimen exhibited a much shorter response time, but the mean value was nearly similar to the East if calculated with the same mass balance gradient.

The western part of Jotunheimen showed a faster flow than the East, also if calculated with db/dH = 0.3 m w.e./100m/a. Some other variables also changed with the mass balance gradient, but there is still a large number, that stayed the same. Regarding this analysis, the differentiation in a more maritime western and a more continental eastern part is still valid and not only dependent on the different mass balance gradients.

In Jotunheimen, the European, and the New Zealand Alps, the number of glaciers differed largely. The statistical population was 125 glaciers in Jotunheimen, 702 in the New Zealand Alps, and 1763 glaciers in the European Alps. This difference of more than ten times between the highest and the lowest value has an influence on the standard deviation. The higher the number of the statistical population the lower is σ. This means, that an error was included by comparing the standard deviations of these regions.

In section 6.1, a t-test was performed between the mean of the parameterization results for all comparable variables of the three regions. Half of the basic input variables were not significant on the 10% level. If a variable is denoted as not significant, that would mean that the statistic population of this variable does not differ significantly between the two chosen data sets. In reversed manner that could mean, that the not significant populations are only dependent samples of the same statistic population. Therefore, the mean of the variables that showed no significance could be judged as values spreading around the ‘real’ mean, the expected value, of the theoretical ‘whole’ statistic population. In conclusion, these variables are not comparable under this aspect. Regarding the performed comparison, this would result in a very close similarity of the compared data sets. The question has to be raised if e.g. glacier area and length are triggered the same way in similar alpine mountain topography, producing similar data-sets.

Compared with the mean net mass balance of the other two regions, the value of $\bar{b}n$ in Jotunheimen was very high. It was about ten times higher than the corresponding values in the European Alps and the ‘dry’ area in the New Zealand Alps. In contrast, the calculated $\bar{b}n$ -value of Nigardsbreen was five times lower than the value of the ‘wet’ area in the New Zealand Alps. Via various calculations, the mean shear stress is used for estimating the mean net mass balance, as already mentioned in section 8.5. In the European and New Zealand Alps, this variable was calculated first, but then an equal value was set for all glaciers.

Neither this method nor the selection of an arbitrarily value was chosen for Jotunheimen. No empirical data for Jotunheimen or no physical based or for Jotunheimen specified term exist. Therefore, the calculation method of HAEBERLI & HOELZLE (1995) was taken as best assumption, bearing in mind the large range of uncertainties that maybe caused the high values of the mean net balance in Jotunheimen.

8.8 Relationship between glacier behavior and climate

The relation between the glacier behaviour and the climate based mainly on the inventory data and the parameterization results. Differences on the influences of climatic factors were already visible on a sub-regional scale. They expressed the differences between the individual regions concerning the climatic regime. Differences in length changes and mass balance could be related to the NAO and its index. According to the large time steps in the current data, a more detailed analysis and interpretation of the glacier behaviour and the connection to climate was not performed.

A problem in the connection between glacier behaviour and climate factors is the availability of measured values from weather stations. These stations are only in special cases located in close vicinity of or on a glacier. On Storbreen, an automatic weather station (AWS) has been installed in 2001 (ANDREASSEN et al. 2008b). It provides meteorological and mass balance data of one point in the ablation area. Unfortunately, the data of the AWS does not reach back in time long enough for this study. At least, a period since the beginning of the 1980s would have been needed to relate the AWS data to a comparable period here. Therefore, as in most cases, the available weather stations were situated in populated areas and in the mountain valleys. The climatic situation at these locations differs from the situation in the glacier regions. At Jostedalsbreen, there is a special case, i.e. the climate data of Bergen fit very well to the data of Jostedalsbreen (NESJE 2005; WINKLER et al. 2009). No weather station is known that would represent the data of Jotunheimen in the same way.

9 Conclusion and outlook

Using satellite imagery and aerial photos for manual mapping of glacier outlines and glacier centrelines at LIA maximum in Jotunheimen was successful on a regional scale. Inventory data of the LIA maximum glaciers could be determined automatically using GIS techniques. Some uncertainties remained in the mapping process, but their influence is not large enough to call into question the reliability of the mapping results. All outcomes can be seen as good results of the mapping.

The inventory data of Jotunheimen at LIA maximum reduced in area and length, and only a few glaciers vanished between LIA maximum and 2003. Overall, the glaciers were relatively larger in size at LIA maximum, especially remarkable at the upper and lower end of the area range. Compared with the European and the New Zealand Alps, the relative glacier retreat is not as great as in these regions.

The parameterization and a comparison with the parameterization data of the European and the New Zealand Alps could be realized and showed a consistent pattern of the glacier behaviour and glacier regime of Jotunheimen glaciers. The division in two climatic and glaciological different parts was confirmed by this method.

The results are convincing although the design of the calculations was made for larger glaciers (HAEBERLI & HOELZLE 1995; HOELZLE et al. 2007). The maximum glacier area of Jotunheimen in the 1970s/80s was only a tenth of the maximum glacier area in the other two regions.

Unfortunately, no other glacier inventory at LIA maximum on a regional scale in Norway was available yet. An application of the parameterization to other regions of Norway, also with larger glaciers, would give more insight on glacier behaviour at LIA maximum in Norway and in general. The comparison between the data of Nigardsbreen and Jotunheimen is not representative because of the use of only one single glacier for Jostedalsbreen. Therefore, this comparison cannot be regarded as a comparison between Jotunheimen and Jostedalsbreen. It will be especially interesting, if the small area loss compared with the non Norwegian regions is also visible compared with other glacier regions in Norway. Therefore, further inventories at LIA maximum of Norwegian glacier areas are needed.

To learn more about the importance and representativity of Jotunheimen concerning whole Norway, results from the parameterization of the 1980s until

2003 can be used. This data from other glacier regions in Norway is available (e.g. Svartisen (PAUL & ANDREASSEN 2009)) or in preparation and a comparison can give insight in data ranges and differences and similarities between the regions. On this basis, conclusions can be drawn concerning glaciological regimes and estimations concerning glacier behaviour, also reconstructed for LIA maximum.
Regarding Jotunheimen, this comparison can verify possible errors due to the small glacier size and due to the thermal regime by not tuning the scheme to polythermal or cold-based glaciers.

The input data for the parameterization were a certain fraction of the total inventory data of Jotunheimen. A comparison and statistical analysis concerning the total inventory would give insight in the reliability and representativity of this selection.

The successful implementation of a classification of the glacier forelands would have been very helpful concerning time management and objectivity of the mapping process. Although testing of a lot of different properties in the inquiry, no convincing solution was found. Possibly, enhancement of this classification can benefit from progresses in the more intense research on (semi-)automatic mapping of debris-covered glaciers.

Relation of climate and glacier behaviour seems possible by using the parameterization results. The time steps chosen for the parameterization are the maximum of the LIA and the 1970s/80s, and, for Jotunheimen, 2003. These time steps correspond with a glacier retreat in Jotunheimen, only interrupted by minor readvances. By using the glacier inventory of 2000 for Switzerland (Kääb et al. 2002; Paul et al. 2002), the parameterization can be also applied to this region for three time steps, comparable with Jotunheimen. A comparison between these data will be very interesting. Variables directly related to climate, e.g. net mass balance, might change remarkably. Therefore, the parameterization results would mirror the climate situation. This would give more evidence about significance of the reconstruction at LIA maximum.

References

AHLMANN, H.W. (1928): Physico-geographical researches in the Horrung massif, Jotunheim. Geografiska Annaler, 10: 307-371.

ALBERTZ, J. (2007). Einführung in die Fernerkundung (3. ed.). Wissenschaftliche Buchgesellschaft, Darmstadt.

ANDREASSEN, L.M., ELVEHØY, H., KJØLLMOEN, B., ENGESET, R.V. & HAAKENSEN, N. (2005): Glacier mass-balance and length variation in Norway. Annals of Glaciology, 42: 317-325.

ANDREASSEN, L.M., PAUL, F., KÄÄB, A. & HAUSBERG, J.E. (2008a): Landsat-derived glacier inventory for Jotunheimen, Norway, and deduced glacier changes since the 1930s. The Cryosphere 2: 131-145.

ANDREASSEN, L.M., VAN DER BROEKE, M.R., GIESEN, R.H. & OERLEMANS, J. (2008b): A 5 year record of surface energy and mass balance from the ablation zone of Storbreen, Norway. Journal of Glaciology, 54(185): 245-258.

ANIYA, M. (1995): Holocene glacial chronology in Patagonia - Tyndall and Upsala glaciers. Arctic and Alpine Research, 27(4): 311-322.

ARENDT, A.A., ECHELMEYER, K.A., HARRISON, W.D., LINGLE, C.S. & VALENTINE, V.B. (2002): Rapid Wastage of Alaska Glaciers and Their Contribution to Rising Sea Level. Science, 297(5580): 382-386, doi: 10.1126/science.1072497.

AUNE, B. (1993): Temperaturnormaler normalperiode 1961 - 1990. DNMI Rapport, Oslo.

BÄTZING, W. (2005). Die Alpen: Geschichte und Zukunft einer europäischen Kulturlandschaft. Beck, München.

BAUMANN, S., ANDREASSEN, L.M. & WINKLER, S. (2008): Mapping Little Ice Age glacier maxima in Jotunheimen, using aerial photography and Landsat imagery. Proceedings of EARSeL-LISSIG Workshop on Remote Sensing of Snow and Glaciers, Berne, available at URL: http://www.earsel.org/workshops/LISSIG2008/Baumann_Paper.pdf.

BAUMANN, S., WINKLER, S. & ANDREASSEN, L.M. (2009): Mapping glaciers in Jotunheimen, South-Norway, during the "Little Ice Age" maximum. The Cryosphere, 3(2): 231-243.

BAXTER, J. (2009): Scandianvian Mountains over 2000 meters (01.2009). URL: http://www.scandinavianmountains.com/intro/ geography.htm (Access: 12.11.2009).

BENISTON, M. (2005): Mountain Climates and Climatic Change: An Overview of Processes Focusing on the European Alps. Pure and Applied Geophysics, 162: 1587-1606.

BICKERTON, R.W. & MATTHEWS, J.A. (1993): 'Little Ice Age' variations of outlet glaciers from the Jostedalsbreen ice-cap, southern Norway: a regional lichenometric-dating study of ice-marginal moraine sequences and their climatic significance. Journal of Quaternary Science, 8: 45-66.

BLATTER, H. & HUTTER, K. (1991): Polythermal conditions in Arctic glaciers. Journal of Glaciology, 37(126): 261-269.

BOGEN, J., WOLD, B. & ØSTREM, G. (1989): Historic glacier variations in Scandinavia. In: OERLEMANS, J. (Ed.): Glacier Fluctuations and Climatic Change. Kluwer Academic Publishers, Dordrecht, pp. 109-128.

BÖHM, R., SCHÖNER, W., AUER, I., HYNEK, B., KROISLEITNER, C. & WEYSS, G. (2007). Gletscher im Klimawandel: vom Eis der Polargebiete zum Gold-

bergkees in den Hohen Tauern. Zentralanstalt für Meteorologie und Geodynamik, Wien.

BOLCH, T., BUCHROITHNER, M., PIECZONKA, T. & KUNERT, A. (2008): Planimetric and volumetric glacier changes in the Khumbu Himal, Nepal, since 1962 using Corona, Landsat TM and ASTER data. Journal of Glaciology, 54(187): 592-600.

BOLCH, T. & KAMP, U. (2006): Glacier Mapping in High Mountains Using DEMs, Landsat and Aster Data. Grazer Schriften der Geographie und Raumforschung, 41: 37-48.

BORTZ, J. (2005). Statistik für Human- und Sozialwissenschaftler (6. ed.). Springer, Heidelberg.

BRAITHWAITE, R.J. (2008): Temperature and precipitation climate at the equilibrium-line altitude of glaciers expressed by the degree-day factor for melting snow. Journal of Glaciology, 54(186): 437-444.

BURROWS, C.J. (2005). Julius Haast in the Southern Alps. Canterbury University Press, Christchurch.

CHINN, T.J.H. (1996): New Zealand glacier responses to climate change of the past century. New Zealand Journal of Geology and Geophysics, 39: 415-428.

CHINN, T.J.H. (2000): Glaciers of Irian Jaya, Indonesia, and New Zealand - Glaciers of New Zealand (05.07.2000). URL: http://pubs.usgs.gov/prof/ p1386h/nzealand/nzealand.html (Access: 15.07.2009).

CHINN, T.J.H. (2001): Distribution of the glacial water resources of New Zealand. Journal of Hydrology (NZ), 40(2): 139-187.

CHINN, T.J.H., SALINGER, J., BLAIR, F. & WILLSMAN, A. (2008): Glaciers and climate. Bulletin of the Federal Mountain Clubs of NZ, No. 171.

CHINN, T.J.H., WINKLER, S., SALINGER, M.J. & HAAKENSEN, N. (2005): Recent glacier advances in Norway and New Zealand: A comparison of their glaciological and meteorological causes. Geografiska Annaler, Series A, Physical Geography, 87(1): 141-157.

CIPRA (2007): Die Alpenkonvention - Instrument für Schutz und nachhaltige Entwicklung (17.01.2007). URL: http://www.cipra.org/ de/alpenkonvention (Access: 20.08.2009).

CSATHO, B.M., SCHENK, T., VAN DER VEEN, C.J. & KRABILL, W.B. (2008): Intermittent thinning of Jakobshavn Isbræ, West Greenland, since the Little Ice Age. Journal of Glaciology, 54(184): 131-147.

CSATHO, B.M., VAN DER VEEN, C.J. & TREMPER, C.M. (2005): Trimline mapping from multispectral Landsat ETM+ imagery. Géographie Physique et Quaternaire, 59(1): 49-62.

DAVIDSON, R. (2008): Reading topographic maps. Types of aerial photographs (2008). URL: http://www.map-reading.com/aptypes.php (Access: 10.11.2009).

DE JONG, R., HAMMARLUND, D. & NESJE, A. (2009): Late Holocene effective precipitation variations in the maritime regions of south-west Scandinavia. Quaternary Science Reviews, 28: 54-64.

DISCOVERY COMMUNICATIONS (2008): Baffin Island (30.03.2008). URL: http://geography.howstuffworks.com/polar-regions/baffin-island. htm (Access: 26.11.2009).

DYKES, R.C., BROOK, M.S. & WINKLER, S. (submitted): The contemporary retreat of Tasman Glacier, Southern Alps, New Zealand, and the evolution of Tasman proglacial lake since AD 2000. Erdkunde - Special Issue.

DYURGEROV, M.B. (2002). Glacier Mass Balance: Data of Measurements and Analysis. Occasional Paper No. 55. University of Colorado, Institute of Arctic and Alpine Research, Boulder, 144 pp.

DYURGEROV, M.B. & MEIER, M.F. (1997): Mass Balance of Mountain and Subpolar Glaciers: A New Global Assessment for 1961-1990. Arctic and Alpine Research, 29(4): 379-391.

DYURGEROV, M.B. & MEIER, M.F. (1999): Analysis of Winter and Summer Glacier Mass Balances. Geografiska Annaler, Series A, Physical Geography, 81(4): 541-554.

ERDAS IMAGINE (2006): ERDAS IMAGINE Tour Guides. pp. 730. Leica Geosystems.

ERIKSTAD, L. & SOLLID, J.L. (1986): Neoglaciation in South Norway using lichenometric methods. Norsk geografisk tidsskrift, 40: 85-105.

FÆGRI, K. (1948): Brevariasjoner i Vestnorge i de siste 200 år. Naturen, 72: 230-243.

FEALY, R. & SWEENEY, J. (2007): Identification of frequency changes in synoptic circulation types and consequences for glacier mass balance in Norway. Norsk Geografisk Tidsskrift, 61(2): 76-91, doi: 10.1080/00291950701374328.

FITZHARRIS, B.B., CHINN, T.J.H. & LAMONT, G.N. (1997): Glacier balance fluctuations and atmospheric circulation patterns over the Southern alps, New Zealand. International Journal of Climatology, 17(7): 745-763.

FITZSIMONS, S.J. & VEIT, H. (2001): Geology and geomorphology of the European Alps and the Southern Alps of New Zealand – A comparison. Mountain Research and Development, 21(4): 340-349.

FØRLAND, E.J. (1993): Nedbørnormaler normalperiode 1961 - 1990. DNMI Rapport, Oslo.

FOSSEN, H., PEDERSEN, R.-B., BERGH, S. & ANDRESEN, A. (2008): Creation of a mountain chain. The building up of the Caledonides; about 500-405 Ma. In: RAMBERG, I.B., BRYHNI, I., NØTTVEDT, A. & RANGNES, K. (Eds.): The making of a land - geology of Norway. Norsk Geologisk Forening, Trondheim, pp. 178-231.

FRANCOU, B., VUILLE, M., WAGNON, P., MENDOZA, J. & SICART, J.-E. (2003): Tropical climate change recorded by a glacier in the central Andes during the last decades of the twentieth century: Chacaltaya, Bolivia, 16°S. Journal of Geophysical Research, 108(D5): 4154, doi: 10.1029/2002JD002723

GAO, J. & LIU, Y. (2001): Applications of remote sensing, GIS and GPS in glaciology: a review. Progress in Physical Geography, 25(4): 520-540.

GARBER, S. (2007): Sputnik and The Dawn of the Space Age (10.10.2007). URL: http://history.nasa.gov/sputnik/ (Access: 09.10.2009).

GARMIN (2005): GARMIN. eTrex series (2005). URL: https://buy.garmin.com/shop/store/assets/pdfs/specs/etrex_series_spec.pdf (Access: 10.12.2009).

GÄRTNER-ROER, I., HAEBERLI, W., HOELZLE, M., PAUL, F. & ZEMP, M. (2009): Internationales Gletscher Monitoring. Global Terrestrial Network for Glaciers (GTN-G). Talk. Deutscher Geographentag. Wien.

GEE, D.G., FOSSEN, H., HENRIKSEN, N. & HIGGINS, A.K. (2008): From the Early Paleozoic Platforms of Baltica and Laurentia to the Caledonide Orogen of Scandinavia and Greenland. Episodes, 31(1): 44-52.

GLCF (2008): Earth Science Data Interface (25.12.2008). URL: http://glcfapp.umiacs.umd.edu:8080/esdi/ftp?id=214595 (Access: 26.11.2009)

GLIMS (2009a): GLIMS: Global Land Ice Measurements from Space. Monitoring the World's Changing Glaciers (04.2009). URL: http://www.glims.org/ (Access: 12.11.2009).

GLIMS (2009b): GLIMS: Links to other programmes (04.2009). URL: http://www.glims.org/About/links.html (Access: 12.11.2009).

GREUELL, W. & BÖHM, R. (1998): 2 m temperatures along melting mid-latitude glaciers, and implications for the sensitivity of the mass balance to variations in temperature. Journal of Glaciology, 44(146): 9-20.

GROSS, G. (1987): Der Flächenverlust der Gletscher in Österreich 1850 - 1920 - 1969. Zeitschrift für Gletscherkunde und Glazialgeologie, 23(2): 131-141.

GROVE, A.T. (2001): The "Little Ice Age" and its geomorphological consequences in Mediterranean Europe. Climatic Change, 48: 121-136.

GROVE, A.T. (2008): A brief consideration of climate forcing factors in view of the Holocene glacier record. Global and Planetary Change, 60: 141-147.

GROVE, J.M. (1988). The Little Ice Age. Methuen, London; New York.

GROVE, J.M. (2004). Little ice ages. Routledge studies in physical geography and environment, 5. Routledge, London, New York.

GÜNTHER, R. & WIDLEWSKI, D. (1986): Die Korrelation verschiedener Klimaelemente mit dem Massenhaushalt alpiner und skandinavischer Gletscher. Zeitschrift für Gletscherkunde und Glazialgeologie, 22: 125-147.

HAEBERLI, W. (1991): Alpengletscher im Treibhaus der Erde. Regio Basiliensis, 32(125): 37-46.

HAEBERLI, W. (1995): Glacier fluctuations and climate change detection - operational elements of a worldwide monitoring strategy. WMO Bulletin, 44: 23-31.

HAEBERLI, W. (2004): Glaciers and ice caps: historical background and strategies of world-wide monitoring. In: BAMBER, J. & PAYNE, J.L. (Eds.): The mass balance of the cryosphere: observations and modelling of contemporary and future changes. Cambridge University Press, Cambridge, pp. 559-578.

HAEBERLI, W., ALEAN, J.C., MÜLLER, P. & FUNK, M. (1989): Assessing risks from glacier hazards in high mountain regions: some experiences in the Swiss Alps. Annals of Glaciology, 13: 96-102.

HAEBERLI, W. & BENISTON, M. (1998): Climate change and its impacts on glaciers and permafrost in the Alps. Ambio, 27(4): 258-265.

HAEBERLI, W., FRAUENFELDER, R., HOELZLE, M. & MAISCH, M. (1999): On Rates and Acceleration Trends of Global Glacier Mass Changes. Geografiska Annaler, Series A, Physical Geography, 81(4): 585-591.

HAEBERLI, W. & HOELZLE, M. (1995): Application of inventory data for estimating characteristics of and regional climate-change effects on mountain glaciers: a pilot study with the European Alps. Annals of Glaciology, 21: 206-212.

HAEBERLI, W., MAISCH, M. & PAUL, F. (2002): Mountain glaciers in global climate-related observation networks. WMO Bulletin, 51(1): 18-25.

HOCK, R. (2003): Temperature index melt modelling in mountain areas. Journal of Hydrology, 282: 104-115, doi: 10.1016/s0022-1694(03)00257-9.

HOEL, A. & WERENSKIOLD, W. (1962). Glaciers and snowfields in Norway. Norsk Polarinstitutt. Skrifter. Oslo University Press, Oslo.

HOELZLE, M. (1994). Permafrost und Gletscher im Oberengadin. Grundlagen und Anwendungsbeispiele für automatisierte Schätzverfahren. Mitteilungen der VAW/ETHZ, 132. vol. Versuchsanstalt für Wasserbau, Hydrologie und

Glaziologie der Eidgenössischen Technischen Hochschule Zürich (VAW), Zürich, 123 pp.

HOELZLE, M., CHINN, T.J.H., STUMM, D., PAUL, F., ZEMP, M. & HAEBERLI, W. (2007): The application of inventory data for estimating past climate change effects on mountain glaciers: A comparison between the European Alps and the Southern Alps of New Zealand. Global and Planetary Change, 56(1-2): 69-82.

HOELZLE, M., DISCHL, M. & FRAUENFELDER, R. (2000): Weltweite Gletscherbeobachtung als Indikator der globalen Klimaänderung. Vierteljahrsschrift der Naturforschenden Gesellschaft Zürich, 145(1): 5-12.

HOELZLE, M., HAEBERLI, W., DISCHL, M. & PESCHKE, W. (2003): Secular glacier mass balances derived from cumulative glacier length changes. Global and Planetary Change, 36: 295-306.

HOLZHAUSER, H., MAGNY, M. & ZUMBUHL, H.J. (2005): Glacier and lake-level variations in west-central Europe over the last 3500 years. The Holocene, 15(6): 789-801, doi: 10.1191/0959683605hl853ra.

HORMES, A., MULLER, B.U. & SCHLUCHTER, C. (2001): The Alps with little ice: evidence for eight Holocene phases of reduced glacier extent in the Central Swiss Alps. The Holocene, 11(3): 255-265.

HUGGEL, C., HAEBERLI, W., KÄÄB, A., HOELZLE, M., AYROS, E. & PORTOCARRERO, C. (2003): Assessment of glacier hazards and glacier runoff for different climatic scenarios based on remote sensing data: A case study for a hydropower plant in the Peruvian Andes. Proceedings of EARSeL-LISSIG-Workshop Observing our Cryosphere from Space, Bern, 22-33.

HURRELL, J.W. (1995): Decadal Trends in the North Atlantic Oscillation: Regional Temperatures and Precipitation. Science, 269(5224): 676-679, doi: 10.1126/science.269.5224.676.

INNES, J.L. (1985): Lichenometry. Progress in Physical Geography, 9: 187-254.

IPCC (2001). Climate change 2001 - the scientific basis. Contribution of Working Group I to the Third Assessment Report of the Intergovernmental Panel on Climate Change. IPCC-Report, 3. vol. Cambridge University Press, Cambridge, New York.

IPCC (2007). Climate Change 2007: The Physical Science Basis. Contribution of Working Group I to the Fourth Assessment Report of the Intergovernmental Panel on Climate Change. Cambridge University Press, Cambridge, New York.

JANSEN, E., DOKKEN, T., NESJE, A., DAHL, S.O., LINGE, H., NINNEMANN, U.S. & OTTERAA, O.H. (2005): Bjerknes Centre for Climate Research - combining past, present and future climate change. Norwegian Journal of Geology, 85(1-2): 33-44.

JÒHANNESSON, T., RAYMOND, C.F. & WADDINGTON, E.D. (1989a): A simple method for determing the response time of glaciers. In: OERLEMANS, J. (Ed.): Glacier Fluctuations and Climatic Change. Kluwer Academic Publishers, Dordrecht, pp. 343-352.

JÒHANNESSON, T., RAYMOND, C.F. & WADDINGTON, E.D. (1989b): Time-scale for adjustment of glaciers to changes in mass balance. Journal of Glaciology, 35(121): 355-369.

JOTUNHEIMEN REISELIV (2007): Jotunheimen 2007. Nationalparkriket, pp. 65. Lom.

KÄÄB, A., PAUL, F., MAISCH, M., HOELZLE, M. & HAEBERLI, W. (2002): The new remote-sensing-derived Swiss glacier inventory: II. First results. Annals of Glaciology, 34(1): 362-366.

KARGEL, J.S., ABRAMS, M.J., BISHOP, M.P., BUSH, A., HAMILTON, G., JISKOOT, H., KÄÄB, A., KIEFFER, H.H., LEE, E.M., PAUL, F., RAU, F., RAUP, B., SHRODER, J.F., SOLTESZ, D., STAINFORTH, D., STEARNS, L. & WESSELS, R. (2005): Multispectral imaging contributions to global land ice measurements from space. Remote Sensing of Environment, 99(1-2): 187-219, doi: 10.1016/j.rse.2005.07.004.

KARLÉN, W. & MATTHEWS, J.A. (1992): Reconstructing Holocene glacier variations from glacier lake sediments: studies from Nordvestlandet and Jostedalsbreen-Jotunheimen, southern Norway. Geografiska Annaler, Series A, Physical Geography, 63: 273-281.

KASER, G., FOUNTAIN, A.G. & JANSSON, P. (2003). A manual for monitoring the mass balance of mountain glaciers with particular attention to low latitude characteristics. A contribution from the International Commission on Snow and Ice (ICSI) to the UNESCO HKH-Friend program. Technical Documents in Hydrology, 59. vol. IHP-VI, Paris.

KJØLLMOEN, B. (Ed.), (2004): Glaciological investigations in Norway in 2003, NVE-report,4-2004. NVE, Oslo.

KJØLLMOEN, B. (Ed.), (2006): Glaciological investigations in Norway in 2005. NVE-report, 2-2006. NVE, Oslo.

KJØLLMOEN, B. (Ed.), (2008): Glaciological investigations in Norway in 2007. NVE-report, 3-2008. NVE, Oslo, 99 pp.

KJØLLMOEN, B. (Ed.), (2009): Glaciological investigations in Norway in 2008. NVE-report, 2-2009. NVE, Oslo, 99 pp.

KLEMSDAL, T. (2000): Natural Landscapes of Norway. In: JUNG, G. (Ed.): Norwegen eine Naturlandschaft? - Ökologie und nachhaltige Nutzung : Tagungsband der Norwegen-Tagung, 26. - 28. November 1999. Oldenburger Geoökologische Studien, Band 4, Oldenburg, pp. 5-52.

KOESTLER, A.G. (1983): Zentral Komplex und NW-Randzone der Jotundecke West-Jotunheimen, Südnorwegen. PhD Thesis, ETH Zürich, Zürich.

KUHN, M. (1984): Mass budget imbalances as criterion for a climatic classification of glaciers. Geografiska Annaler, Series A, Physical Geography, 66(1-2): 229-238.

KUHN, M. (1995): The mass balance of very small glaciers. Zeitschrift für Gletscherkunde und Glazialgeologie, 31: 171-179.

LAUMANN, T. & NESJE, A. (2009): A simple method of simulating the future frontal position of Briksdalsbreen, western Norway. Holocene, 19(2): 221-228, doi: 10.1177/0959683608100566.

LAUMANN, T. & REEH, N. (1993): Sensitivity to climate change of the mass balance of glaciers in southern Norway. Journal of Glaciology, 39(133): 656-665.

LAWSON, W. & FITZSIMONS, S.J. (2001): Glaciers and the environment. In: STURMAN, A. & SPRONKEN-SMITH, R. (Eds.): The physical environment. A New Zealand perspective. Oxford University Press, Melbourne, New York, pp. 269-289.

LIDMAR-BERGSTRÖM, K., OLLIER, C.D. & SULEBAK, J.R. (2000): Landforms and uplift history of southern Norway. Global and Planetary Change, 24(3-4): 211-231.

LIE, Ø., DAHL, S.O., NESJE, A., MATTHEWS, J.A. & SANDVOLD, S. (2004): Holocene fluctuations of a polythermal glacier in high-alpine eastern Jotunheimen, central-southern Norway. Quaternary Science Reviews, 23: 1925-1945.

LIESTØL, O. (1967): Storbreen glacier in Jotunheimen, Norway. Norsk polarinstitutt skrifter, 141: 1-63.

LINDERHOLM, H.W., JANSSON, P. & CHEN, D. (2007): A high-resolution reconstruction of Storglaciären mass balance back to 1780/81 using tree-ring data and circulation indices. Quaternary Research, 67(1): 12-20, doi: 10.1016/j.yqres.2006.08.005.

MACHGUTH, H. (2003): Messung und dreidimensionale Modellierung der Massenbilanzverteilung auf Gletschern der Schweizer Alpen. Diploma thesis, Universität Zürich, Zürich, 158 pp.

MAISCH, M., WIPF, A., DENNELER, B., BATTAGLIA, J. & BENZ, C. (2000). Die Gletscher der Schweizer Alpen: Gletscherhochstand 1850, Aktuelle Vergletscherung, Gletscherschwund, Szenarien (2. ed.). vdf, Hochschulverlag an der ETH, Zurich.

MANN, M.E. (2000): CLIMATE CHANGE: Lessons for a New Millennium. Science, 289(5477): 253-254, doi: 10.1126/science.289. 5477.253.

MANNIG, B. (2007): Überblick über das Klima Norwegens anhand von ausgewählten Klimastationen. Unpublished map. University of Würzburg. Würzburg.

MARTINSEN, O.J. & NØTTVEDT, A. (2008): Norway rises from the sea. In: RAMBERG, I.B., BRYHNI, I., NØTTVEDT, A. & RANGNES, K. (Eds.): The making of a land - geology of Norway. Norsk Geologisk Forening, Trondheim, pp. 442-479.

MATTHEWS, J.A. (1974): Families of lichenometric dating curves from the Storbreen gletschervorfeld, Jotunheimen, Norway. Norsk geografisk tidsskrift, 28: 215-235.

MATTHEWS, J.A. (1975): Experiments on the reproducibility and reliability of lichenometric dates, Storbreen gletschervorfeld, Jotunheimen, Norway. Norsk geografisk tidsskrift, 29: 97-109.

MATTHEWS, J.A. (1977): A lichenometric test of the 1750 end-moraine hypothesis: Storbreen gletschervorfeld, southern Norway. Norsk geografisk tidsskrift, 31: 129-136.

MATTHEWS, J.A. (1991): The late Neoglacial ('Little Ice Age') glacier maximum in southern Norway: new ^{14}C-dating evidence and climatic implications. The Holocene, 1(3): 219-233.

MATTHEWS, J.A. (2005): 'Little Ice Age' glacier variations in Jotunheimen, southern Norway: a study in regionally controlled lichenometric dating of recessional moraines with implications for climate and lichen growth rates. The Holocene, 15(1): 1-19.

MATTHEWS, J.A., BERRISFORD, M.S., DRESSER, P.Q., NESJE, A., DAHL, S.O., BJUNE, A.E., BAKKE, J., JOHN, H., BIRKS, B., LIE, Ø., DUMAYNE-PEATY, L. & BARNETT, C. (2005): Holocene glacier history of Bjørnbreen and climatic reconstruction in central Jotunheimen, Norway, based on proximal glaciofluvial stream-bank mires. Quaternary Science Reviews, 24(1-2): 67-90, doi: 10.1016/j.quascirev.2004.07.003.

MATTHEWS, J.A. & BRIFFA, K.R. (2005): The 'Little Ice Age': re-evaluation of an evolving concept. Geografiska Annaler, Series A, Physical Geography, 1: 17-36.

MATTHEWS, J.A., DAHL, S.O., NESJE, A., BERRISFORD, M.S. & ANDERSSON, C. (2000): Holocene glacier variations in central Jotunheimen, southern Norway based on distal glaciolacustrine sediment cores. Quaternary Science Reviews, 19(16): 1625-1647.

MATTHEWS, J.A. & DRESSER, P.Q. (2008): Holocene glacier variation chronology of the Smørstabbtindan massif, Jotunheimen, southern Norway, and the recognition of century- to millennial-scale European Neoglacial Events. The Holocene, 18(1): 181-201.

MATTHEWS, J.A. & KARLEN, W. (1992): Asynchronous neoglaciation and Holocene climate-change reconstructed from Norwegian glacilacustrine sedimentary sequences. Geology, 20(11): 991-994.

MOEN, A. (1999). Nasjonalatlas for Norge Vegetasjon. Norges geografiske, oppmåling (2. ed.). StatensKartverk, Hønefoss.

MÜLLER, F., CAFISCH, T. & MÜLLER, G. (1976). Firn und Eis der Schweizer Alpen: Gletscherinventar. Geographisches Institut der ETH Zürich publ. 57. Zürich: Versuchsanstalt für Wasserbau, Hydrologie und Glaziologie der ETH Zürich.

NCDC (2008): Climate Science: Investigating Climatic and Environmental Processes. Decadal Processes (<10^2 years) (20.08. 2008). URL: http://www.ncdc.noaa.gov/paleo/ctl/clisci100.html (Access: 17.11.2009).

NESJE, A. (2005): Briksdalsbreen in western Norway: AD 1900-2004 frontal fluctuations as a combined effect of variations in winter precipitation and summer temperature. The Holocene, 15(8): 1245-1252.

NESJE, A. (2009): Latest Pleistocene and Holocene alpine glacier fluctuations in Scandinavia. Quaternary Science Reviews, 28: 2119-2136, doi: 10.1016/j.quascirev.2008.12.016.

NESJE, A., BAKKE, J., DAHL, S.O., LIE, Ø. & MATTHEWS, J.A. (2008a): Norwegian mountain glaciers in the past, present and future. Global and Planetary Change, 60: 10-27.

NESJE, A. & DAHL, S.O. (1993): Lateglacial and Holocene glacier fluctuacions and climate variation in Western Norway - a review. Quaternary Science Reviews, 12(4): 255-261.

NESJE, A. & DAHL, S.O. (2003): The `Little Ice Age`- only temperature? The Holocene, 13(1): 139-145, doi: 10.1191/0959683603hl603fa.

NESJE, A., DAHL, S.O., THUN, T. & NORDLI, Ø. (2008b): The 'Little Ice Age' glacial expansion in western Scandinavia: summer temperature or winter precipitation? Climate Dynamics, 30: 789-801, doi: 10.1007/s00382-007-0324-z.

NESJE, A., KVAMME, M., RYE, N. & LØVLIE, R. (1991): Holocene glacial and climate history of the Jostedalsbreen region, western Norway - evidence from lake-sediments and terrestrial deposits. Quaternary Science Reviews, 10(1): 87-114.

NESJE, A., LIE, Ø. & DAHL, S.O. (2000): Is the North Atlantic Oscillation reflected in Scandinavian glacier mass balance records? Journal of Quaternary Science, 15(6): 587-601.

NESJE, A., MATTHEWS, J.A., DAHL, S.O., BERRISFORD, M.S. & ANDERSSON, C. (2001): Holocene glacier fluctuations of Flatebreen and winter-precipitation changes in the Jostedalsbreen region, western Norway, based on glaciolacustrine sediment records. Holocene, 11(3): 267-280.

NORDGULEN, Ø. & ANDRESEN, A. (2008): The Precambrian. In: RAMBERG, I.B., BRYHNI, I., NØTTVEDT, A. & RANGNES, K. (Eds.): The making of a land - geology of Norway. Norsk Geologisk Forening, Trondheim, pp. 62-119.

NORDLI, Ø., LIE, Ø., NESJE, A. & BENESTAD, R. (2005): Glacier mass balance in southern Norway modelled by circulation indices and spring-summer temperature AD 1781 - 2000. Geografiska Annaler, Series A, Physical Geography, 87: 431-445.

NVE (Ed.), (2006): Modelling the climate sensitivity of Storbreen and Engabreen, Norway. NVE-Report, 3-2006. NVE, Oslo, 35 pp.

NYE, J.F. (1960): The response of glaciers and ice-sheets to seasonal and climatic changes. Proceedings of the Royal Society of London, Series A(256): 559-584.

OBERRIGHT, J.E. (2004): Artificial Satellites (2004). URL: http://www.nasa.gov/worldbook/artificial_satellites_worldbook.html (Access: 09.10.2009).

OERLEMANS, J. (Ed.), (2001): Glaciers and climate change. Balkema, Rotterdam, 148 pp.

OERLEMANS, J. (2005): Extracting a climate signal from 169 glacier records. Science, 308(5722): 675-677, doi: 10.1126/science. 1107046.

ØSTREM, G. (1964): Ice-cored moraines in Scandinavia. Geografiska Annaler, XLVI, 3: 282-337.

ØSTREM, G. & BRUGMAN, M. (1991). Glacier mass-balance measurements. A manual for field and office work. NHRI science report, no. 4. National Hydrology Research Institute, Inland Waters Directorate, Conservation and Protection, Environment Canada, Saskatoon, Saskatchewan.

ØSTREM, G., DALE SELVIG, K. & TANDBERG, K. (1988). Atlas over breer i Sør-Norge, 61. vol. NVE, Oslo.

ØSTREM, G. & HAAKENSEN, N. (1993): Glaciers of Europe – Glaciers of Norway. In: WILLIAMS, R.S.J. & FERRINGO, J.G. (Eds.): Satellite Image Atlas of Glaciers of the World. USGS Professional Paper 1386–E–3. USGS, pp. 63-109.

ØSTREM, G. & ZIEGLER, T. (1969). Atlas over breer i Sør-Norge. NVE, Oslo.

ØYEN, P.A. (1893): Isbræstudier i Jotunheimen. Nytt Magasin for Naturvidenskabere, 31: 26-27.

PATERSON, W.S.B. (1994). The physics of glaciers, 3. vol. Butterworth-Heinemann, Oxford, Auckland, Boston, Johannesburg, Melbourne, New Delhi.

PAUL, F. (2001): Evaluation of different methods for glacier mapping using Landsat TM. Proceedings of EARSeL-SIG Workshop Land Ice and Snow, Dresden, 239-245.

PAUL, F. (2007). The New Swiss Glacier Inventory 2000 - Application of Remote Sensing and GIS. Schriftenreihe Physische Geographie, Glaziologie und Geomorphodynamik, 52. vol. Geographisches Institut der Universität Zürich, Zurich, 210 pp.

PAUL, F. (2009): Guidlines for the compilation of glacier inventory data from digital sources. PAUL, F., pp. 20. available at URL: http://globglacier.ch/docs/guidelines_inventory.pdf.

PAUL, F. & ANDREASSEN, L.M. (2009): A new glacier inventory for the Svartisen region, Norway from Landsat ETM+ data: challenges and change assessment. Journal of Glaciology, 55(192): 607-618.

PAUL, F., HUGGEL, C. & KÄÄB, A. (2004a): Combining satellite multispectral image data and a digital elevation model for mapping debris-covered glaciers. Remote Sensing of Environment, 89: 510-518.

PAUL, F., HUGGEL, C., KÄÄB, A., KELLENBERGER, T. & MAISCH, M. (2003): Comparison of TM-derived glacier areas with higher resolution data sets. Proceedings of EARSeL-LISSIG-Workshop Observing our Cryosphere from Space, Bern, 15-21.

PAUL, F. & KÄÄB, A. (2005): Perspectives on the production of a glacier inventory from multispectral satellite data in Arctic Canada: Cumberland Peninsula, Baffin Island. Annals of Glaciology, 42: 59-66.

PAUL, F., KÄÄB, A. & HAEBERLI, W. (2007): Recent glacier changes in the Alps observed by satellite: Consequences for future monitoring strategies. Global and Planetary Change, 56(1-2): 111-122.

PAUL, F., KÄÄB, A., MAISCH, M., KELLENBERGER, T. & HAEBERLI, W. (2004b): Rapid disintegration of Alpine glaciers observed with satellite data. Geophysical research letters, 31: L21402, doi: 10.1029/2004GL020816.

PAUL, F. & SVOBODA, F. (2009): A new glacier inventory on southern Baffin Island, Canada, from ASTER data: II. Data analysis, glacier change and applications. Annals of Glaciology, 50(53): 22-31.

POHJOLA, V.A. & ROGERS, J.C. (1997): Atmospheric circulation and variations in Scandinavian glacier mass balance. Quaternary Research, 47(1): 29-36.

RASMUSSEN, L.A. (2004): Altitude variation of glacier mass balance in Scandinavia. Geophysical research letters, 31: L13401, doi: 10.1029/2004GL020273.

RASMUSSEN, L.A. & ANDREASSEN, L.M. (2005): Seasonal mass-balance gradients in Norway. Journal of Glaciology, 51(175): 601-606.

RASMUSSEN, L.A., ANDREASSEN, L.M., BAUMANN, S. & CONWAY, H. (submitted): Little Ice Age precipitation in southern Norway. The Holocene: 1-14.

RASMUSSEN, L.A., ANDREASSEN, L.M. & CONWAY, H. (2007): Reconstruction of mass balance of glaciers in southern Norway back to 1948. Annals of Glaciology, 46: 255-260.

RASMUSSEN, L.A. & CONWAY, H. (2004): Climate and Glacier Variability in Western North America. Journal of Climate, 17: 1804-1815.

RASMUSSEN, L.A. & CONWAY, H. (2005): Influence of upper-air conditions on glaciers in Scandinavia. Annals of Glaciology, 42: 402-408.

RAUP, B., KÄÄB, A., KARGEL, J.S., BISHOP, M.P., HAMITON, G., LEE, E., PAUL, F., RAU, F., SOLTESZ, D., KHALSA, S.J.S., BEEDLE, M. & HELM, C. (2007): Remote sensing and GIS technology in the Global Land Ice Measurements from Space (GLIMS) Project. Computers & Geosciences, 33: 104-125.

REICHERT, B.K., BENGTSSON, L. & OERLEMANS, J. (2001): Midlatitude forcing mechanisms for glacier mass balance investigated using general circulation models. Journal of Climate, 14(17): 3767-3784.

REUBER, O. & REUBER, M. (1999): Geologie des Jotunheimen (1999). URL: http://www.reuber-norwegen.de/JotunInfoGeol.html (Access: 12.11.2009).

RICHARD, J.A. & XIUPING, J. (2006). Remote Sensing Digital Image Analysis. An Introduction (4. ed.). Springer Verlag, Berlin.

ROGERS, J.C. (1984): The association between the North-Atlantic Oscillation and the Southern Oscillation in the northern hemisphere. Monthly Weather Review, 112(10): 1999-2015.

RÖTHLISBERGER, F. (1986). 10000 Jahre Gletschergeschichte der Erde. Sauerländer Verlag, Aarau.

ROTT, H., SCHERLER, K.E., REYNAUD, L., BARBERO, R.S. & ZANON, G. (1993): Glaciers of Europe - Glaciers of the Alps. In: WILLIAMS, R.S.J. & FERRINGO, J.G. (Eds.): Satellite Image Atlas of glaciers of the World. USGS Professional Paper 1386-E-1. USGS.

SALINGER, J. (2001): Climate variations in New Zealand and Southwest Pacific. In: STURMAN, A. & SPRONKEN-SMITH, R. (Eds.): The physical environment. A New Zealand perspective. Oxford University Press, Melbourne, New York, pp. 130-149.

SCHAEFER, J.M., DENTON, G.H., KAPLAN, M., PUTNAM, A., FINKEL, R.C., BARRELL, D.J.A., ANDERSEN, B.G., SCHWARTZ, R., MACKINTOSH, A., CHINN, T.J.H. &

SCHLÜCHTER, C. (2009): High-Frequency Holocene Glacier Fluctuations in New Zealand Differ from the Northern Signature. Science, 324: 622-625.

SCHOLZ, H. & JONASSON, C. (2004): Einführung in die Geologie Skandinaviens. Geographische Rundschau, 2: 43-49.

SHAKESBY, R.A., MATTHEWS, J.A. & SCHNABEL, C. (2008): Cosmogenic ^{10}Be and ^{26}Al ages of Holocene moraines in southern Norway II: evidence for individualistic responses of high-altitude glaciers to millennial-scale climatic fluctuations. The Holocene, 18(8): 1165-1177, doi: 10.1177/ 0959683608096592.

SHAKESBY, R.A., MATTHEWS, J.A. & WINKLER, S. (2004): Glacier variations in Breheimen, southern Norway: relative-age dating of Holocene moraine complexes at six high-altitude glaciers. The Holocene, 14(6): 899-910.

SHAKESBY, R.A., SMITH, J., MATTHEWS, J., WINKLER, S., DRESSER, P.Q., BAKKE, J., DAHL, S.O., LIE, Ø. & NESJE, A. (2007): Reconstruction of Holocene glacier history from distal sources: glaciofluvial stream-bank mires and a glaciolacustrine sediment core near Sota Sæter, Breheimen, southern Norway. The Holocene, 17(6): 729-745.

SHUMSKII, P.A. (1964). Principles of Structural Glaciology. The Petrography of Fresh-water Ice as a Method of Glaciological Investigation. Dover Publications Inc., New York.

SIDJAK, R.W. & WHEATE, R.D. (1999): Glacier mapping of the Illecillewaet icefield, British Columbia, Canada, using Landsat TM and digital elevation data. International Journal of Remote Sensing, 20(2): 273-284.

SIX, D., REYNAUD, L. & LETREGUILLY, A. (2001): Alpine and Scandinavian glaciers mass balances, their relations with the North Atlantic Oscillation. Comptes rendus de l'academie des sciences, Sciences de la terre et des planetes, 333(11): 693-698.

SOLLI, A. & NORDGULEN, Ø. (2008): Bedrock map of Norway and the Caledonides in Sweden and Finland - 1:2 000 000. Geological Survay of Norway.

SOLOMINA, O., BARRY, R. & BODNYA, M. (2004): The retreat of tien shan glaciers (Kyrgyzstan) since the Little Ice Age estimated from aerial photographs, lichenometric and historical data. Geografiska Annaler, Series A, Physical Geography, 86(2): 205-215.

SOLOMINA, O., HAEBERLI, W., KULL, C. & WILES, G. (2008): Historical and Holocene glacier-climate variations: General concepts and overview. Global and Planetary Change, 60(1-2): 1-9, doi: 10.1016/ j.gloplacha.2007.02.001.

STEINER, D., PAULING, A., NUSSBAUMER, S.U., NESJE, A., LUTERBACHER, J., WANNER, H. & ZUMBUHL, H.J. (2008): Sensitivity of European glaciers to precipitation and temperature – two case studies. Climatic Change, 90(4): 413-441, doi: 10.1007/s10584-008-9393-1.

STURMAN, A. (2001a): Local and regional weather and climate. In: STURMAN, A. & SPRONKEN-SMITH, R. (Eds.): The physical environment. A New Zealand perspective. Oxford University Press, Melbourne, New York, pp. 94-112.

STURMAN, A. (2001b): Synoptic controls on weather. In: STURMAN, A. & SPRONKEN-SMITH, R. (Eds.): The physical environment. A New Zealand perspective. Oxford University Press, Melbourne, New York, pp. 76-93.

STURMAN, A. & WANNER, H. (2001): A comparative review of the weather and climate of the Southern Alps of New Zealand and the European Alps. Mountain Research and Development, 21(4): 359-369.

SVOBODA, F. & PAUL, F. (2009): A new glacier inventory on southern Baffin Island, Canada, from ASTER data: I. Applied methods, challenges and solutions Annals of Glaciology, 50(53): 11-21.

TONIAZZO, T. & SCAIFE, A.A. (2006): The influence of ENSO on winter North Atlantic climate. Geophysical research letters, 33(24): L24704, doi: 10.1029/2006gl027881.

TRENHAILE, A.S. (2004). Geomorphology: a Canadian perspective (2. ed.). Oxford University Press, Toronto.

U.S. DEPARTMENT OF THE INTERIOR (2009a): Landsat 5 History (10.12.2009). URL: http://landsat.usgs.gov/about_landsat5.php (Access: 09.10.2009).

U.S. DEPARTMENT OF THE INTERIOR (2009b): Landsat Missions Timeline (10.12.2009). URL: http://landsat.usgs.gov/about_mission_ history.php (Access: 09.10.2009).

UNEP & WGMS (2008): Global Glacier Changes: facts and figures. UNEP, World Glacier Monitoring Service, Zurich, 88 pp.

VINCENT, C., LE MEUR, E., SIX, D. & FUNK, M. (2005): Solving the paradox of the end of the Little Ice Age in the Alps. Geophysical research letters, 32(9): L09706, doi: 10.1029/2005gl022552.

VORREN, T.O., MANGERUD, J., BLIKRA, L.H., NESJE, A. & SVEIAN, H. (2008): The emerge of modern Norway. In: RAMBERG, I.B., BRYHNI, I., NØTTVEDT, A. & RANGNES, K. (Eds.): The making of a land - geology of Norway. Norsk Geologisk Forening, Trondheim, pp. 534-559.

VUILLE, M., FRANCOU, B., WAGNON, P., JUEN, I., KASER, G., MARK, B.G. & BRADLEY, R.S. (2008): Climate change and tropical Andean glaciers: Past, present and future. Earth-science reviews 89, No. 3, pp. 79. Elsevier, Amsterdam, New York.

WANNER, H., BEER, J., BÜTIKOFER, J., CROWLEY, T.J., CUBASCH, U., FLÜCKIGER, J., GOOSSE, H., GROSJEAN, M., JOOS, F., KAPLAN, J.O., KÜTTEL, M., MÜLLER, S.A., PRENTICE, I.C., SOLOMINA, O., STOCKER, T.F., TARASOV, P., WAGNER, M. & WIDMANN, M. (2008): Mid- to Late Holocene climate change: an overview. Quaternary Science Reviews, 27(19-20): 1791-1828.

WANNER, H., HOLZHAUSER, H., PFISTER, C. & ZUMBÜHL, H. (2000): Internannual to century scale climate variability in the European Alps. Erdkunde, 54: 62-69.

WINKLER, S. (2001): Untersuchungen zur Klima- und Morphodynamik in skandinavischen Gebirgsregionen während des Holozän – ein Vergleich ihrer Wechselwirkungen und Prozesssysteme im überregionalen Kontext kaltgemäßigter maritimer Gebirgsregionen. Unpublished Habilitation Thesis, Universität Trier, Trier.

WINKLER, S. (2002): Von der "Kleinen Eiszeit" zum "globalen Gletscherrückzug". Eignen sich Gletscher als Klimazeugen?, Colloquia Academia. Akademievorträge junger Wissenschafter. Akademie der Wissenschaften und der Literatur Mainz, Abhandlungen der Mathematisch-naturwissenschaftlichen Klasse Nr. 3, Franz Steiner Verlag, Stuttgart, pp. 57.

WINKLER, S. (2003): A new interpretation of the date of the 'Little Ice Age' glacier maximum at Svartisen and Okstindan, northern Norway. The Holocene, 13(1): 83-95.

WINKLER, S. (2004a): Hochgebirgsgletscher. Die jüngere weltweite Entwicklung der Hochgebirgsgletscher vor dem Hintergrund der holozänen Gletschergeschichte. Geographie und Schule, 26(148): 2-8.

WINKLER, S. (2004b): Lichenometric dating of the 'Little Ice Age' maximum in Mt Cook National Park, Southern Alps, New Zealand. The Holocene, 14(6): 911-920, doi: 10.1191/0959683604hl767rp.

WINKLER, S. (2009). Gletscher und ihre Landschaften. Eine illustrierte Einführung. PRIMUS Verlag, Darmstadt, 183 pp.

WINKLER, S. (in print): Verstehen wir die Reaktion maritimer Gletscher? – Untersuchungen des Gletscherverhaltens der letzten 20 Jahre in Südnorwegen. NORDEN, 19.

WINKLER, S., ELVEHØY, H. & NESJE, A. (2009): Glacier fluctuations of Jostedalsbreen, western Norway, during the past 20 years: the sensitive response of maritime mountain glaciers. The Holocene, 19(3): 395-414, doi: 10.1177/0959683608101390.

WINKLER, S. & HAAKENSEN, N. (1999): Kritische Überprüfung der Möglichkeit zur Prognose des Gletscherverhaltens auf der Grundlage von Modellierungen - dargestellt anhand von regionalen Beispielen aus Norwegen. Petermanns Geographische Mitteilungen, 143(4): 291-304.

WINKLER, S., HAAKENSEN, N., NESJE, A. & RYE, N. (1997): Glaziale Dynamik in Westnorwegen – Ablauf und Ursachen des aktuellen Gletschervorstoßes am Jostedalsbreen. Petermanns Geographische Mitteilungen, 141(1997/1): 43-63.

WINKLER, S. & NESJE, A. (2009): Perturbation of climatic response at maritime glaciers? Erdkunde, 63(3): 229-244.

WINKLER, S., ROER-GÄRTNER, I., ZEMP, M., CHINN, T.J.H., NUSSBAUMER, S.U. & ZUMBÜHL, H. (submitted): Mountain Glaciers as climate indicators - in spatial and temporal differentiation. Erdkunde - Special Issue.

WOLKEN, G.J. (2006): High-resolution multispectral techniques for mapping former Little Ice Age terrestrial ice cover in the Canadian High Arctic. Remote Sensing of Environment, 101: 104-114.

ZEMP, M., PAUL, F., HOELZLE, M. & HAEBERLI, W. (2008): Glacier fluctuations in the European Alps 1850-2000: an overview and spatio-temporal analysis of available data. In: ORLOVE, B., WIEGANDT, E. & LUCKMAN, B. (Eds.): The darkening peaks: Glacial retreat in scientific and social context. University of California Press, Berkely, pp. 152-167.

Appendix A – Parameters and variables of the parameterization

Name	Term	Calculation	Unit
Surface area	S	–	km²
Length	L_0	–	km
Minimum altitude	H_{min}	–	m a.s.l.
Maximum altitude	H_{max}	–	m a.s.l.
Length change	δL	$L_{0,old}$-$L_{0,new}$	m
Mean altitude	H_{mean}	$(H_{max}+H_{min})/2$	m a.s.l.
Equilibrium line altitude	ELA	~ H_{mean}	m a.s.l.
Range	ΔH	H_{max}-H_{min}	m
Length of the central flowline in ablation area	L_a	$0.5*L_0$ für $L_0 \leq 2$ km; $0.75*L_0$ für $L_0 > 2$ km	km
Average surface slope	α	$\arctan(\Delta H/L_0)$	rad
Average surface slope in ablation area	α_a	$\arctan[(H_{mean}-H_{min})/L_a]$	rad
Mean basal shear-stress	τ	$0.005+1.598*\Delta H-0.435*(\Delta H)^2$ für $\Delta H \leq 1.6$; 1.5 für $\Delta H > 1.6$	bar
Average ice thickness at central flowline	h_f	$\tau/(f*\rho*g*\sin\alpha)$	m
Average ice thickness at central flowline in ablation area	$h_{f,a}$	$\tau/(f*\rho*g*\sin\alpha_a)$	m
Average ice thickness over whole glacier	h_F	$(\pi/4)*h_f$	m
Total glacier volume	V	$F*h_F$	km^3
Maximum ice thickness	h_{max}	$2.5*h_{f,a}$	m
Depth-averaged mean flow velocity along central flowline in ablation area	$u_{m,a}$	$[(3*b_t/4)*(L_a/2)]/h_{f,a}$	m/a
Velocity of ice deformation	$u_{d,a}$	$2*A*\tau^n*h_f/(n+1)$	m/a
Sliding velocity in ablation area	$u_{b,a}$	$u_{s,a} - u_{d,a}$	m/a
Mean surface flow velocity along central flowline in ablation area	$u_{s,a}$	~ $u_{m,a}$	m/a
Velocity ratio	VR	$u_{b,a} / u_{s,a}$	–
Response time	t_{resp}	h_{max}/b_t	a
Reaction time	t_{react}	L_a/c	a
Relaxation time	t_{relax}	t_{resp}-t_{react}	a
Kinematic wave velocity	c	$4*u_{s,a}$	m/a
Annual ablation at glacier tongue	b_t	$(db/dH)*(H_{mean}-H_{min})$	m w.e./a
Change in ELA	δELA	$(H_{min,old}-H_{min,new})/2$	m
Mass balance disturbance	δb	δELA*(db/dH)	m w.e./a
Mean mass balance	$\bar{b}_n$	$\delta b/(2*n_{resp})$	m w.e./a
Gravitational acceleration	g	9.81	$m*s^{-2}$
Density of ice	ρ	917	$kg*m^{-3}$
Flow parameter	A	0.16	$a^{-1}*bar^{-3}$
Flow parameter	n	3	–
Shape factor	f	1	–
Mass balance gradient	db/dH	–	m w.e./100m*a^{-1}

Appendix B – t-Test

The t-test was performed to compare to means from individual probes and to analyse the significant independence of the probes. The test shows, whether the difference of the two means is significantly different from zero (null hypothesis). The equations are taken from BORTZ (2005).

The standard deviation of the difference of two means is:

$$\hat{\sigma}_{\bar{x}_1-\bar{x}_2} = \sqrt{\frac{\hat{\sigma}_1^2}{n_1} + \frac{\hat{\sigma}_2^2}{n_2}}$$

$\hat{\sigma}_{\bar{x}_1-\bar{x}_2}$ = assumed standard deviation of the difference of the means,

$\hat{\sigma}_1^2$ = assumed variance of statistic population 1,

$\hat{\sigma}_2^2$ = assumed variance of statistic population 2,

n_1 = statistic population of probe 1, n_2 = statistic population of probe 2.

The assumed standard deviation of the difference of the means is needed to calculate

$$\hat{t} = \frac{\bar{x}_1-\bar{x}_2}{\hat{\sigma}_{\bar{x}_1-\bar{x}_2}}$$

.

Taken a two-tailed significance level α with a calculated degree of freedom (Φ),

$\Phi = n_1 + n_2 - 2$,

the significance is tested by $\hat{t} > t_{\alpha;\Phi}$.

This method was performed with all means from the parameterization in the comparison:

- Jotunheimen – European Alps;
- Jotunheimen – New Zealand Alps;
- European Alps – New Zealand Alps.

Jotunheimen (1) – European Alps (2) – Parameterization data

$n_1 = 125$, $n_2 = 1763$, $\Phi = 125 + 1763 - 2 = 1886$;
$t_{5\%,\ 1886} = 1.96$, $t_{1\%,\ 1886} = 2.576$, $t_{10\%,\ 1886} = 1.645$;
Results: 0 = no, 1 = yes.

1980s/70s

Var.	$\bar{x}_1$	$\bar{x}_2$	$\hat{\sigma}_2^2$	$\hat{\sigma}_2^2$	$\hat{\sigma}$	$\hat{t}$ abs.	$\hat{t} > t_{5,\Phi}$	$\hat{t} > t_{1,\Phi}$	$\hat{t} > t_{10,\Phi}$
S	1.46	1.44	3.04	13.59	0.18	0.09	**0**	**0**	**0**
H_{max}	2051	3271	21803	103736	15.27	79.83	1	1	1
H_{min}	1607	2620	21402	69922	14.52	69.79	1	1	1
L_0	1.65	1.63	1.17	2.34	0.10	0.17	**0**	**0**	**0**
L_a	1.04	1.01	0.80	1.47	0.09	0.39	**0**	**0**	**0**
H_m	1829	2945	13922	46022	11.73	95.22	1	1	1
α	0.31	24.25	0.02	60.90	0.19	128.52	1	1	1
τ	0.62	0.79	0.04	0.10	0.02	8.55	1	1	1
h_f	26.41	30.08	231.96	313.07	1.43	2.57	1	**0**	1
$h_{f,a}$	32.81	23.62	650.01	193.06	2.30	3.99	1	1	1
V_E	0.05	0.07	0.01	0.17	0.01	1.83	**0**	**0**	1
h_{max}	82	89	4063	5195	5.95	1.16	**0**	**0**	**0**
b_t	1.56	2.44	0.98	2.29	0.10	9.22	1	1	1
$u_{m,a}$	18.12	15.67	164.89	455.70	1.26	1.95	**0**	**0**	1
$u_{d,a}$	0.91	2.58	1.56	21.45	0.16	10.62	1	1	1
$u_{b,a}$	17.20	13.09	143.02	311.30	1.15	3.58	1	1	1
VR	0.96	0.89	0.00	0.01	0.01	11.83	1	1	1
t_{resp}	68.94	18.02	3229.48	50.54	5.09	10.01	1	1	1
t_{react}	0.02	37.37	0.00	306.47	0.42	89.58	1	1	1
t_{relax}	68.93	19.35	3227.76	130.94	5.09	9.74	1	1	1

LIA maximum

Var.	$\bar{x}_1$	$\bar{x}_2$	$\hat{\sigma}_2^2$	$\hat{\sigma}_2^2$	$\hat{\sigma}$	$\hat{t}$ abs.	$\hat{t} > t_{5,\Phi}$	$\hat{t} > t_{1,\Phi}$	$\hat{t} > t_{10,\Phi}$
S	2.00	2.22	5.28	15.91	0.23	0.98	**0**	**0**	**0**
L_0	2.23	2.30	2.21	2.86	0.14	0.47	**0**	**0**	**0**
V	0.09	0.11	0.02	0.05	0.01	1.65	**0**	**0**	**0**

Jotunheimen (1) – New Zealand Alps (2) – Parameterization data

n_1 = 125, n_2 = 702, Φ = 125 + 702 - 2 = 825;
$t_{5\%,\,825}$ = 1.96, $t_{1\%,\,825}$ = 2.576, $t_{10\%,\,825}$ = 1.645;
Results: 0 = no, 1 = yes.

1980s/70s

Var.	$\bar{x}_1$	$\bar{x}_2$	$\hat{\sigma}_2^2$	$\hat{\sigma}_2^2$	$\hat{\sigma}$	$\hat{t}$ abs.	$\hat{t} > t_{5,\Phi}$	$\hat{t} > t_{1,\Phi}$	$\hat{t} > t_{10,\Phi}$
S	1.46	1.40	3.04	23.10	0.24	0.26	**0**	**0**	**0**
H_{max}	2051	2238	21803	83859	17.14	10.88	1	1	1
H_{min}	1607	1543	21402	95120	17.51	3.67	1	1	1
L_0	1.65	1.58	1.17	3.97	0.12	0.56	**0**	**0**	**0**
L_a	1.04	1.19	0.80	2.23	0.10	1.48	**0**	**0**	**0**
H_m	1829	1904	13922	48816	13.45	5.55	1	1	1
α	0.31	0.50	0.02	1.63	0.05	3.73	1	1	1
τ	0.62	0.83	0.04	0.10	0.02	9.61	1	1	1
h_f	26.41	28.37	231.96	393.03	1.55	1.26	**0**	**0**	**0**
V_E	0.05	0.09	0.01	0.43	0.03	1.41	**0**	**0**	**0**
h_{max}	82	105	4063	7665	6.59	3.48	1	1	1
b_t	1.56	4.79	0.98	13.06	0.16	19.89	1	1	1
$u_{m,a}$	18.12	36.86	164.89	2029.63	2.05	9.13	1	1	1
$u_{d,a}$	0.91	2.87	1.56	29.30	0.23	8.38	1	1	1
$u_{b,a}$	17.20	33.99	143.02	1661.16	1.87	8.96	1	1	1
VR	0.93	0.95	0.00	0.01	0.01	1.76	**0**	**0**	1
t_{resp}	68.94	35.68	3229.48	2526.41	5.43	6.13	1	1	1
t_{react}	0.02	11.57	0.00	135.11	0.44	26.33	1	1	1
t_{relax}	68.93	19.35	3227.76	130.94	5.09	9.74	1	1	1
h_F_E	26.48	22.28	228.96	242.41	1.48	2.84	1	1	1
h_F_T	22.47	18.91	164.97	174.71	1.25	2.84	1	1	1
V_T	0.07	0.07	0.02	0.31	0.02	0.01	**0**	**0**	**0**
$\bar{b}n$	-0.04	-0.41	0.00	0.12	0.01	26.89	1	1	1

LIA maximum

Var.	$\bar{x}_1$	$\bar{x}_2$	$\hat{\sigma}_2^2$	$\hat{\sigma}_2^2$	$\hat{\sigma}$	$\hat{t}$ abs.	$\hat{t} > t_{5,\Phi}$	$\hat{t} > t_{1,\Phi}$	$\hat{t} > t_{10,\Phi}$
S	2.00	1.73	5.28	489.40	0.86	0.32	**0**	**0**	**0**
L_0	2.23	2.00	2.21	4.55	0.16	1.48	**0**	**0**	**0**

European Alps (1) – New Zealand Alps (2) – Parameterization data

n_1 = 1763, n_2 = 702, Φ = 1763 + 702 - 2 = 2463;
$t_{5\%,\ 2463}$ = 1.96, $t_{1\%,\ 2463}$ = 2.576, $t_{10\%,\ 2463}$ = 1.645;
Results: 0 = no, 1 = yes.

1980s/70s

Var.	$\bar{x}_1$	$\bar{x}_2$	$\hat{\sigma}_2^2$	$\hat{\sigma}_2^2$	$\hat{\sigma}$	$\hat{t}$ abs.	$\hat{t} > t_{5,\Phi}$	$\hat{t} > t_{1,\Phi}$	$\hat{t} > t_{10,\Phi}$
S	1.44	1.40	13.59	23.10	0.20	0.22	**0**	**0**	**0**
H_{max}	3271	2238	103736	83859	13.35	77.35	1	1	1
H_{min}	2620	1543	69922	95120	13.23	81.43	1	1	1
L_0	1.63	1.58	2.34	3.97	0.08	0.60	**0**	**0**	**0**
L_a	1.01	1.19	1.47	2.23	0.06	2.82	**0**	**0**	**0**
H_m	2945	1904	46022	48816	9.78	106.53	1	1	1
α	24.25	0.50	60.90	1.63	0.19	123.68	1	1	1
τ	0.79	0.83	0.10	0.10	0.01	2.94	1	1	1
h_f	30.08	28.37	313.07	393.03	0.86	1.99	**0**	**0**	**0**
V_E	0.07	0.09	0.17	0.43	0.03	0.51	**0**	**0**	**0**
h_{max}	88.90	104.95	5195.01	7665.19	3.72	4.31	1	1	1
b_t	2.44	4.79	2.29	13.06	0.14	16.67	1	1	1
$u_{m,a}$	15.67	36.86	455.70	2029.63	1.77	11.94	1	1	1
$u_{d,a}$	2.58	2.87	21.45	29.30	0.23	1.22	1	1	1
$u_{b,a}$	13.09	33.99	311.30	1661.16	1.59	13.11	1	1	1
VR	0.89	0.95	0.01	0.01	0.00	14.01	1	1	1
t_{resp}	18.02	35.68	50.54	2526.41	1.90	9.27	1	1	1
t_{react}	37.37	11.57	306.47	135.11	0.61	42.63	1	1	1

LIA maximum

Var.	$\bar{x}_1$	$\bar{x}_2$	$\hat{\sigma}_2^2$	$\hat{\sigma}_2^2$	$\hat{\sigma}$	$\hat{t}$ abs.	$\hat{t} > t_{5,\Phi}$	$\hat{t} > t_{1,\Phi}$	$\hat{t} > t_{10,\Phi}$
S	2.22	1.73	15.91	489.40	0.84	0.59	**0**	**0**	**0**
L_0	2.30	2.00	2.86	4.55	0.09	3.28	1	1	1

Caption of all tables in Appendix B that have not been explained in the text or appendix list:

abs. = absolute
h_F_E = Ice thickness over whole glacier with elliptic bed geometry
h_F_T = Ice thickness over whole glacier with triangular bed geometry
Var. = Variable
V_E = Volume with elliptic bed geometry
V_T = Volume with triangular bed geometry

$\hat{\sigma} = \hat{\sigma}_{\bar{x}_1 - \bar{x}_2}$